Photo halftones
for microfilming use

Period Covered

21 May 1965 through 21 November 1967

Contract No. 950985

JET PROPULSION LABORATORY
CALIFORNIA INSTITUTE OF TECHNOLOGY
PASADENA, CALIFORNIA

DEVELOPMENT OF A STERILIZABLE RUGGEDIZED VIDICON FOR LUNAR AND PLANETARY PHOTOGRAPHY

Final Report

Period Covered

21 May 1965 through 21 November 1967

Contract No. 950985

Prepared for

California Institute of Technology
JET PROPULSION LABORATORY
4800 Oak Grove Drive
Pasadena, California

Prepared by

S. A. Ochs
Project Engineer

Approved by

F. D. Marschka
Project Supervisor

Approved by

R. W. Engstrom
Manager, Advanced Development

Prepared by

Electronic Components and Devices
RADIO CORPORATION OF AMERICA
Industrial Tube Division
Lancaster, Pennsylvania

December 1967

Foreword

This Final Report was prepared by Radio Corporation of America, Electronic Components and Devices, Industrial Tube Division, Lancaster, Pennsylvania, under JPL Contract No. 950985. The JPL Project Engineers were L. Ralph Baker and Henry Canvel.

The report covers the period from May 21, 1965 to November 21, 1967. The work was performed by Conversion Tube Operations: D. W. Epstein, Manager; R. W. Engstrom, Manager of Advanced Development; F. D. Marschka, Project Supervisor; S. A. Ochs, Project Engineer; D. D. Neuer, Engineering Technician. The following engineers also made major contributions: J. L. Rhoads, J. G. Ziedonis, W. M. Kramer and J. A. Zollman

This work was performed for the Jet Propulsion Laboratory, California Institute of Technology, sponsored by the National Aeronautics and Space Administration under Contract NAS7-100.

ABSTRACT

A one-inch vidicon was developed which can withstand ethylene-oxide and dry-heat sterilization as well as exposure to severe shock and vibration. The tube has a ceramic-metal modular construction and is potted in a magnetic shield. Electrostatic focusing and magnetic deflection are employed. Electrical performance is encouraging with resolution of over 500 TV lines having been observed.

TABLE OF CONTENTS

TABLE OF CONTENTS
(CONT'D.)

TABLE OF CONTENTS
(CONT'D.)

LIST OF FIGURES

SECTION I

Objective and General Description of Project

The objective goal of JPL Contract No. 950985 was to design, develop and construct an exceptionally rugged 1" vidicon for slow-scan operation. The tube should be able to yield a high-quality television signal after having undergone the testing procedure outlined in Table I.

Table I

Test Requirements

1. Ethylene-oxide decontamination: six 28-hour cycles at 50° C.
2. Dry-heat sterilization: six 92-hour cycles at 135° C.
3. Static acceleration: ± 190 g for 20 min. along three orthogonal axes (6 tests)
4. Sinusoidal vibration:
   (a) ± 0.5 in. displacement, 5-16 Hz, 6 min. duration
   (b) 5 g rms, 17-50 Hz, 6 min.
   (c) 15 g rms, 50-100 Hz, 4 min.
   (d) 35 g rms, 100-2000 Hz, 18 min.
   (e) 25 g rms, wide-band noise, 15-2000 Hz, 9 min.

   All tests along three axes (15 tests).
5. Shock:
   (a) ± 3000 g half-sine pulse, 225 u sec. rise-time
   (b) ± 3000 g half-sine pulse, 100 u sec. rise-time

   All shocks applied 5 times in each of 6 directions (60 tests).

The sterilization requirements primarily presented a problem for the photoconductor, while the other tests concerned the tube as a whole. The project therefore had two goals: Task 1, the development of a slow-scan photoconductor capable of surviving the dry-heat sterilization; and Task 2, the design, fabrication and testing of the complete ceramic vidicon.

The work done under this contract was performed in two consecutive periods. During Phase A, which lasted fifteen months, the objectives of Task 1 were achieved and an initial tube design was produced under Task 2. Phase B covered sixteen months and consisted of the development of a final tube design and a period of tube fabrication and testing.

SECTION II

Task 1

I. PHOTOCONDUCTOR DEVELOPMENT

The development of a sterilizable slow-scan photoconductor followed the general outline presented in proposal DP 5132 as amended.

The substrate used consisted of vitreous quartz of extremely high quality as far as surface defects were concerned. The faceplates were selected according to their freedom from visible imperfections when viewed by microscope of 30X magnification under light of grazing incidence. Although the inspection criterion was a complete absence of visible imperfections, few substrates in actual fact met this specification.

The initial tubes made on this project were very promising as far as general performance and resistance to dry-heat sterilization were concerned. However, they had a serious problem of spottiness. White, grey and black spots were visible in the television picture and appeared to be caused by imperfections in the photoconductor layer. Attempts at removing this problem included: (1) improvement of the vacuum conditions during the photoconductor evaporation, (2) improved filtering of the inert gas which is admitted to the system upon completion of the evaporation, (3) shortening the time during which the photolayer is exposed to air before exhaust of the tube on which it is mounted, and (4) improved faceplate preparation. Although all of these measures may have contributed to the reduction of spurious signals, it became increasingly clear during the course of the project that the chief source of spottiness lay in the faceplate cleaning procedures.

Repeated re-evaluation and improvements of the faceplate washing and drying procedures resulted in a very substantial reduction of spottiness. Although this problem cannot be considered as having been completely solved, spurious signals were reduced to the point where they are only of secondary importance.

No evidence was observed of any increase in spottiness due to the sterilization procedures.

The final faceplate cleaning procedure decided upon consisted of the following steps: (1) Wash substrates in a water solution of Alconox detergent by swabbing with cotton balls, (2) Rinse substrates in hot deionized water and then, in cold deionized water, (3) Follow with a closely controlled rinsing and drying procedure in a vapor dryer charged with isopropyl alcohol.

The degree of cleanliness of the substrates at this stage was preserved as closely as possible until the faceplate was loaded in the vaporator. It is not likely that any appreciable contamination could occur during this interval since the cleaning facilities and the evaporator are both located in the same clean room.

The evaporations were performed in a dry pumping system evacuated by sorption and ion pumps without the use of organic vapors. The jigging was designed such that the signal electrode and the photoconductive layer

could be deposited without breaking vacuum. Because of the above, the substrate was not exposed to air from the time it was loaded into the evaporator to completion of the photosurface. Therefore, the possibility of contamination occurring between the signal plate and the photoconductor was minimized.

The application of glow-discharge cleaning was evaluated. It appeared that this process was not needed for producing the desired photoconductor characteristics or for good layer adherence to the substrate. Since glow-discharge cleaning was considered as the possible cause of some gross spots found in early tubes, it was decided not to continue to use this cleaning method any further.

The signal electrode (back plate) used in all tubes consisted of rhodium which was evaporated from a rhodium-plated tungsten-wire heater. The resistance of the signal electrodes, as monitored on test slides, varied between 90K and 900K ohms per square. Tube performance appeared to be independent of variations in signal-electrode resistance so long as the resistance was below one megohm per square. The optical transmission of a rhodium coating as used in this work is approximately 65 to 70% relative to air.

The photolayer used was of the RCA developed ASOS type. Since electrical performance changed so little with the sterilization bakes, an elaborate program of photoconductor development was not necessary. Only a minor modification in the evaporation schedule was made (at tube No. 11) in order to effect a slight decrease in dark current, although it does not appear that an appreciable change was caused. Except for this small adjustment, all evaporations were made using essentially the same evaporation profile.

The finished faceplates were removed from the evaporator, inspected optically and then mounted in RCA 7735A vidicons. These commercial tubes are 1" vidicons with magnetic focus and deflection. Their heater operates at 6.3 volts and 0.6 amperes.

During the period of Task 1, the following two test specifications were applied to this contract:

(1) JPL Spec. XSO-30275-TST-A, "Environmental Test Specification Compatibility Test for Planetary Dry Heat Sterilization Requirements," which required three 36-hour cycles at 145°C; and
(2) JPL Spec. GMO-50198-ETS, "Environmental Test Specification Compatibility Tests for Ethylene Oxide Decontamination Requirements," comprising a 24-hour exposure to a prescribed gas mixture at 24°C, followed by a 24-hour exposure to the gas at 40°C.

During Phase B another test specification, JPL Spec. VOL-50503-ETS "Environmental Specification Voyager Capsule Flight Equipment Type Approval and Flight Acceptance Test Procedures for the Heat Sterilization and Ethylene Oxide Decontamination Environments," was applied to this contract. Its pertinent requirements were those included in Table I.

While all the work on Task 1 was performed in accordance with the first mentioned two specifications (as reported in parts II through IV), it was felt desirable to establish whether the photoconductor would withstand the newer test requirements equally well. Therefore, additional heat sterilization tests were made during Phase B, as reported in part V of this section.

II. STERILIZATION AND DECONTAMINATION

The vidicons were baked in an electrically-heated air-tight chamber provided with a dry nitrogen atmosphere. Up to 8 tubes were treated simultaneously. The tubes rested on Teflon supports inside a stainless steel box which was placed in the heating chamber. The temperature was monitored by two or three chromel-alumel thermocouples, which were usually placed in contact with the faceplate rings of different tubes. A separate thermocouple placed in contact with the stainless steel box was connected to a Brown Electronik recording controller which regulates the electric power for heating the chamber.

During a typical heating cycle, the temperature of the experimental tubes was raised to 145°C plus or minus 2°C and maintained there for 36 hours. At the end of the cycle the tubes were allowed to stabilize at room temperature. In all cases, several hours or days elapsed between heating cycles.

For the ethylene-oxide decontamination, tubes were placed in the air-tight chamber and exposed to an atmosphere containing twelve percent ethylene-oxide and 88 percent Freon 12, by weight. The relative humidity was controlled as per paragraphs 3.5 and 3.6.1 of JPL Specification GMO50198-ETS. The temperature was kept at 40°C and monitored as described above. The required amount of water was metered with a pipette and injected into the chamber through a stopcock. The vidicons exposed to this test were treated for 24 hours.

III. TESTING

The vidicons were tested at standard television rate, 60 fields per second interlaced, with 525 lines per frame. A raster of 0.48" width and 0.36" height was scanned. The following measurements were made:

A. Dark Current Vs. Target Voltage

Readings were taken at successively higher values of target voltage (usually to 60V). For each reading, the electron beam was increased until it was just able to discharge the target surface. The current was measured with a Keithley 414 micro-microammeter. Due to the slow response of the meter, it took considerable time for equilibrium to be established at any given target voltage. In order to obtain meaningful results within a practical time, all dark current readings were taken one minute after the target was first discharged at the particular target voltage in question.

The temperature of the faceplate was found to be an important parameter influencing dark current. Therefore, in many tests, the faceplate temperature was monitored with a thermocouple and attempts were made to keep the faceplate at a constant temperature by means of a flow of cooled air.

B. Signal Current Vs. Target Voltage

The sensitivity of the photoconductor was measured in terms of the signal current due to a faceplate illumination of one footcandle. Readings were taken at different target voltages increasing in steps of 10V, as long as sufficient electron beam was available.

C. Light Transfer Characteristic

Signal current was measured as a function of faceplate illumination (at intensities of 0.01, 0.10 and 1.0 footcandle) with the faceplate at 20V. The gamma of the photoconductor, i.e. the slope of the characteristic when plotted on log-log coordinates, was then measured.

D. Spectral Characteristics

The tube was operated at a target voltage of 20V and the uniform target illumination adjusted to the value yielding a signal current of 0.200 uA. Narrow band optical filters were then interposed between the light source and the target, and the corresponding signal current was measured for each wavelength. A correction factor was then applied to each measurement to make allowance for the brightness of the tungsten light source at the wavelength in question and for the transmission of the particular filter used.

E. Resolution

A EIA resolution pattern was projected onto the faceplate. With the target at 20V, the light intensity was varied until a signal current of 0.200 uA was produced. The beam was decreased in magnitude until it was just able to discharge the highlight portions on the target.

The ultimate resolution was measured in the central region of the target and at the corners. In some cases, the beam focus was readjusted between these two readings so as to give optimum resolution. This procedure was adopted since the resolution capability of the photoconductor, rather than that of the beam, was desired.

F. Grey-Scale Rendition

The dynamic range of the tubes was measured in terms of the number of grey-scale steps which could be recognized on the EIA resolution pattern. The same operating parameters were used as for the measurement of resolution.

G. Erasure

The erase characteristics of the tubes were measured in terms of the signal remaining at the third scan after the removal of uniform illumination. The tube was operated at a pre-determined target voltage, usually 20V, and the light intensity adjusted such that the signal current was 0.200 uA. The lower half of the faceplate was then masked so that a reference black level signal was produced.

A chopper, located between the light source and the tube, interrupted the light for one-third of a second every second. The signal output was displayed on an oscilloscope and the lag measured in terms of the signal produced at the third scan after the light had been interrupted.

IV. EXPERIMENTAL RESULTS

A total of fifty-one vidicons were made. Six of these did not receive the three sterilization cycles and final test: One (#11) had too many spots to be useful; three (#15, 22, 23) were overheated during the sterilization procedure so that the indium faceplate seal melted and vacuum was lost; the glass bulbs of two tubes (#27, 47) cracked during the second bake cycle.

TableII shows some of the data obtained from these fifty-one tubes. It can be seen that the changes in the various characteristics caused by the dry-heat sterilization procedure are far from consistent and are relatively small compared to the variations from tube to tube. However, certain significant features emerge quite clearly and provide a basis for predicting the effect of the sterilization process on any given tube.

A. Dark Current

Dark current, at a fixed target voltage, was considered the tube characteristic which would be most susceptible to change under the sterilization procedure. Table III shows the distribution of 45 vidicons as to change in dark current at two target voltages. At each value of the ratio

$$\frac{\text{Dark Current after Sterilization}}{\text{Initial Dark Current}}$$

the number of tubes is given for which this ratio was obtained. The same data are displayed graphically in Figs. 1 and 2, for target voltages of 20V and 30V, respectively.* Here the abscissas represent the dark current ratio, divided into segments of width 0.3. For instance, the segment marked 1.7 includes the values of the dark current ratio in the range from 1.55 to 1.85. The ordinates indicate the number of tubes belonging to each segment. Smooth curves were drawn which approximate this distribution of the experimental tubes.

---

*The dark currents of tubes No. 25 and 26 at E_t = 20V were so small that the measurements were very inaccurate. The entries for these two based on Fig. 1, therefore, were based on the dark currents measured at E_t = 30V.

Table II

Selected Data from Experimental Vidicons
Before and After Three Sterilization Bakes

NG	Dark Current (E_t = 20V) Initial	Final	Signal Current (E_t = 20V, Ill. = 1 fc) Initial	Final	Resolution (E_t = 20V, IS = 200 uA) Initial	Final	Residual Signal (at third scan, E_t = 20V) Initial	Final	Grey-Scale Initial	Final	Gamma Initial	Final
1	4.2 nA	3.7 nA	259 nA	315 nA	600 lines	600 lines	80%	80%	8 steps	8 steps	0.55	0.63
2	5.0	7.0	265	350	500	600	80	81	8	8	.60	.64
3	6.7	10.0	514	480	600	500	80 (E_t=30V)	77	8	10	.70	.75
4	3.0	14.3	418	555	600	550	82(E_t=15V)	83	-	10	.70	.67
5	8.0	11.5	392	454	500	425	74(E_t=30V)		10	10	.72	.70
6	11.0	15.0	489	440	500	425	79		10	10	.65	.67
7	4.5	4.0	400	400	650	550	76		10	10	.73	.75
8	2.0	4.6	340	390	650	525	72		10	10	.71	.80
9	2.9	4.5	350	360	550	350	80		10	10	.65	.62
10	4.3	5.5	420	400	550	350	81		10	10	.66	.65
11									not tested, very bad spots			
12	5.6	29.0	375	500		350	76			7	.69	.71
13	7.5	10.0	423	540	650	600	82		10	10	.70	.72
14	3.4	8.5	447	512	550	375	82		10	8	.70	.66
15	6.5		500		500		80		10		.70	
16	2.0	1.9	303	428	400	400	80	75	10	7	.70	.68
17	0.7	2.5	285	422	450	375	82	79	10	7	.66	.70
18	3.9	6.0	366	460	500	600	78	78	8	10	.74	.77
19	2.7	3.0	367	440	550	600	80	76	8	10	.77	.72
20	7.2	9.0	433	611	500	425	80	78	8	10	.74	.69
21	6.5	10.0	474	630	200	400	81	80	8	10	.73	.68
22	<.01		450		550		86		7		.68	

Table II (Cont'd.)

NG	Dark Current (E_t = 20V) Initial	Final	Signal Current (E_t = 20V, Ill. = 1 fc) Initial	Final	Resolution (E_t = 20V, IS = 200 uA) Initial	Final	Residual Signal (at third scan, E_t = 20V) Initial	Final	Grey-Scale Initial	Final	Gamma Initial	Final
23	2.5 nA		428 nA		525 lines		86%		7 steps		.67	
24	1.3	1.0 nA	224	410 nA	450	300 lines	78(30V)	84%	8	8 steps	.71	.62
25	<0.1	<1	240	395	500	350	78(30V)	80	7	9	.64	.60
26	<1	1.9	240	367	600	400	83	87	10	10	.59	.64
27	1.3		260		650		87		10		.62	
28	5.0	16.0	445	620	600	400	82	80	10	10	.70	.72
29	3.4	9.0	380	500	600	375	84	80	10	10	.66	.68
30	2.3	11.6	413	510	550	500	84		10	10	.67	.65
31	4.6	4.4	237	360	300	525	82		10	10	.70	.66
32	3.0	2.9	290	318	550	500	79		10	10	.69	.64
33	3.5	7.0	370	423	500	600	80		10	10	.67	.66
34	3.0	6.2	415	400	600	600	80		10	10	.69	.67
35	4.3	9.0	355	500	525	450			10	10	.63	.71
36	3.0	6.7	385	442	550	550			10	9	.69	.66
37	3.0	7.0	385	500	500	450			10	10	.71	.73
38	8.5	20.8		559	400	500			8	10	.61	.66
39	8.6	21.4	475	565	525	550			10	10	.67	.65
40	9.0	6.4	390	412	50	600			5	10	.65	.71
41	5.0	5.6	375	422	400	500			10	9	.70	.64
42	5.0	6.6	435	765	350	500			10	10	.69	.66
43	4.0	9.0	475	560	550	550			10	10	.68	.68
44	8.5	15.0	540	489	450	325			10	10	.62	.67

Table II (Cont'd.)

N_G	Dark Current (E_t = 20V) Initial	Final	Signal Current (E_t = 20V, Ill. = 1 fc) Initial	Final	Resolution (E_t = 20V, IS = 200 uA) Initial	Final	Residual Signal (at third scan, E_t = 20V) Initial	Final	Grey-Scale Initial	Final	Gamma Initial	Final
45	6.8 nA	12.4 nA	423 nA	508 nA	400 lines	325 lines			9 steps	10 steps	.61	.69
46	5.4	7.8	443	426	550	525			10	10	.72	.71
47	5.1		410		475				10		.71	
48	8.1	6.5	486	557	575	600			10	10	.69	.73
49	18.1	38.1	519	698	300	200			7	9	.69	.69
50	17.5	30.2	594	747	450	325			10	9	.64	.67
51	6.2	10.0	378	501	600	475			10	10	.63	.70

Table III

Distribution of 45 Tubes in Terms of Dark-Current Ratio

Dark Current After Sterilization / Initial Dark Current	Number of Tubes E_t = 20V	Number of Tubes E_t = 30V
0.7	1	0
0.8	2	2
0.9	2	0
1.0	3	1
1.1	2	1
1.2	1	1
1.3	3	1
1.4	4	2
1.5	3	2
1.6	1	6
1.7	3	5
1.8	2	1
1.9	0	3
2.0	1	4
2.1	3	3
2.2	2	1
2.3	2	2
2.4	1	1
2.5	2	2
2.6	1	0
2.7	0	0
2.8	0	0
2.9	0	1
3.0	0	0
3.1	0	0
3.2	1	0
3.3	0	1
3.4	0	0
3.5	0	1
3.6	1	0
3.7	0	0
3.8	0	0
3.9	0	1
4.0	1	0
4.8	1	0
5.0	1	0
5.1	0	1
5.2	1	0
6.1	0	2

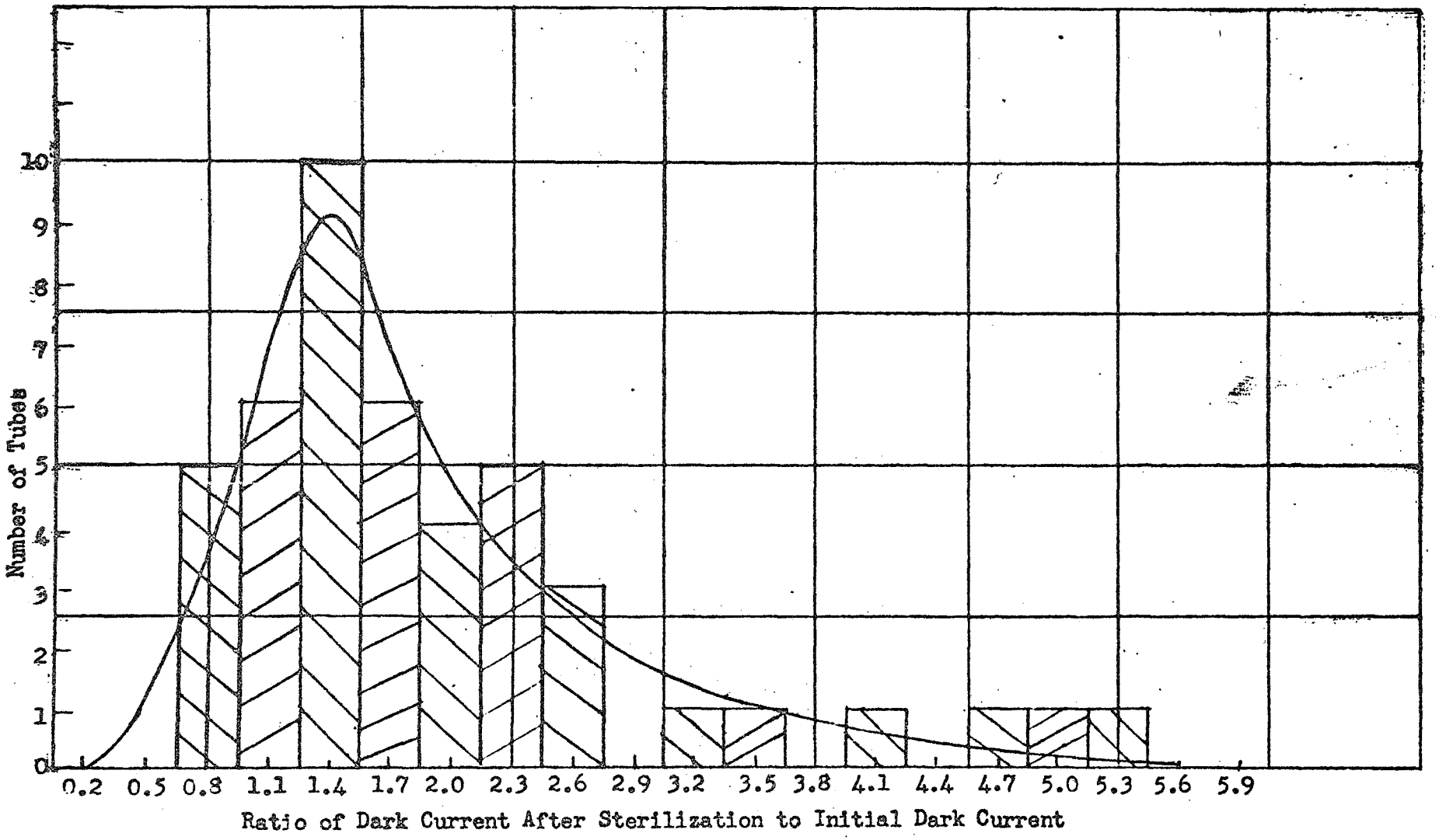

Figure 1. Distribution of Tubes in Terms of Dark Current After Sterilization to Initial Dark Current. Target Voltage = 20 v.

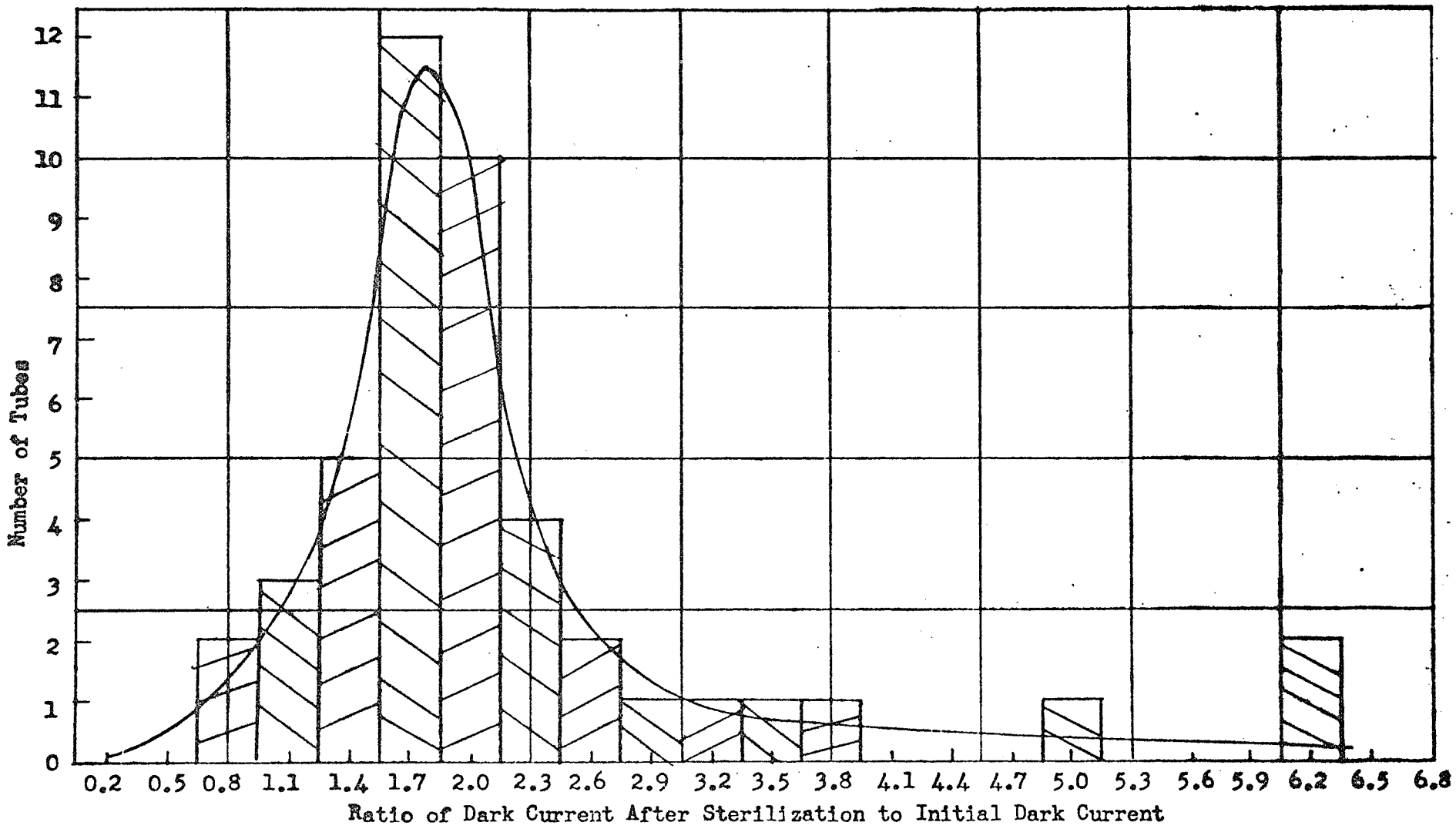

Figure 2. Distribution of Tubes in Terms of Dark Current After Sterilization to Initial Dark Current. Target Voltage= 30 v.

It can be seen in Fig. 1 that at a target voltage of 20V the most probable value of the dark current ratio was in the range 1.40 ± 0.15. However more than half of the tubes had a ratio higher than this value. The mean value of the ratio was 1.65. Sixty percent of the tubes had a ratio of 2.0 or less, 85% a ratio of 2.5 or less.

For a target voltage of 30V, the most probable value of the dark current ratio was 1.80 ± 0.15, while the mean value was 1.85. Sixty-five percent of the tubes had a ratio of or below 2.0, 85% a ratio of or below 2.5.

The above results are complicated by the temperature dependence of the dark current. It was found that variations in dark current due to changes in the faceplate temperature can be comparable to the changes caused by the sterilization bakes. Therefore, attempts were made in most tests to keep the faceplates at the same temperature for all measurements. The temperature was measured with a thermocouple mounted against the front surface of the faceplate. A flow of cooled air was passed over this surface and adjusted so as to keep the temperature at the desired value. However, it often was not feasible to control the temperature to better than one or two degrees C and, in addition, the temperature of the photoconductive layer, on the back side of the faceplate, may have had a significantly different value from that indicated by the thermocouple.

In order to obtain an indication of the significance of variations in temperature, measurements were made of the dark current of some representative tubes at different temperatures. Figure 3 shows the results of such measurements on five tubes, made at a target voltage of 20V, on a semilog plot. In the case of the 2 tubes where more than two measurements were obtained the uncertainty of the results is clearly seen in the spread of the experimental points. This spread most likely is an indication of the difference between the nominal thermocouple readings and the true photoconductor temperatures. However, there can be little doubt about the sizable rate of rise in dark current with temperature. Most measurements were made at an indicated temperature of between 22°C and 30°C. It can be seen that a variation in temperature of 2°, within this range, can easily account for a dark current change of 20%.

As can be seen from Table II, wide variations existed between the dark current values obtained from different tubes. Little correlation is found between the sensitivity and dark current measurements of any given tube. Therefore, it appears possible that the dark current can be kept small even in tubes of high sensitivity.

In Fig. 4 the dark current characteristics for 3 typical tubes are shown before and after the full sterilization process. The approximate faceplate temperature at which the measurements were made

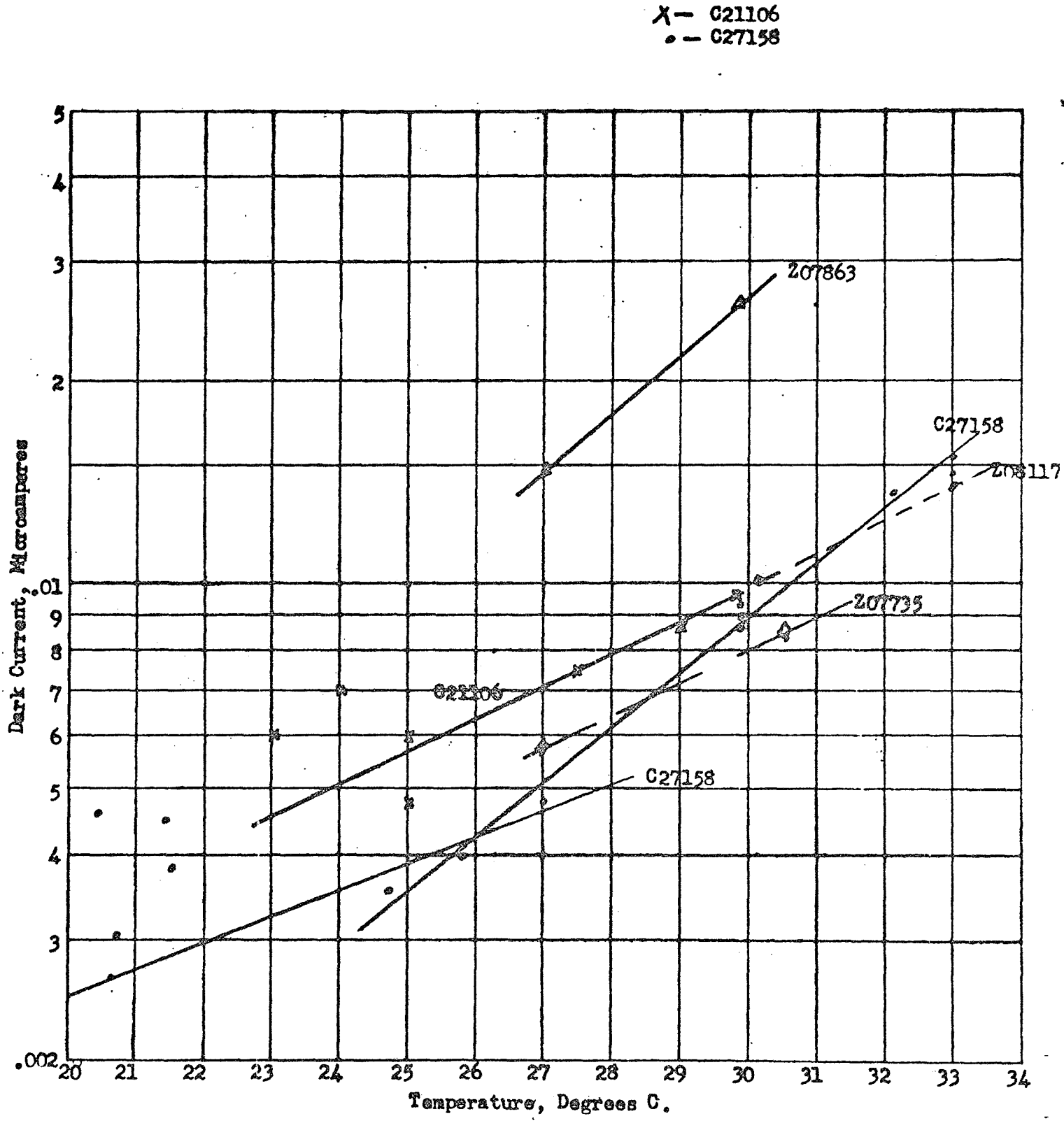

Figure 3. Semilog Plot of Dark Current (of Five Tubes) vs. Temperature. Target Voltage = 20 v.

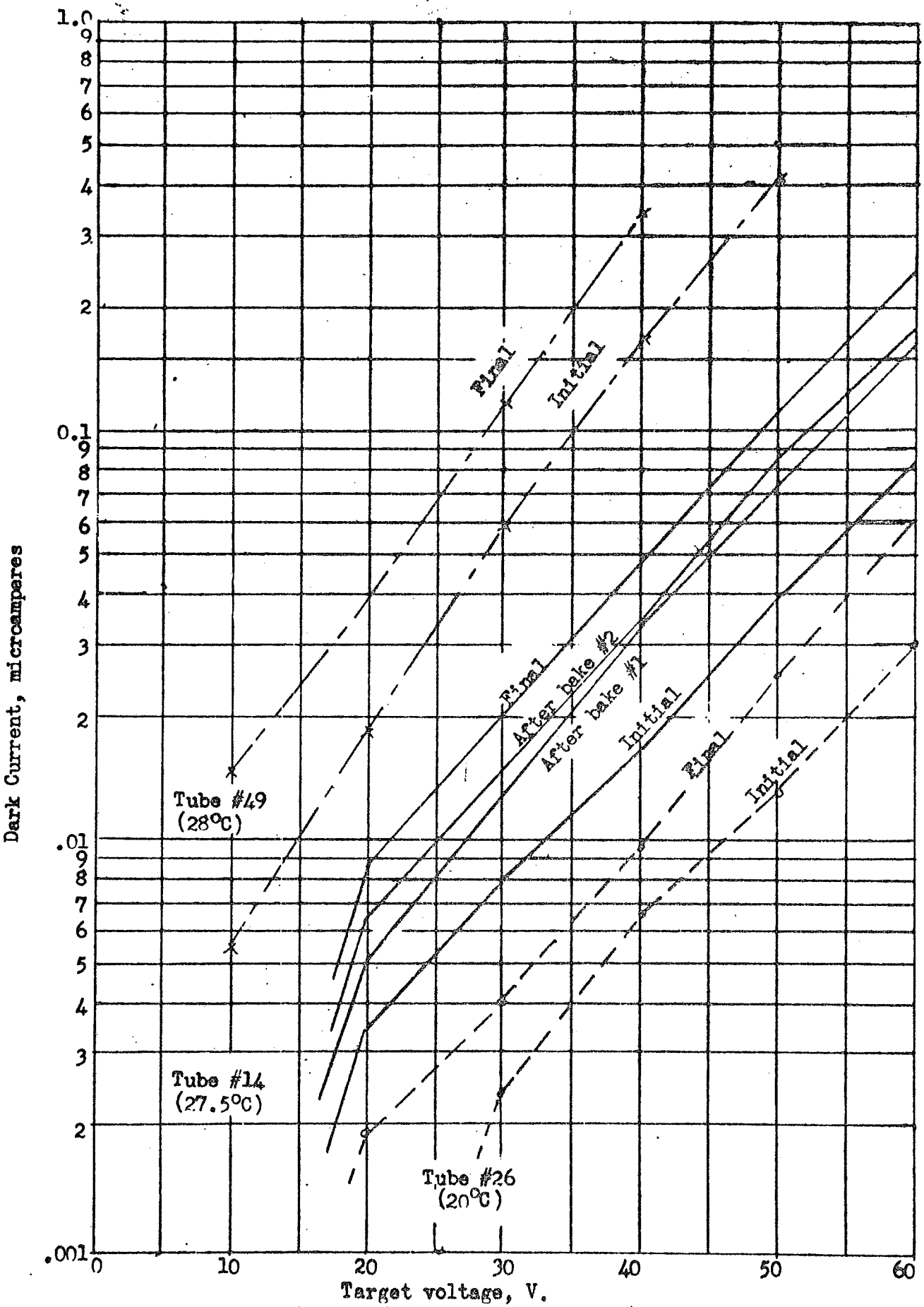

Figure 4. Semilog Plot of Dark Current (of three tubes) vs. Target Voltage, Before and After Dry-Heat Sterilization.

for each tube is indicated. For one tube (#14), the results obtained after the first and second sterilization bakes also are given. In general it was found that the increase in dark current due to the first bake was greater than for the subsequent bakes.

The results reported above suggest that for any given tube it is likely that sterilization will cause an increase in dark current at constant target voltage of less than 100%.

B. Sensitivity

In general, the sensitivity of the photoconductor chosen for this project was found to increase as a result of the dry-heat sterilization, but by a smaller percentage than the dark current. Figure 5 is a graphical presentation of the distribution of 44 vidicons as to change in signal current at 20V target voltage, for uniform illumination of one footcandle intensity. The most probable ratio of sensitivity after sterilization, to initial sensitivity, as well as the mean value of this ratio, according to these results is about 1.25.

Although temperature changes of the faceplate caused some corresponding variations in signal current, these represented a much smaller percentage change than the corresponding effect with dark current. In the case of one tube in which the faceplate temperature was changed from 23°C to 30°C, at one footcandle illumination and 20V target voltage, the signal current rose by less than 10%.

Typical plots of signal current vs. target voltage at 1.0 fc faceplate illumination are given in Fig. 6 for two experimental tubes. As was found in the case of dark current, the increase in sensitivity after the first bake was greater than after the second and third.

The measurements indicated that the sensitivity of any future tube with the photoconductor used in this project, can be expected to increase by about 25% during sterilization.

C. Light Transfer Characteristic

The log-log plots of signal current vs. target illumination for the various tubes in most measurements were slightly concave upward, i.e. the slope of the curves was lower at smaller light levels. The gamma values given in Table II are the average slopes of the various curves. In Fig. 7 the distribution of tubes in terms of gamma is shown, before and after sterilization. The average values of gamma for the two sets of measurements are the same within the accuracy of the data. The difference in shape of the two distribution graphs also is within the expected uncertainty of the measurements. It can, there-

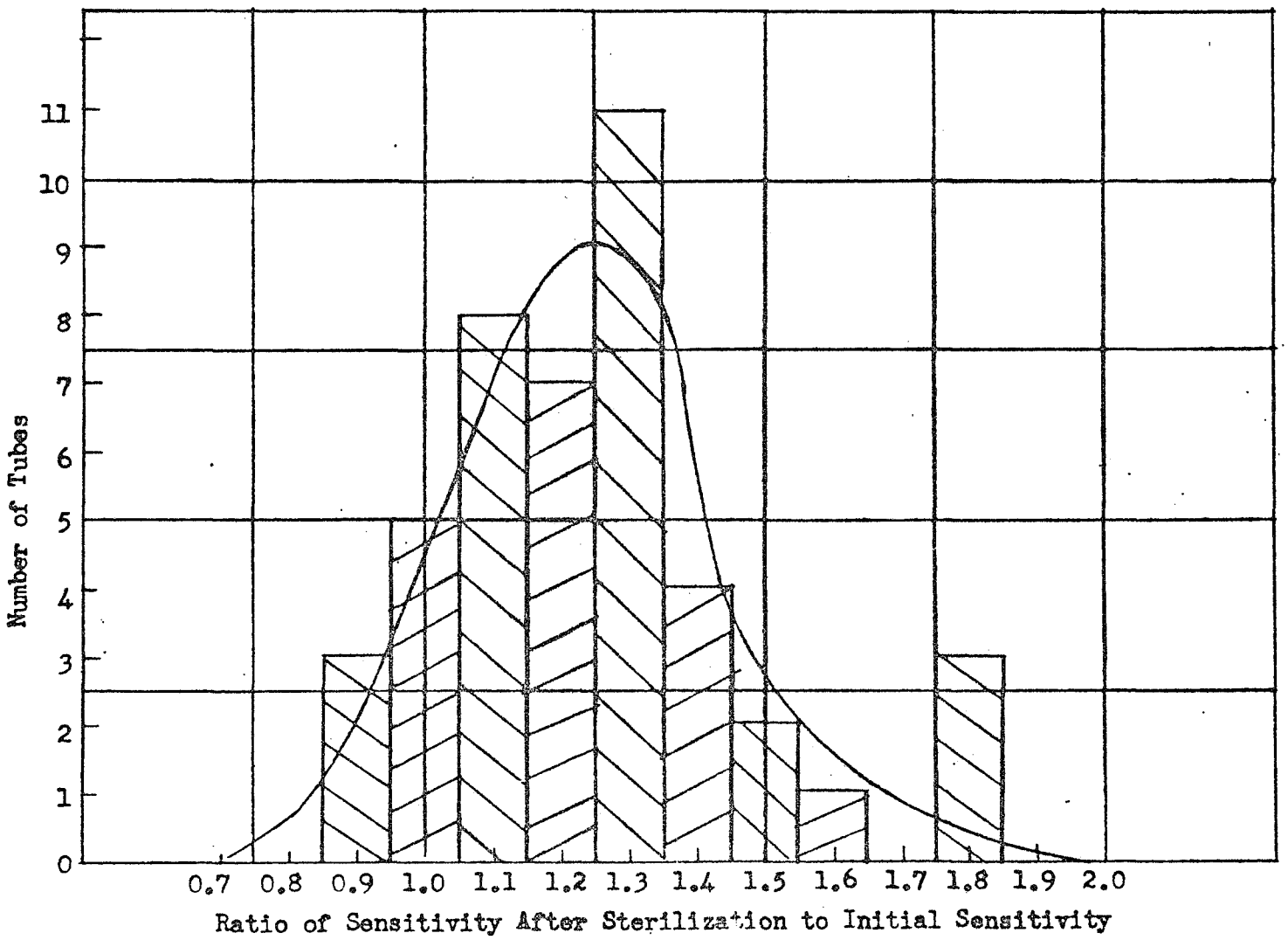

Figure 5. Distribution of Tubes in Terms of Sensitivity (Signal Current at 1.0 ft-cd Target Illumination) After Sterilization to Initial Sensitivity. Target Voltage = 20 v.

Page intentionally left blank

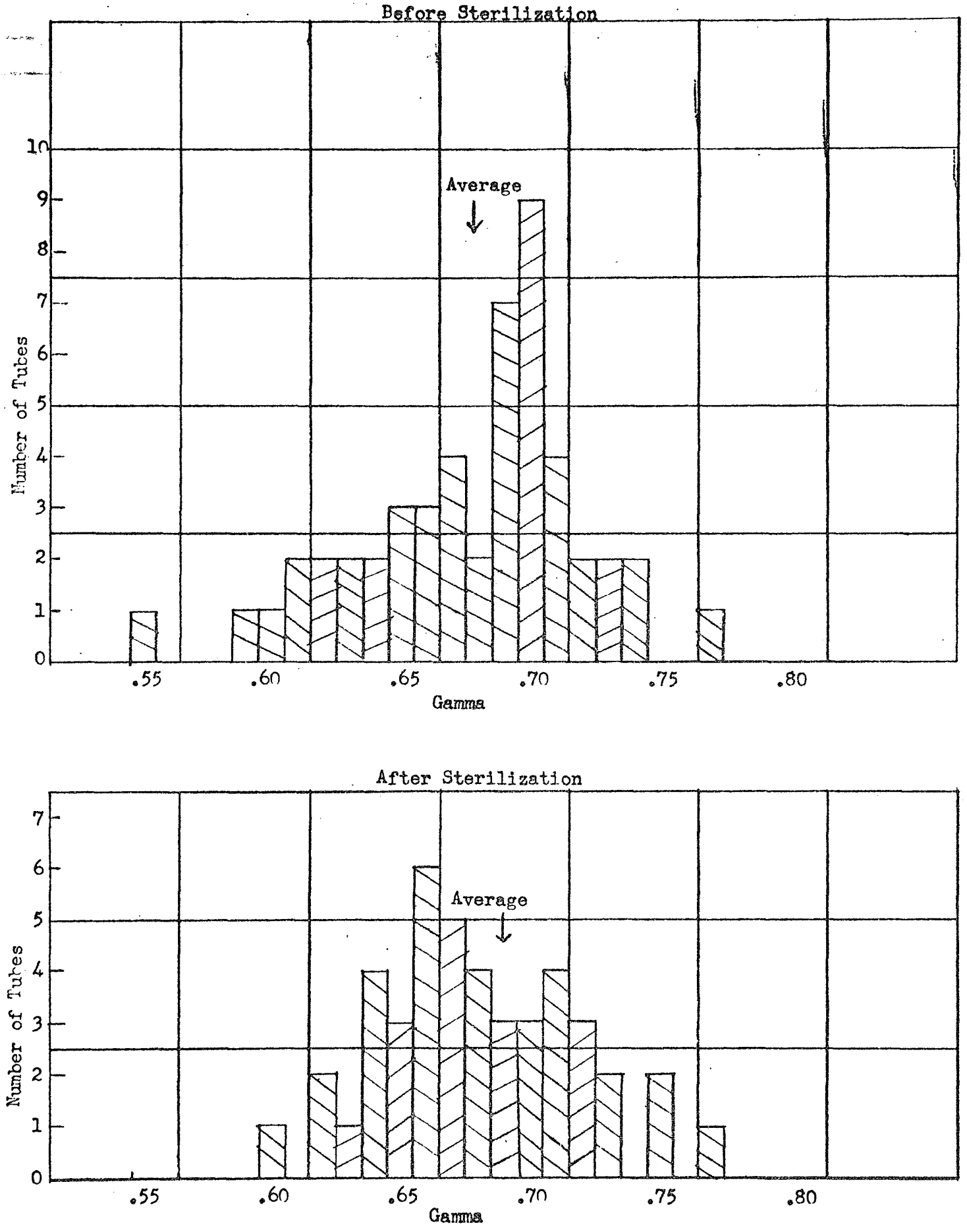

Figure 7. Distribution of Tubes, Before and After Sterilization, in Terms of Gamma. Target Voltage = 20V.

fore, be concluded that the light transfer characteristic of the experimental photoconductor is not sensitive to the sterilization process as far as shape and slope of the curve are concerned. The gamma of the photoconductor generally falls in the range of 0.68 ± 0.04.

A set of measurements were made on one tube (No. 22) when scanned with a one-second frame time. The data were taken before the tube was dry-heat sterilized. Unfortunately, the tube was lost when the oven overheated during the third sterilization bake causing failure of the indium seal, at the faceplate. Due to time limitations, no other such slow-scan measurements were made on later tubes.

The data obtained from tube No. 22 are shown in Fig. 8. The measurements were made at various exposure times ranging from 0.01 sec. to 0.5 sec. The straight line drawn so as to average the experimental points corresponds to a gamma of 0.71. The value of gamma measured for this tube at standard television rate was 0.68. It is seen that a measurable signal was obtained below an exposure of 0.002 ft.-cd.-sec. and that saturation appears to set in somewhat above 0.15 ft.-cd.-sec.

D. Spectral Response

Figure 9 shows the average spectral response of eleven tubes before and after sterilization. Measurements were made at six wavelengths ranging from 500 to 666 millimicrons. The experimental results for each tube were adjusted so that the values quoted correspond to the same amount of power at all wavelengths incident on the faceplate. The curves for the different tubes were then normalized to the same maximum response value, which in all cases occurred at the 566 mu reading. The two curves in Fig. 9 represent the average of these normalized response characteristics. It is seen that after sterilization the response at wavelengths above and below the peak of the curve has somewhat increased relative to the peak response, i.e. the curve has become slightly flatter.

Data taken on four earlier tubes, made before the slight modification in the photoconductor, showed less consistent results than the eleven tubes mentioned above which were made with the later form of photoconductor. The maximum response for the four earlier tubes occurred at somewhat shorter wavelengths (at or below 500 mu) than for the later tubes.

E. Resolution

The distribution of tubes, before and after sterilization, in terms of ultimate resolution is shown in Fig. 10. The average resolution was found to have decreased from an initial value of 500 lines to a final value of 460 lines. Of the forty-four tubes tested for resolution before and after full sterilization: twenty-seven tubes decreased in resolution,

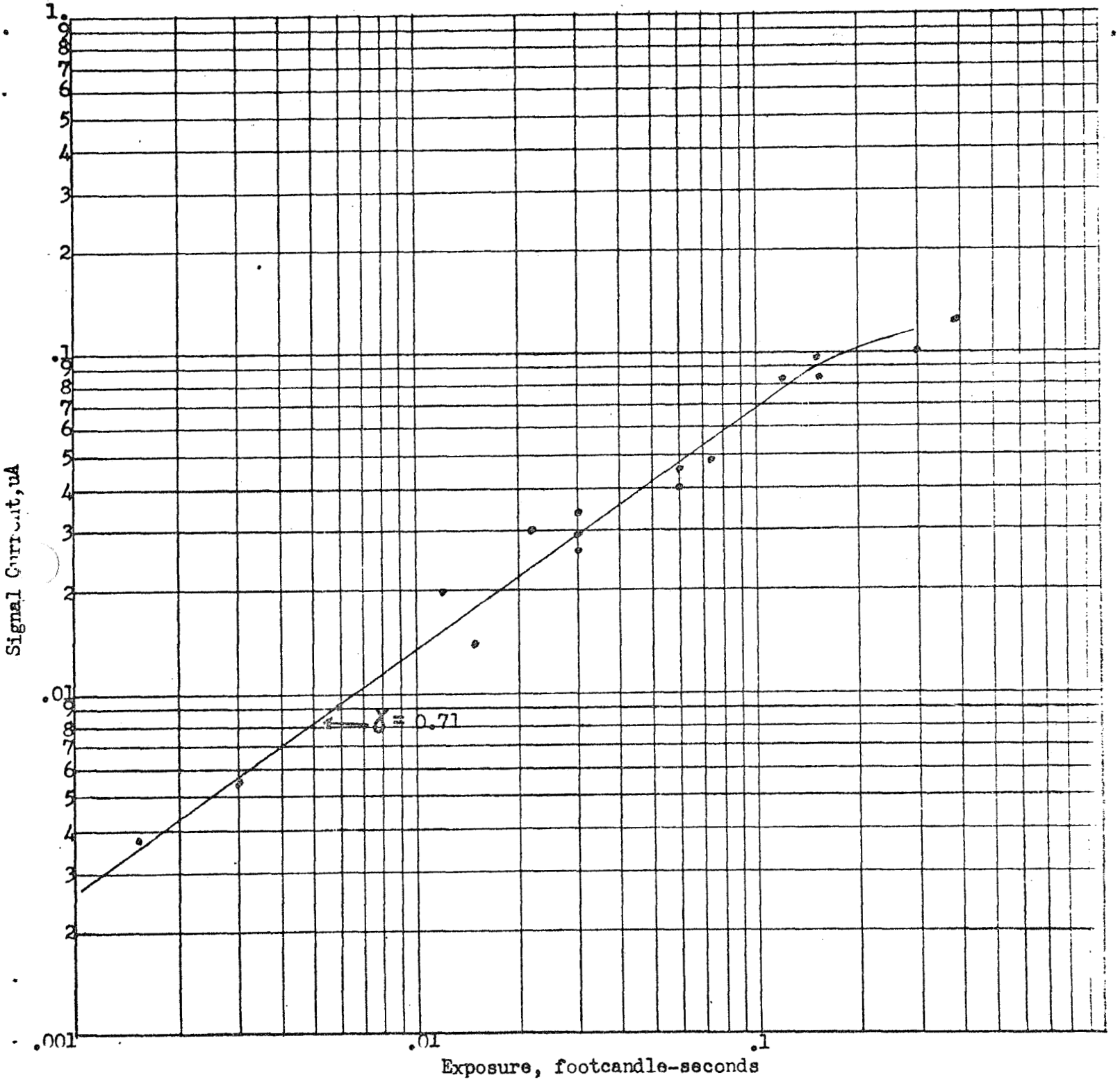

Figure 8. Light Transfer Curve of Tube No. 22 at Slow-Scan Rate. Frame Time = 1 second. Target Voltage = (26± 1)V.

30

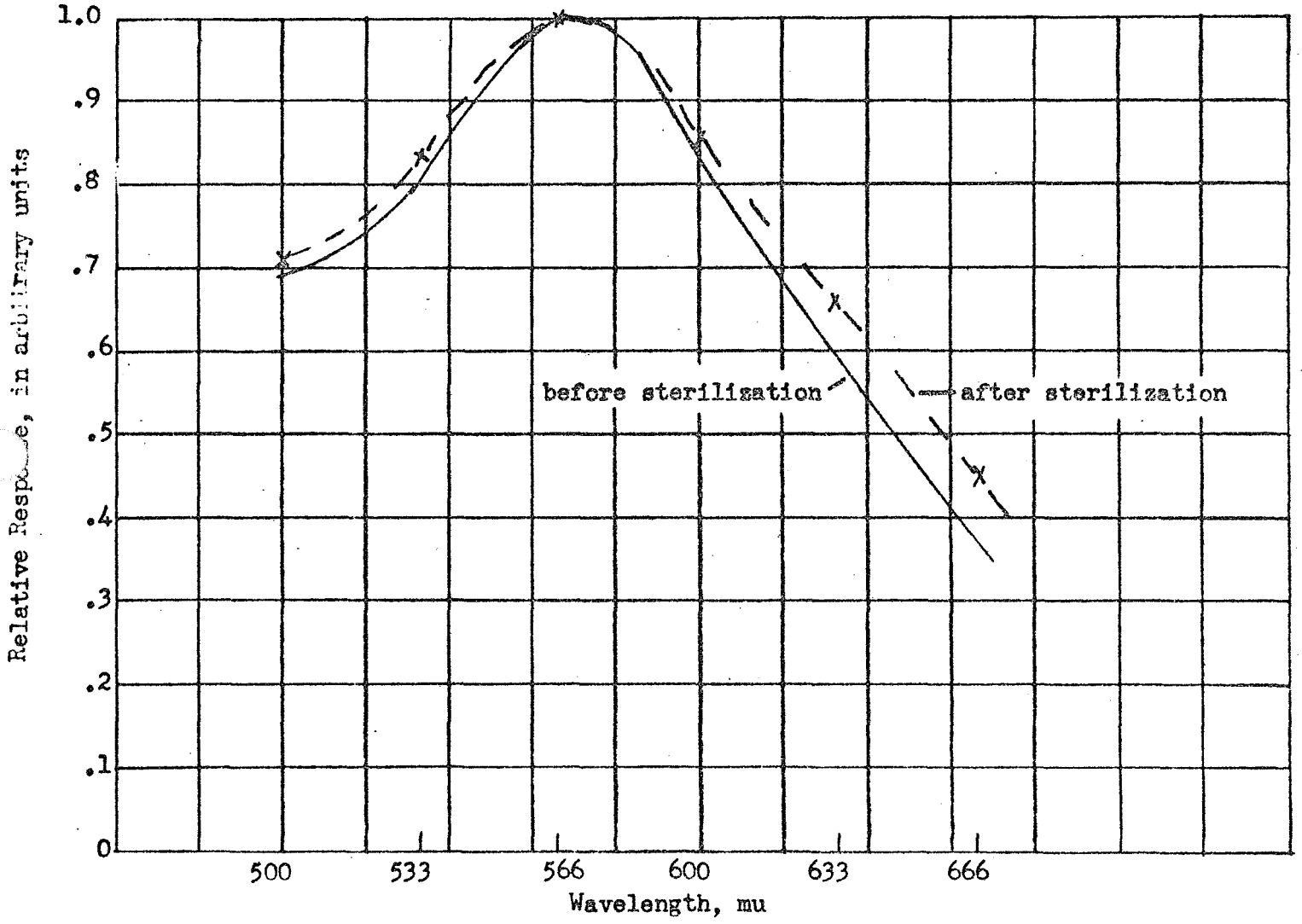

Figure 9. Average Spectral Response (of 11 tubes) Before and After Sterilization. Target Voltage = 20 V.

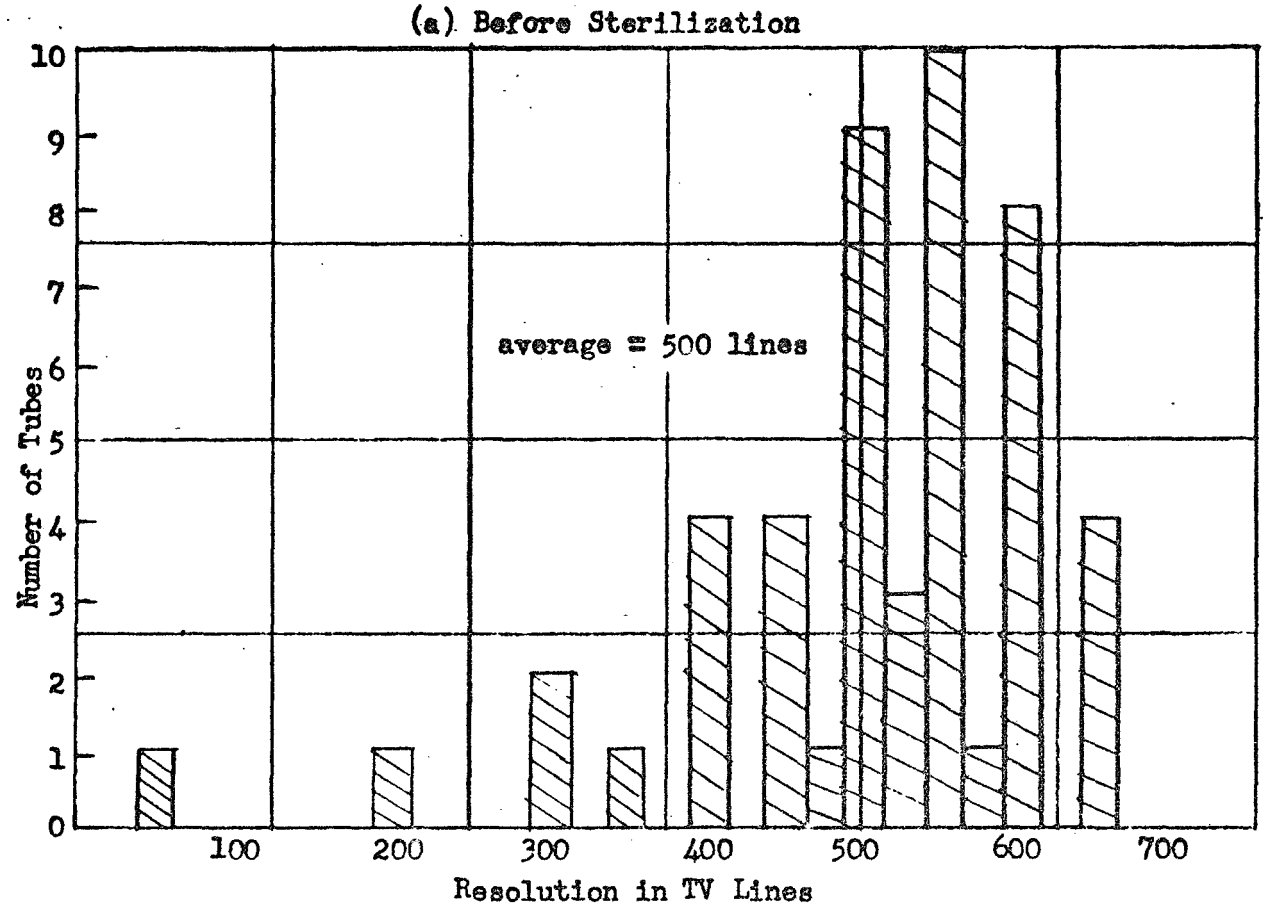

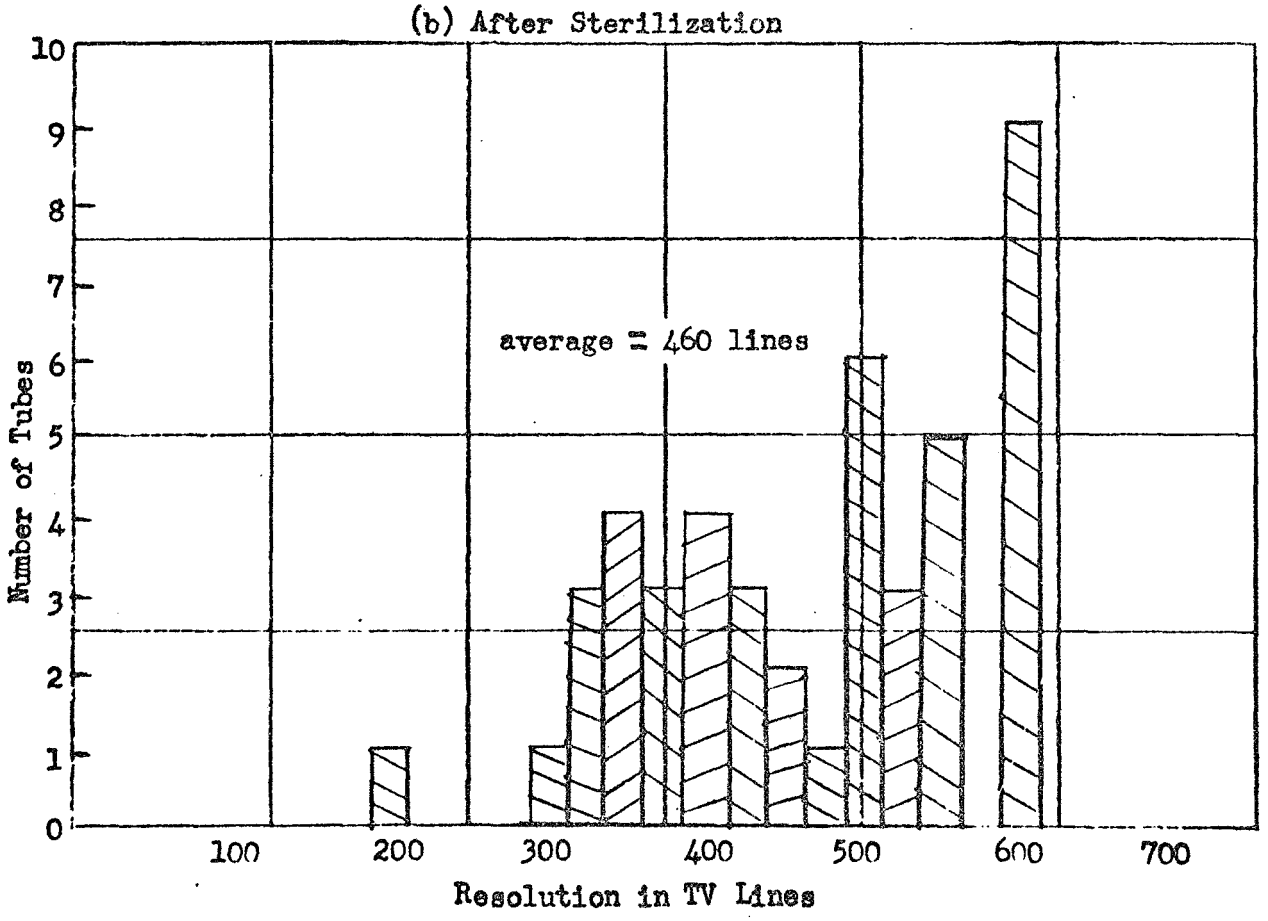

Figure 10. Distribution of Tubes, Before and After Sterilization, in Terms of Resolution. Target Voltage = 20 v., Signal Current = 0.2 ua.

five remained unchanged, and twelve increased during sterilization. It therefore appears that the exposure of the experimental photoconductor to three dry-heat sterilization cycles can be expected to result in a small deterioration of its resolution capability.

F. Grey-scale

In Fig. 11 the distribution of vidicons is shown, before and after sterilization, as to gray-scale rendition. It can be seen that three-quarters of each set of tubes could distinguish the full ten gray-scale steps. The average number of gray-scale steps was essentially the same, 9-1/4 before and 9-1/2 after sterilization.

The gray-scale pattern used for this measurement was limited to ten steps. It is likely that some of the tubes would have been capable of distinguishing a larger number of steps.

G. Erasure

The residual signal, at the third scan after removal of the illumination, was measured on 33 tubes before sterilization and on 15 tubes after sterilization. No significant change was observed. As indicated in Fig. 12, the average residual signal in either case was 80-1/2% of the original signal.

V. SUPPLEMENTARY TEST RESULTS

Some time after the conclusion of Task 1 seven RCA 7735A-type vidicons with ASOS photoconductors were exposed to the dry-heat sterilization tests required by JPL Spec. VOL-50503-ETS outlined in part I of this section.

It was demonstrated that the effect of the revised sterilization procedure was similar to that observed during Task 1, as reported in part IV, using the earlier specifications.

On the average, the seven tubes showed the following changes as a result of the heat treatment: At 20V target voltage, dark current increased by 70% and signal current (for one footcandle faceplate illumination) by 15%. Resolution, gamma, after-image and gray-scale rendition did not show any appreciable change.

The new requirements for the ethylene-oxide decontamination did not appear to be sufficiently different from the earlier specifications to justify additional tests.

VI. SUMMARY

The aim of Task 1 was to develop and demonstrate a photoconductor suitable for slow-scan operation and able to survive the necessary sterilization requirements.

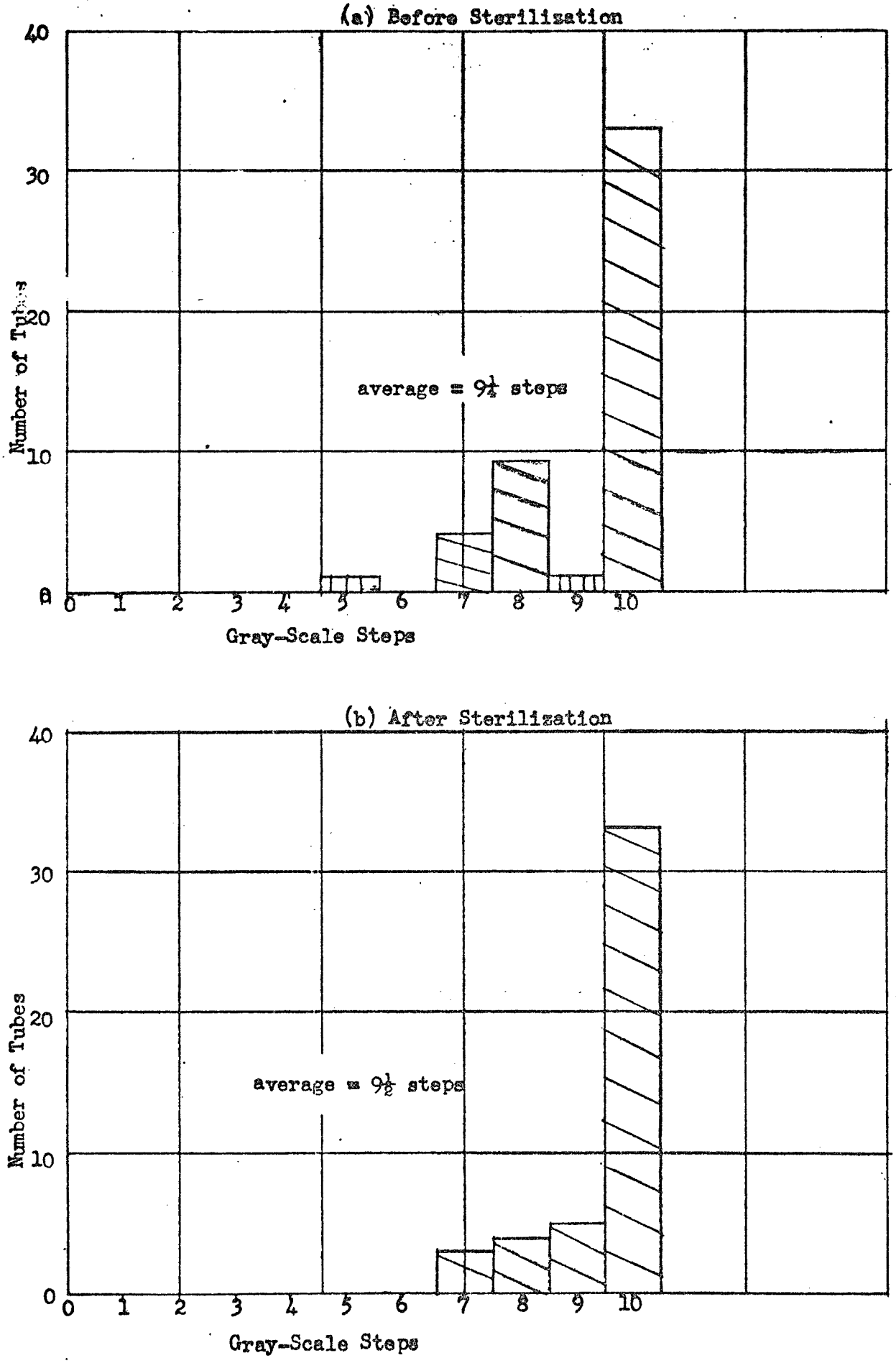

Figure 11. Distribution of Tubes, Before and After Sterilization, in Terms of Gray-Scale Rendition. Target Voltage = 20 v.

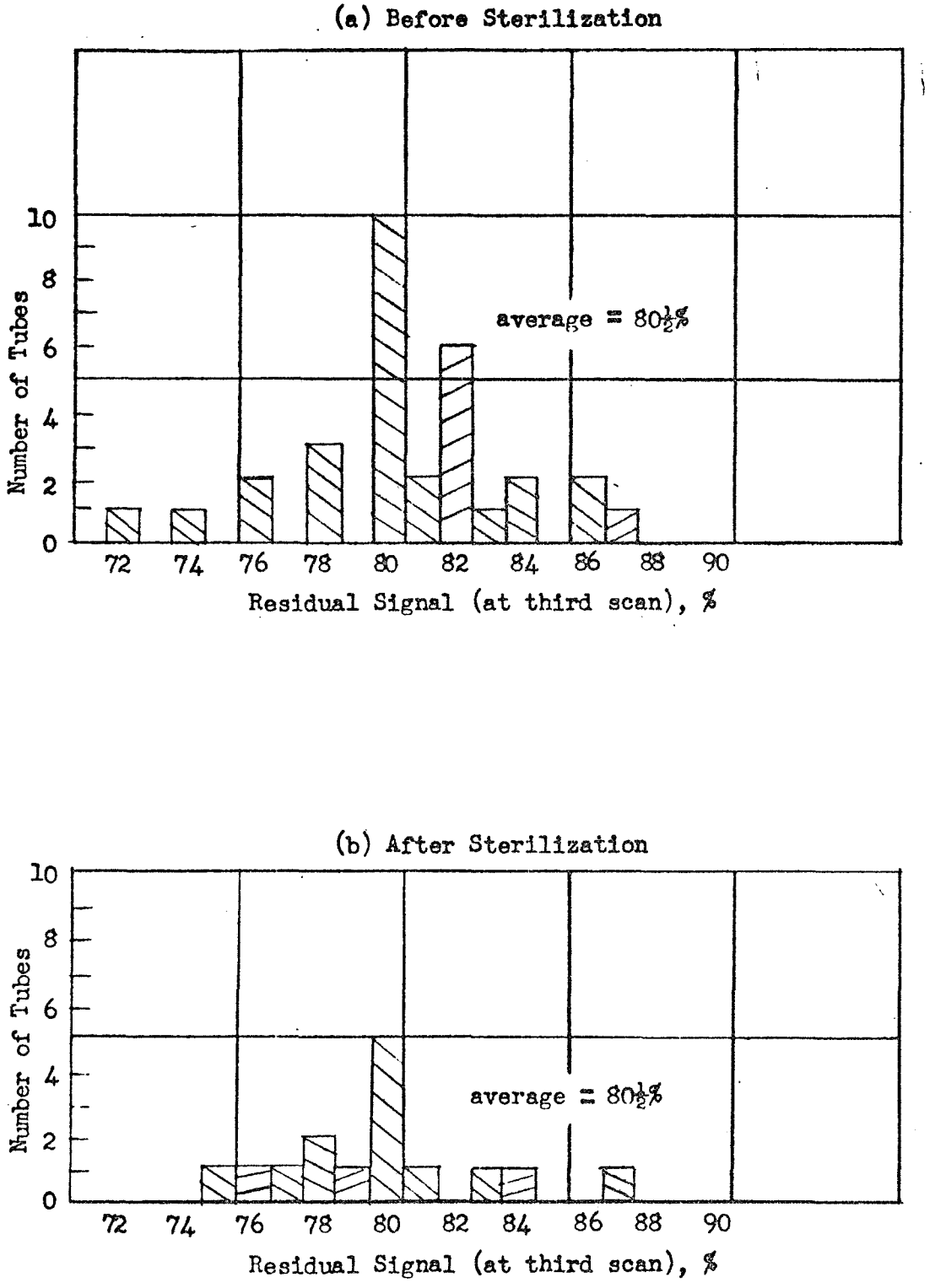

Figure 12. Distribution of Tubes, Before and After Sterilization, in Terms of Residual Signal at Third Scan after Removal of Light. Target Voltage = 20 V., Original Signal Current = 0.2 ua.

Work performed in preparation for this contract already had indicated that an ASOS photosurface with rhodium signal plate on a high-quality quartz substrate is relatively immune to the dry-heat sterilization process.

Fifty-one tubes were made using the ASOS photosurface. Forty-five of these tubes were exposed to the full set of three 36-hour 145°C sterilization bakes. The remaining six tubes were lost, due to various incidental circumstances not connected with the behavior of the photoconductor.

Three tubes were also exposed to the ethylene-oxide decontamination process without any appreciable effect.

The effect of the sterilization bakes consisted primarily of an increase in dark-current and a smaller rise in sensitivity. The data indicates that the dark current can be expected to grow by less than 100% and the sensitivity by about 25%. These changes are well within the range of these quantities as found in different tubes and it is felt that they are highly acceptable. In addition a small deterioration in resolution and, possibly, a minor shift in the spectral response toward longer wavelengths were observed. No systematic changes were found in gamma, gray-scale rendition or lag.

The measurements made during Task 1 were necessarily limited in scope. The chief emphasis was not so much on ascertaining the precise characteristics of the photoconductor under study, as it was on testing its stability under sterilization and decontamination procedures.

Practically no work was done at slow-scan rates, although the photoconductor is intended to be used under such conditions. Both the greater availability of standard-rate equipment and the considerable time-saving in testing at faster rates, made it impractical to do this work at less than sixty fields per second. There is no reason to believe that the effect of the sterilization bakes is any different at slower scan rates than it is at the standard television rate.

As a final presentation of the results obtained on Task 1, Fig. 13 shows the average performance of all the tubes which were tested before and after the complete sterilization procedure. Dark current and signal current (at one-footcandle faceplate illumination) are shown as a function of target voltage. These curves can serve as a guide in predicting the behavior of a photosurface made in the manner of those described in this report.

The photoconductor tests made subsequent to Task 1 proper indicated that the effects of the revised test specifications are similar to those observed in Task 1.

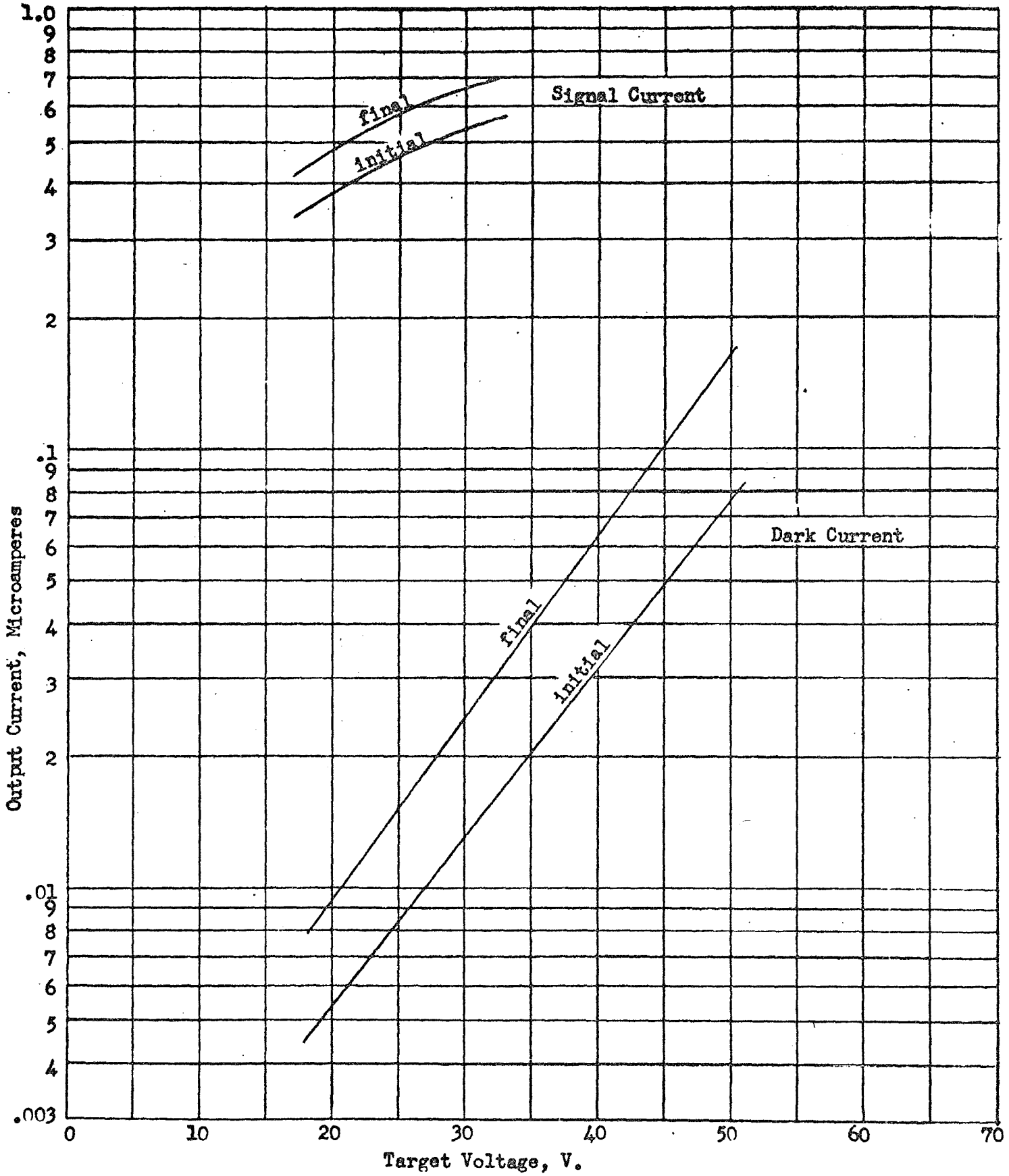

Figure 13. Semilog Plot of Average Dark Current and Average Signal Current at 1.0 ft-cd Faceplate Illumination vs. Target Voltage, Before and After Sterilization. Number of Tubes Included for Dark Current = 45, for Signal Current = 20.

SECTION III

Task 2

I. DESIGN

The camera tube developed under this contract is a ceramic 1" vidicon of extreme ruggedness. In order to meet the required specifications, a novel approach had to be taken for the construction of the tube, its enclosure, and its internal elements.

Four basic requirements guided the design:

(a) All structural features had to be able to withstand the required sterilization and environmental tests.
(b) The cathode surface and photoconductor could not be exposed to brazing temperatures.
(c) The tube should have no magnetic materials except in the bottom section.
(d) Only a limited time was available for designing and procuring the components, jigs and fixtures needed for starting tube construction.

In order to minimize the power requirements and weight of the vidicon, the original design called for an electrostatically focused and deflected tube. Later it was found that elimination of the electrostatic deflection system (the "deflectron") would result in a savings in weight, in greater picture uniformity and in improvements in the tube fabrication process. In addition, a magnetic deflection coil became available which was not only very light, but also able to withstand the required environmental conditions. The power requirement of this coil did not appear to be much greater than that of the deflectron. The tube design was therefore changed to an electrostatically focused and magnetically deflected ("hybrid") version. This final design also incorporated several improvements in construction technique which resulted from experience gained with the earlier design.

A. Original Design

The design achieved during Phase A of this contract is indicated in Fig. 14, while Fig. 15 depicts an actual, unpotted tube.

As a means of ruggedization, the entire structure was designed to consist of brazed ceramic and metal components. The only exception is the quartz faceplate which is attached by an indium seal. Strength tests on faceplate subassemblies showed that this sealing method is satisfactory.

External View (Without Potting or Shielding)

Cross Sectional View

All dimensions are in inches

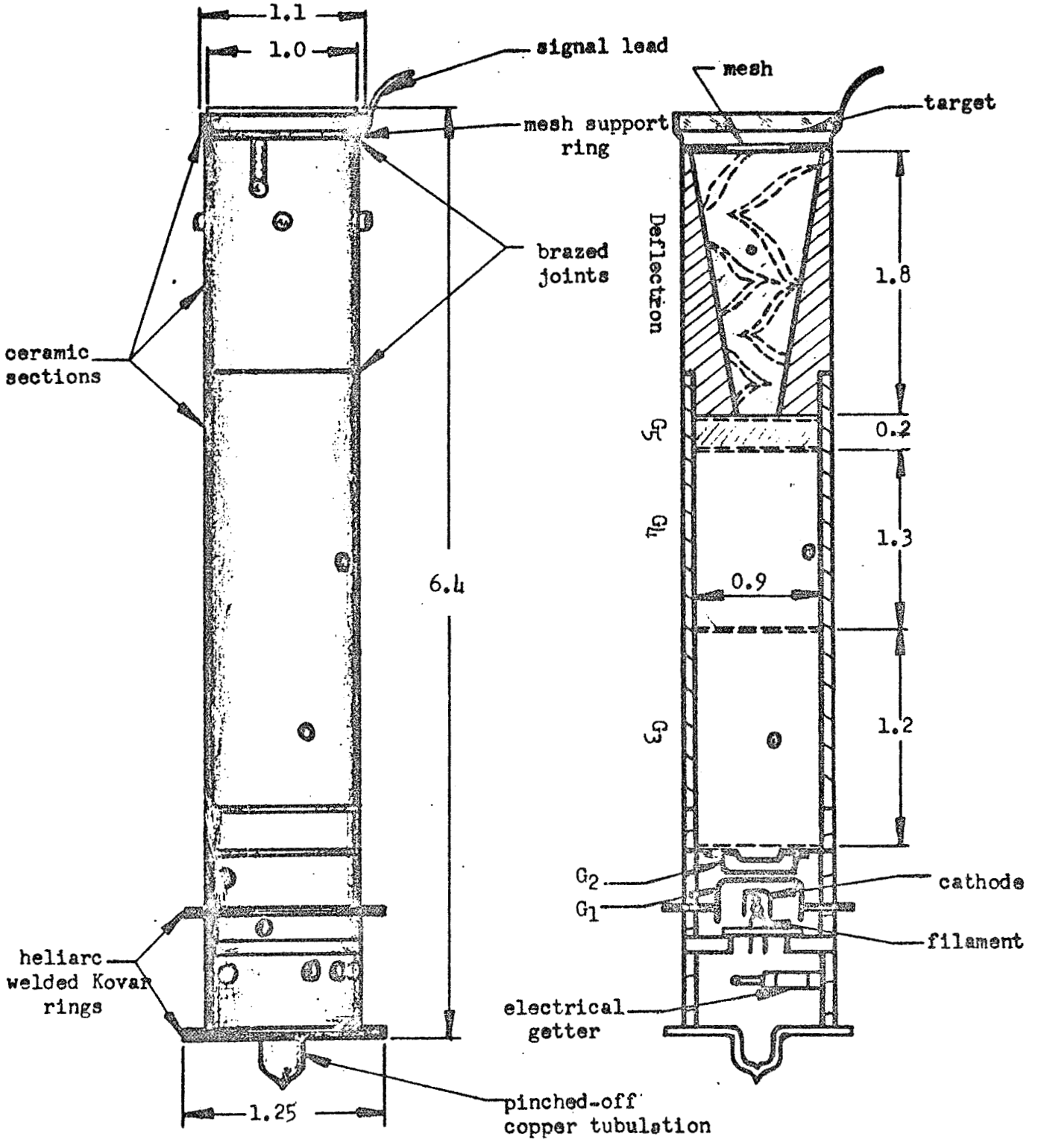

Fig. 14. External and Cross Sectional View of Complete (Unpotted) Ceramic Vidicon of Original Design

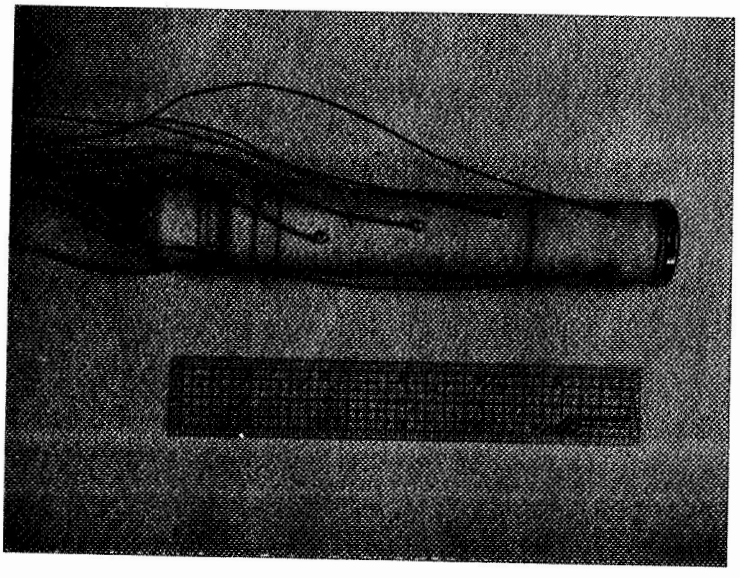

Fig. 15. Ceramic Vidicon - Original Design

The lens and deflectron electrodes originally were made of evaporated copper, sometimes covered with electroplated gold. Such electrodes were found capable of withstanding the brazing operations. Other internal electrodes consist of preformed metal parts.

In order to provide electrical connections to the inside of the tube, molybdenum pins were designed which are brazed into the ceramic tube wall. Leads are attached to the outside end of each pin by soldering or welding. Several electrical connections are made via the brazed joints which hold the various tube components together.

Brazing jigs were developed which ensure good alignment of the various tube components as well as reliable brazed joints. Similarly, jigs were designed for holding and cooling the kovar flanges during the heliarc welding operations, and optimum welding parameters were determined.

Work done prior to this contract indicated that mechanically tensioned (rather than fired) nickel mesh has the highest resistance to damage under exposure of shock of all available mesh materials. Further tests, performed under this contract, reaffirmed this fact. The mesh design, therefore, is based on 1000-line (per inch) nickel mesh, mechanically tensioned on a flat nichrome ring which is screw mounted to a support ring. The latter is a molybdenum disk which is part of the stacked ceramic-metal tube body (see Fig. 14).

The three-element electrostatic electron lens and the five-cycle deflectron were designed according to standard procedures, with particular emphasis being given to minimizing lens and deflection aberrations. The deflectron was made a part of the third lens electrode (G5). Therefore, the center potential of the deflectron should be at the same voltage as G5.

The deflectron portion of the tube was made as a separate ceramic section which forms part of the tube envelope.

It was decided early in the contract that it would be desirable to use the low-power (0.6 watt) "dark heater" gun which had been previously developed by RCA. However, a method had to be found of ruggedizing its construction while maintaining accurate alignment and spacing of its parts. The resultant design is shown in Fig. 16.

Standard parts were used in constructing the gun, but were mounted in a novel fashion. The G2 electrode, which consisted of several sections, was first welded together with accurate alignment (checked by microscope) of its upper (defining) and lower apertures. The G2 and G1 electrodes were then brazed to a ceramic spacer and to the G2 support ring, thereby becoming an integral part of the tube structure. Good alignment was achieved by using a brazing jig which positions the gun electrodes in their proper location relative to the axis of the tube.

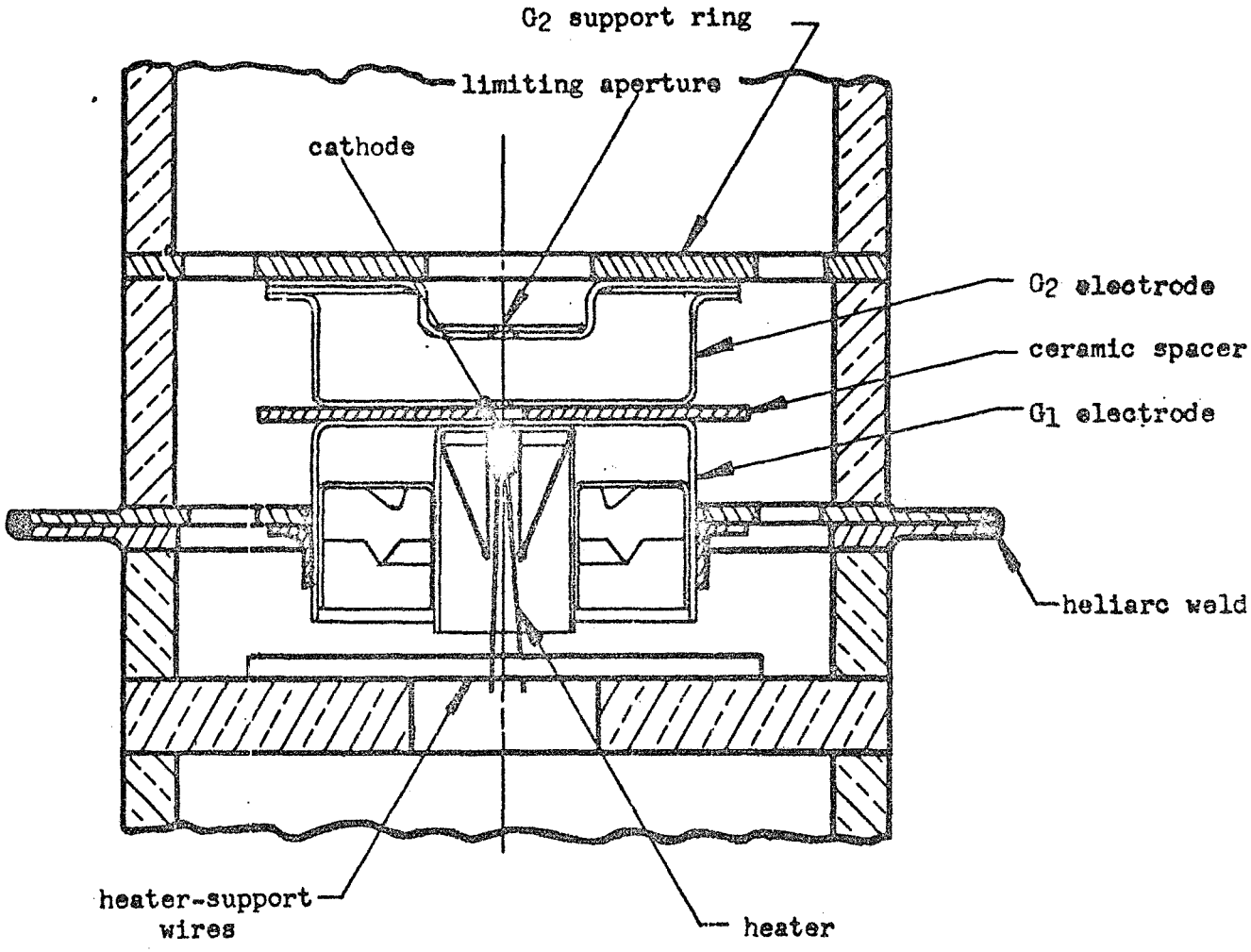

Fig. 16. Cross Sectional View of Gun Section of Ceramic Vidicon

92

In a subsequent operation, the cathode subassembly was mounted inside the G1 cup. A precision jig was designed to ensure accurate spacing between the cathode surface and the G1 electrode.

The lower section of the tube (less copper tubulation) was then attached by heliarc weld. It provided two kovar wires to which the heater legs were attached after the heater had been slipped into the cathode sleeve.

The getters chosen for this application were exothermic units flashed by current fed into the tube through the wall pins. It was found that the ceramic tube walls are sufficiently translucent to permit visual monitoring of the flashing operation.

The tube was evacuated through a copper tubulation on a kovar header which was attached by a heliarc weld. After the proper pump-down, bake and cathode activation, the tube was removed from the pump by means of a pinch-off at the copper tubulation.

B. Final Design

1. General Discussion - The experience gained during Phase A of this contract was used during Phase B to redesign the ceramic vidicon and to make several changes in the fabrication technique. Fig. 17 is a sketch of the final version of the tube showing some of the features of the latest design, and Fig. 18 is a photograph of a tube.

The decision was made to employ electrostatic focus and magnetic deflection on the basis of several considerations. The advantages of this hybrid design, over the earlier all-electrostatic version, are:

(a) greater uniformity of beam landing over the whole raster;
(b) the elimination of the need for a deflectron; and
(c) a shortening of the tube length by about 16%.

The drawbacks of the hybrid vidicon are the need for magnetic deflection coils and a small increase in deflection-power requirements.

Elimination of the conically-shaped deflectron is desirable because:

(a) The production of a precise electrode pattern is difficult.
(b) The form on which the deflectron is deposited adds weight to the tube.
(c) Accurate alignment of the electron gun is easier when the inside wall of the tube consists of a straight cylinder.

As can be seen in Fig. 18, the ceramic portion of the tube body consists of a single section without any molybdenum-to-ceramic seals. Since

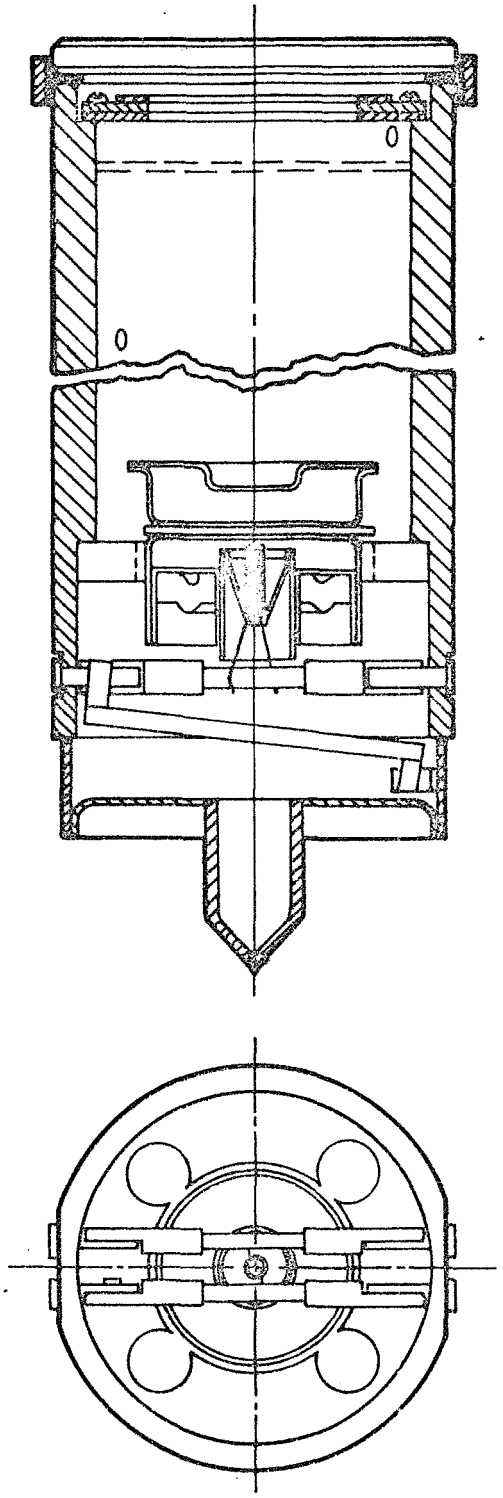

Fig. 17. Cross Section, Final Design

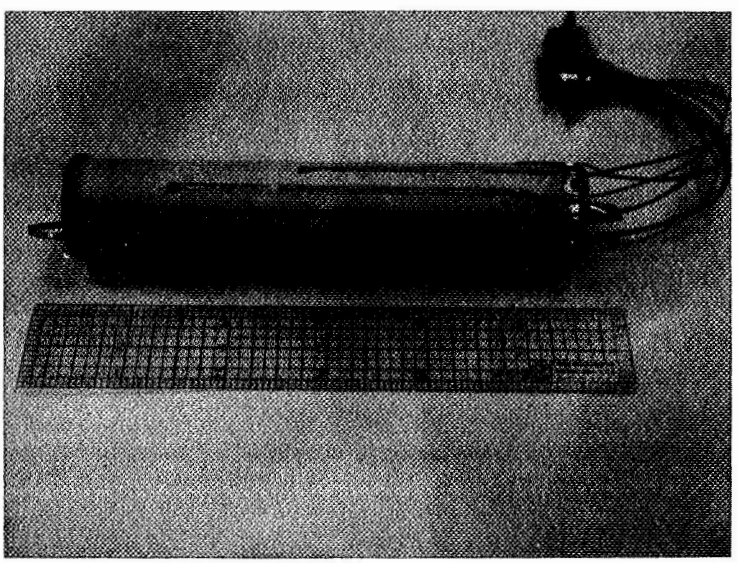

Fig. 18. Ceramic Vidicon, Final Design

the lens section of the tube is of uniform diameter and free of brazed joints, it can be ground to a high degree of accuracy in addition to being stronger than the corresponding part of the original design and less likely to have vacuum leaks.

The hybrid design permits the use of a brazing jig which aligns the gun components relative to the inner wall of the tube, rather than referring to the outer surface. As a result, higher precision can be expected in the positioning of the electron gun.

The mass of the tube, including potting and shielding, was reduced considerably in the newer design. The two heliarc-welded kovar seals of relatively large diameter used in the original version were replaced by a single seal of smaller diameter. Also, the heads of the molybdenum contact pins were recessed into the tube wall. As a result of these changes, the thickness of potting compound and the diameter of the magnetic shield could be reduced. As mentioned before, weight is saved by the elimination of the deflectron. The mass of the magnetic-deflection coils is only about four grams, and since the coils are imbedded in the potting compound, they displace an amount of potting compound of about equal mass. The reduction in tube mass and in thickness of the potting compound causes an increase in the resonance frequency of the potted tube, which should decrease the acceleration experienced by the tube for a given shock pulse applied to the shield.

An approximate comparison of the mass of the tube and of its potting and shielding, for the original and the hybrid versions, is as follows:

	Original Design	Hybrid Design
Mass of vidicon	150	105 g
Mass of potting, shielding and leads	170	95
Total Mass	320 g	200 g

The deflection coils consist of photo-etched copper patterns deposited on a thin dielectric sheet. Fig. 19 is a close-up of two of the four spiral coils which make up a complete "yoke." Each coil contains forty turns. The copper layer is about 0.002" thick and is deposited on 0.005" fiber glass. Fig. 20a shows a deflection yoke before it is rolled into the proper cylindrical shape and Fig. 20b a yoke ready to be slipped onto a tube. In Fig. 21 a ceramic vidicon is shown with its photo-etched yoke in place.

Although yokes of this type consume about two watts, they could be redesigned to require less than half as much power. An electrostatic deflection system, such as used in the original design, requires about one-half watt.

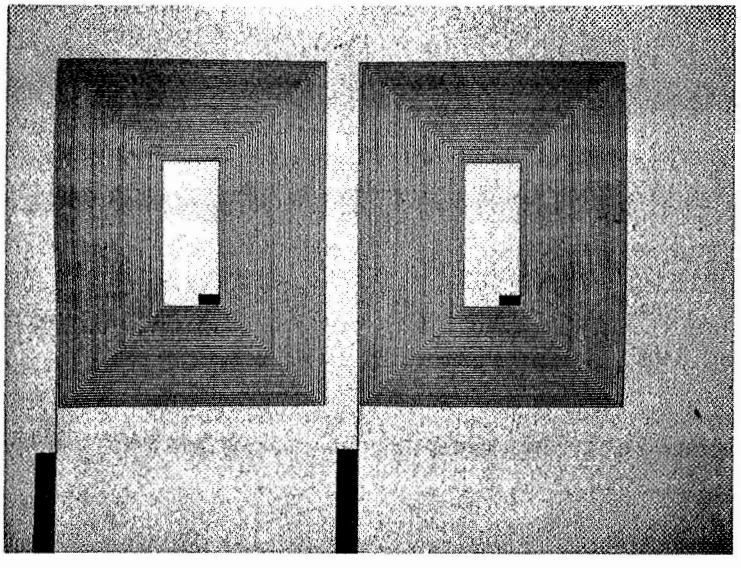

Fig. 19. Close-up of Deflection Coil

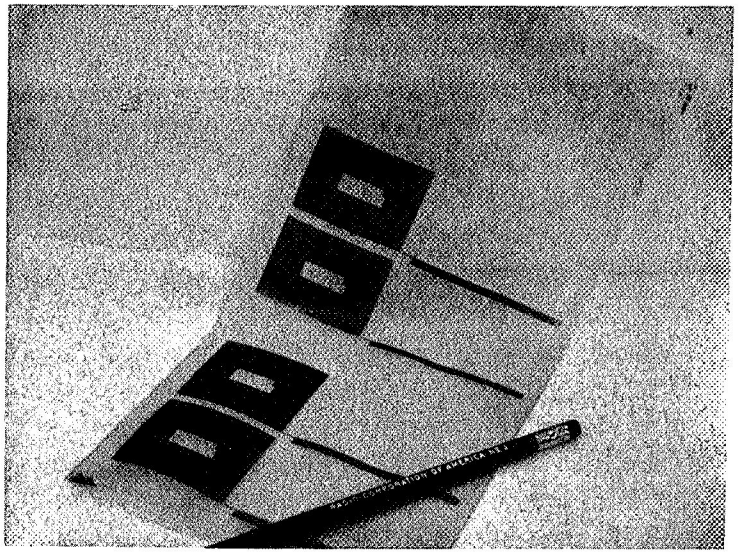

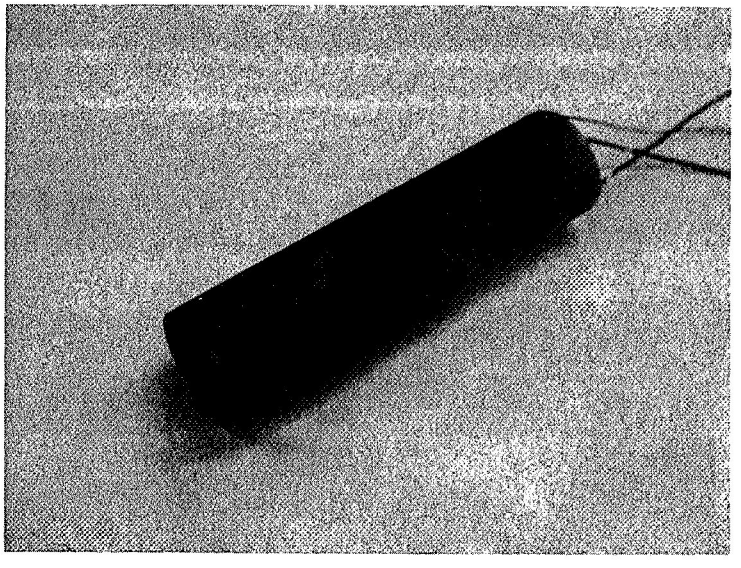

Fig. 20. Photo-etched Deflection Yoke

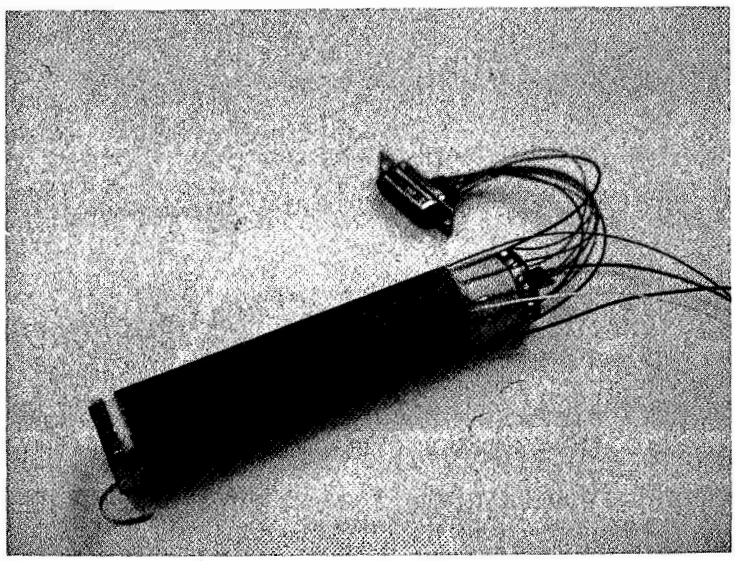

Fig. 21. Ceramic Vidicon With Deflection Yoke

The gun structure of the hybrid tube is supported at the G1 cup by a ceramic ring which is brazed to a shoulder on the inside of the tube. The construction of the electron gun itself is similar to that of the original tube. The redesigned mounting arrangement is stronger than the earlier version, particularly as far as transverse shocks are concerned.

The mesh is screwed onto a molybdenum ring which is brazed to a shoulder in the tube body at the end of the lens section. The mesh and its support ring are otherwise of the same construction as used previously.

The faceplate is attached by means of an indium seal in the same manner as that of the original design.

Several changes were made in the lower end of the tube. As shown in Fig. 17, the heavy kovar wires, which support the heater legs, were redesigned. They are attached to the four molybdenum pins by means of stainless steel connectors, instead of being brazed to a ceramic support as done originally. The internal connections between the cathode, G1 and G2 electrodes and their respective molybdenum pins are made with nichrome ribbons. The getter was changed from the original type to an endothermic unit with greater barium emission.

The kovar bottom section is brazed onto the end surface of the ceramic cylinder by means of a butt joint. The kovar header, with attached copper tubulation, is fastened to the bottom section by a heliarc weld.

The finished tube is potted in a specific formulation of a polyurethane Type PR1538, Products Research Co. The magnetic shield consists of 0.025" thick Moly Permalloy, which had been suggested for this purpose by JPL. Shock tests made on 0.020" thick samples of Moly Permalloy indicated that they lose less than 1% shielding efficiency when exposed to five shocks of 3000 g amplitude and 0.45 millisecond duration in each of six orthogonal directions.

The appearance of a potted tube is shown in Fig. 22.

2. Design of Electron Lens - The electrostatic lens chosen for this tube is of the unipotential, or "einzel", lens type consisting of three coaxial cylinders. The two outside electrodes are at approximately the same positive potential with respect to the intermediate cylinder. Such lenses were shown by Gundert* to give a minimum of spherical aberration and have been used successfully in several electrostatically focused camera tubes.

*E. Gundert, "Aperture Defect of Electrostatic Electron Lenses," Die Telefunkenroehre, No. 19-20, pp. 61-98, March 1941

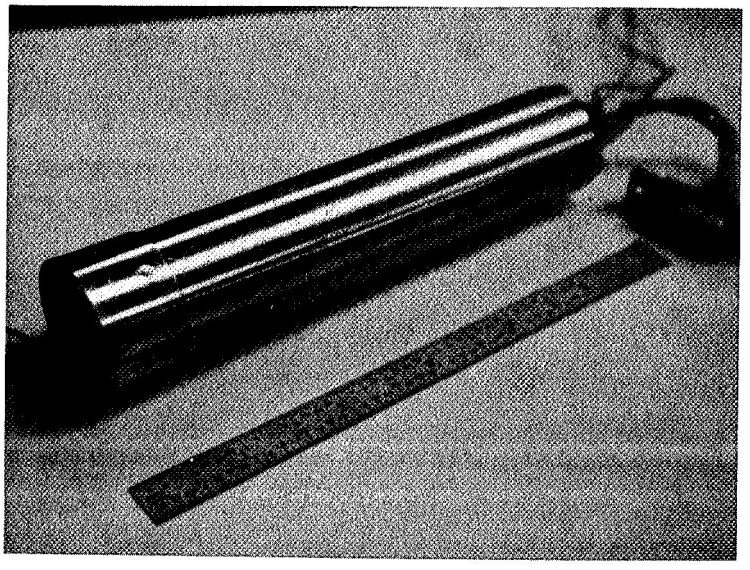

Fig. 22. Ceramic Vidicon in Magnetic Shield

The design of the lens used in the ceramic vidicon was based on a set of relations between pertinent lens parameters derived by Dr. E. G. Ramberg of RCA Laboratories. These equations were applied to several sets of trial values for the lens dimensions and used to give estimates of the spherical aberration to be expected for each case. Combining this value with the spot size obtained by geometric considerations for an aberration-free lens, results in a prediction of the beam diameter expected at the target. The considerations involved in this procedure are described more completely below.

We will approximate the electro-optical system by a thin lens located at the center of the central electrode. Consider an electron incident on this lens at a distance r from the axis and parallel to it. An ideal lens would cause this electron to intersect the axis at the Gaussian focal plane. Instead, the electron transverses the Gaussian plane at a distance Δr from the axis, where Δr is approximately proportional to r^3. We can therefore define a spherical aberration constant S by the relationship

$$\Delta r = S r^3.$$

If the electron paths make small angles α with the axis, then

$$\tan \alpha = r/u \doteq \alpha \text{ (with } \alpha \text{ in radians)}$$

where $= u$ object distance (see sketch)

and $\Delta r = S u^3 \alpha^3$

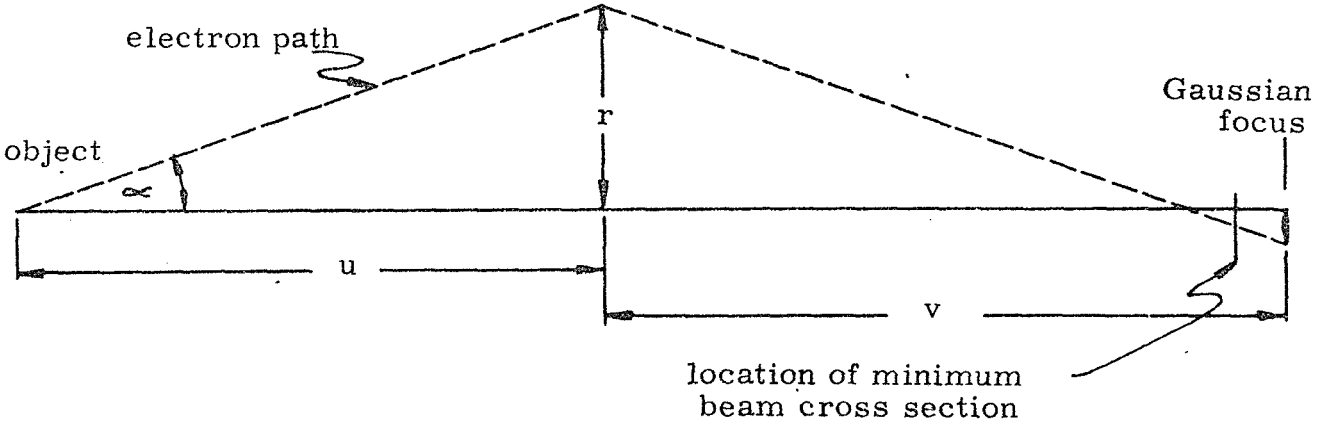

The minimum cross section of the beam occurs at a plane ahead of the Gaussian focus. If the diameter of the beam is $2\Delta r$ at the Gaussian plane, then the minimum diameter is about $(M + 1)\Delta r/2$, where M is the lens magnification. The aberration of the electron image, at the plane of minimum beam cross section, then becomes

$$\Delta d_i = (M + 1)\Delta r/2 = (M + 1)S\alpha^3\alpha^3/2.$$

The aberration constant S is a fairly complex function of the length l_2 of the central electrode and of the lens diameter D. For l_2/D greater than unity, S is, to a first approximation, inversely proportional to D^2. Therefore, it is desirable to make D large. However, this requires a proportionately longer tube. In addition, the requirement of this contract to limit the tube diameter to 1", as well as considerations of the strength of the tube envelope, set an upper limit on the value of D.

The choice of the object distance u depends on several considerations. The above equation for Δd_i suggests that u should be as small as possible. However, for a given value of the image distance v, a decrease in u results in a larger geometric magnification M (= v/u) of the electron image. The value of v cannot be reduced below a value determined by the requirements of a practical deflection yoke. The deflection region has to have sufficient length to permit the use of photo-etched coils of reasonable dimensions and power consumption. The yoke must be situated within a span extending from the middle of the center electrode of the lens to within a distance D of the target.

With the lengths l_2 and v thus fairly well prescribed, u can only vary in a rather limited range.

The magnitude of α, the half-angle of the beam cone issuing from the electron gun, is determined by the geometry of the gun and the performance of the thermionic cathode. Its value, for the case of slow-scan operation, was assumed to be 1^o. No serious consideration was given to limiting α to a smaller value, by means of an auxiliary beam stop, because of the technical complications involved in mounting and accurately aligning the necessary aperture and because it was doubtful whether sufficiently good cathode emission would be obtained to permit such a reduction in beam angle.

The following dimensions represented a suitable compromise of considerations concerning lens performance, tube dimensions and structural requirements:

Total length of lens, L = 4.30"
Length of central electrode, l_2 = 1.12"
Lens diameter, D = 0.80"
Lens magnification, M = 1.10

The object distance then is

$$M = L/(M + 1) = 4.30/2.10 = 2.04"$$

and the focal length of the lens

$$f = uM/(M + 1) = 2.04 \times 1.1/2.1 = 1.07".$$

Computations indicated that for this lens the ratio of the potential of the outside electrodes to that of the central electrode is:

$$V_2/V_1 = 0.13$$

and the spherical aberration constant

$$S = 6.17.$$

The spherical aberration then is

$$\Delta d_i = (M + 1) S u^3 \alpha^3/2$$
$$= 2.1 \times 6.17 \times (2.04\pi/180)^3/2$$
$$= 2.92 \times 10^{-4}".$$

The diameter d_e of the limiting aperture in the G2 electrode is about $1.5 \times 10^{-3}"$. The spot size of an aberration-free electron beam at the target due to the lens magnification is therefore

$$M \times d_1 = 1.1 \times 1.5 \times 10^{-3} = 1.65 \times 10^{-3}"$$

and the total beam diameter, including spherical aberration,

$$d = M \times d_1 + \Delta d_i = (1.65 + 0.29) \times 10^{-3} = 1.94 \times 10^{-3}".$$

This estimate of spot size presumes an electron beam of uniform current density and a well defined edge. Actually, the beam does not possess such a square profile but has a relatively narrow central peak and a gradual decrease toward the edge. The computed beam diameter only represents a working figure which may approximate the diameter of the beam at which its current density is half of the maximum value. An actual beam will not give full signal for an object of dimension d, while it may resolve an object of considerably smaller dimension.

The dimensions of the electrodes used in the ceramic vidicon are indicated in Fig. 23.

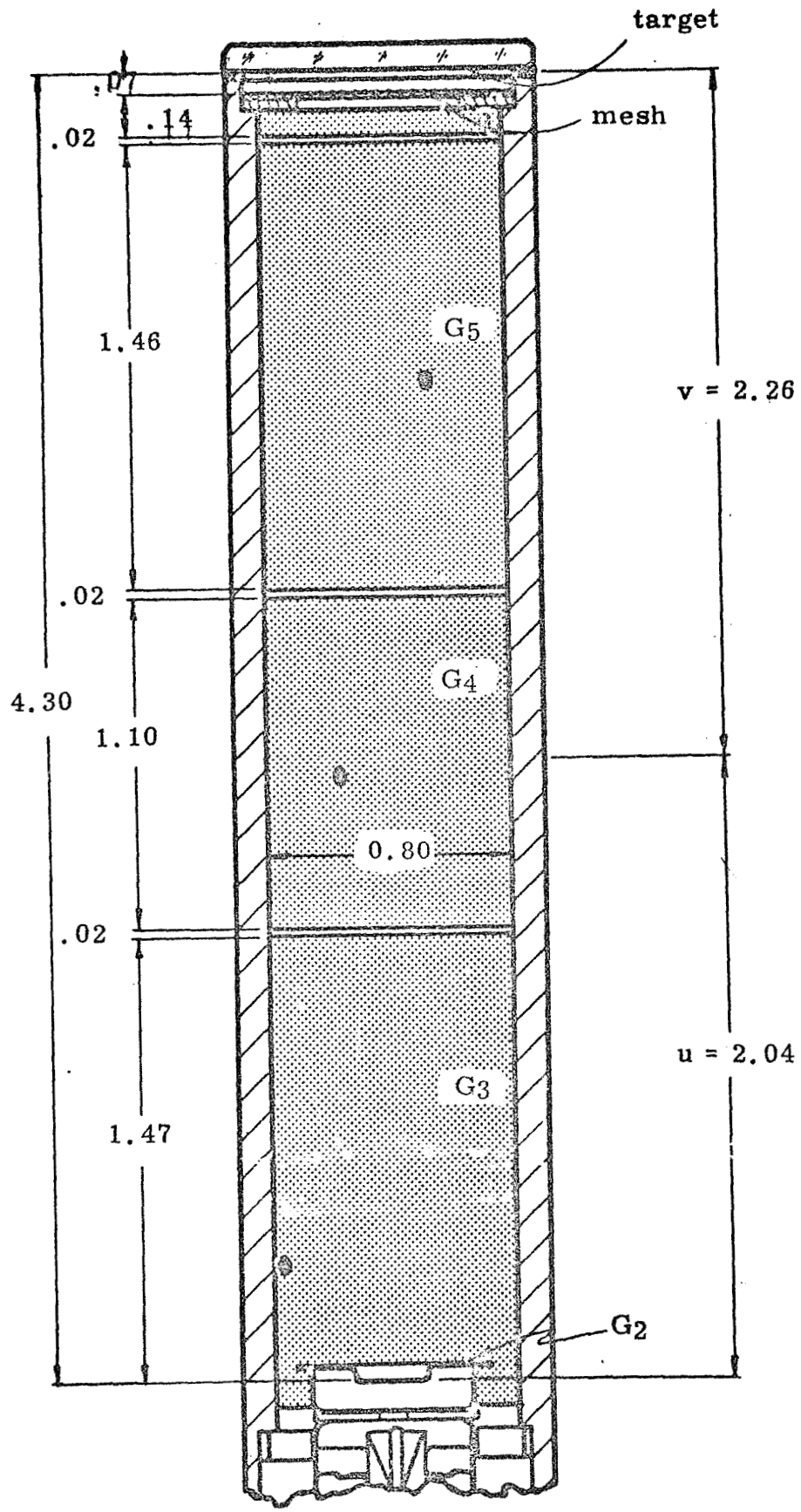

Fig. 23. Electrode Dimensions

3. Tube Structure and Parts - A complete listing of the parts and drawings used in fabricating the ceramic vidicon developed on this project is shown in the Appendix.

II. TUBE FABRICATION

The various components of a complete ceramic vidicon are assembled according to the program outlined in Fig. 24. This procedure will now be described in greater detail.

A. Brazed Tube Body

Flat portions are ground at the feedthrough pin holes on the external surface of the ceramic tube envelope in order that the pin heads will be recessed. The tube envelope is then metalized at all areas where brazed joints will later be formed and at the inside surface where the einzel lens is located. Metalized stripes are applied to the outside surface to provide connections, along the tube body, from all feed-through pins. The lens coating is applied as a continuous layer. Separations between the three lens segments are then cut, by grinding with a diamond wheel, before the metalizing coating is fired. After firing, the metalized areas are plated with nickel.

The G_1 and G_2 cups are made of molybdenum, or by brazing flat molybdenum bottom sections onto stainless steel cylinders. The beam disk assembly is then carefully aligned on the G_2 cup and welded to it. A nichrome ribbon is welded to the G_2 cup for electrical connection. All parts which are to be brazed to the ceramic tube envelope are then nickel plated.

Two brazing operations are performed for finishing the tube body. In the first, the kovar bottom ring and molybdenum connector pins for the mesh, lens electrodes, G_2 and cathode are attached. Nickel tabs, for the internal connections, are brazed onto the G_2 and cathode pins.

In the second braze, the mesh support ring, the ceramic G_1 support ring, the G_1 and G_2 cups, the ceramic G_1-G_2 spacer, the G_1 pin and the four heater pins are attached. A precision jig (Fig. 25) is used to insure accurate alignment of the gun components with the axis of the tube body. An oxide coating on the jig prevents tube components from being brazed to the jig material.

The front end surface of the tube envelope is finally polished smooth in preparation for the faceplate which is sealed on at a later stage.

B. Completion of Tube Assembly

After the tube body has been checked for leaks, the remaining internal components are mounted and the faceplate and tubulation are attached.

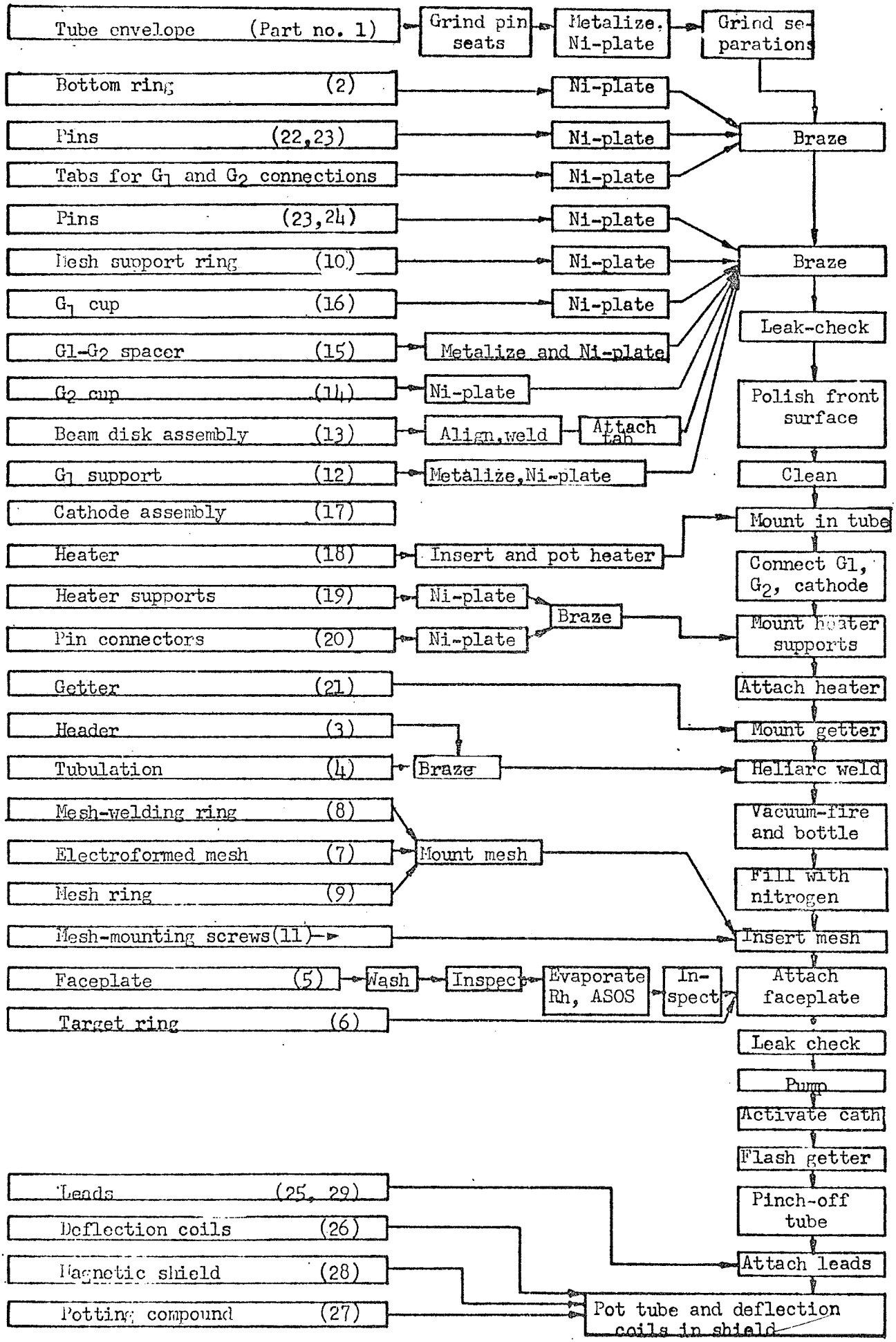

Fig. 24 Flow Chart

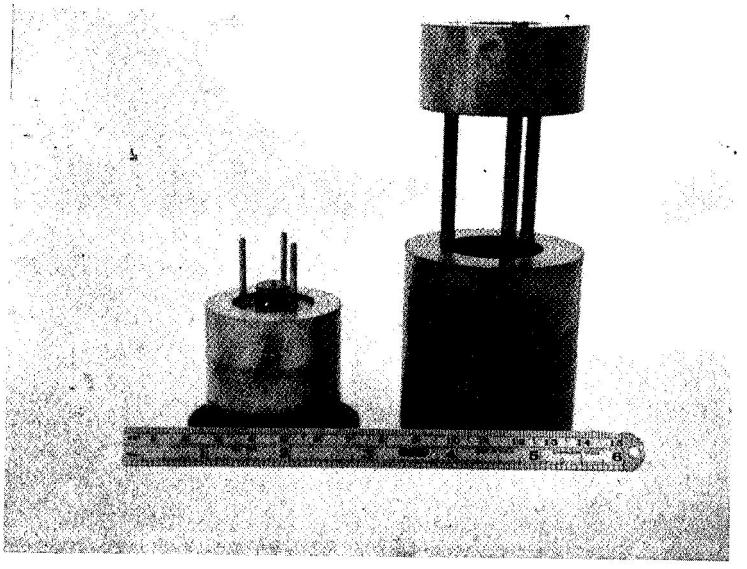

Fig. 25. Brazing Jig

The heater is potted into the cathode assembly in a loose alumina powder capped with a refractory cement (Fig. 26). After the heater has been introduced into the cathode sleeve, the alumina powder (Linde A-1475) is poured in slowly. The cathode assembly is vibrated during this operation in order to assist the flow of the alumina powder and thus prevent the formation of voids. The powder is held in the cathode cup by means of a layer of Sauereisen cement. This cement is not added, however, until after the cathode assembly has been mounted in the tube and the heater legs have been attached to their supports. This procedure preserves the flexibility of the heater legs as needed until they are properly positioned in the tube.

The cathode assembly is introduced into the G_1 cup with a specially designed jig (Fig. 27) which utilizes a micrometer motion to position the cathode surface at the proper distance (0.018") from the G_1 electrode. Accurate spacing is maintained by the use of built-in welding electrodes which permit the cathode assembly to be resistance-welded in place while being held in the mounting jig. Resistance welds are also used to connect the cathode and the G_1 and G_2 electrodes to their respective molybdenum feedthrough pins.

The kovar rods which act as heater supports and the connectors used to attach them to the feedthrough pins are nickel plated and then brazed with a pin connector at each end of each heater support. These units are then resistance-welded to the four corresponding feedthrough pins as indicated on Fig. 17.

After all internal electrode connections have been made and the Sauereisen cement has been applied to the heater, the getter is connected between one of the four heater pins and the kovar bottom ring. The getter is an endothermic unit (i.e. it does not generate a net amount of heat while being flashed, so that full control is maintained during the operation) and consists of two 1" long iron channels, connected in parallel, and filled with the getter charge. It is mounted in such an orientation that the barium evaporation is directed away from the electron gun, but not into the copper tubulation.

The kovar header, with brazed-on copper tubulation, is heliarc-welded onto the bottom ring. The tube is held in a copper fixture which makes good thermal contact to the bottom ring so that the ceramic-to-kovar seal experiences very little heating during the welding process.

Before the mesh and faceplate are mounted on the tube, the latter is vacuum-baked inside a hard-glass bottle in order to degas its internal surfaces. It is held, for at least four hours, at 425°C which is a higher temperature than permissible once the mesh, photosurface and indium seal have been added. After this bake, the tube is exposed

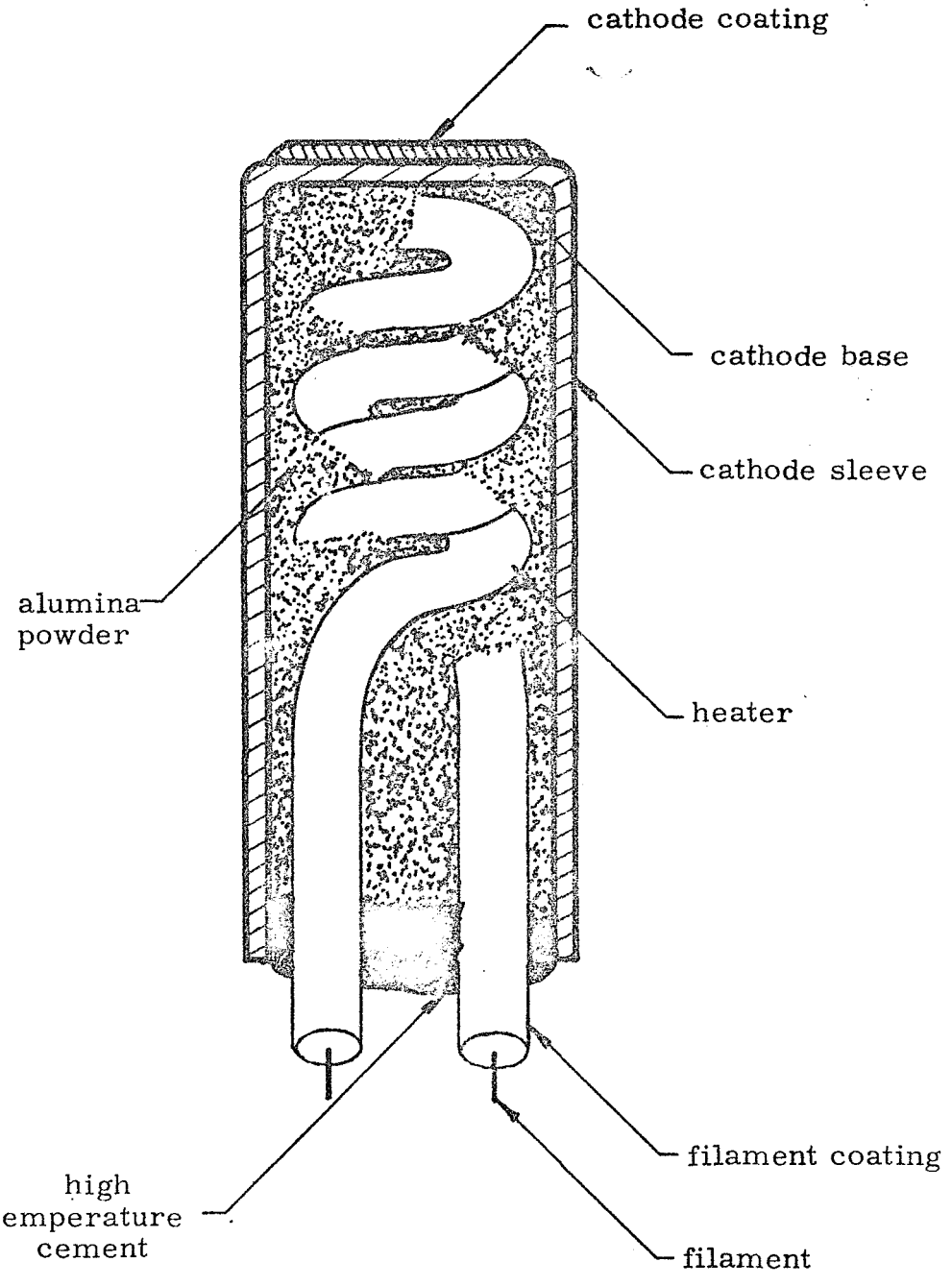

Fig. 26. Cross Section of Potted Heater

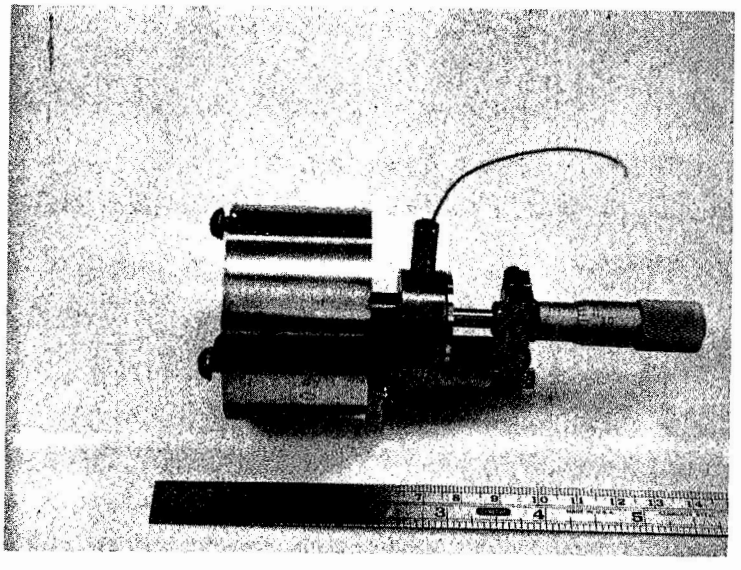

Fig. 27. Cathode Mounting Jig

to atmospheric pressure for a minimum length of time while its assembly is being completed and before it is given its final evacuation.

The electroformed nickel mesh contains 1000 lines per inch. The mesh is stretched over the nichrome mesh ring (with a square hole) and then attached by means of the 0.005" thick nichrome welding ring which is resistance-welded through the mesh to the mesh ring. It was found that in order to obtain a taut and wrinkle-free mounting, the mesh not only has to be drawn uniformly tight but also great care must be taken in the welding operation so that no part of the mesh is exposed to excessive heat. The finished mesh assembly is mounted in the tube with four stainless steel screws.

A special jig is used to ensure proper application of pressure while the indium seal is being made, and to position the faceplate and target ring. Great care must be taken in cleaning the ceramic surface prior to sealing and to remove all particles which might cause leaks.

The tube is given a final helium leak test before the exhaust bake.

C. Tube Exhaust

The ceramic vidicons are exhausted on oil-free vacuum systems using sorption and ion pumps. With the bakeout temperature limited to 140°C, long bake times are used, generally over twelve hours.

Appropriate changes had to be made in the procedures for cathode activation in order to adapt them to the conditions imposed by this tube. Although adequate cathode emission has been obtained, cathode performance has not been consistently good. The probable cause is the difficulty of proper outgassing of the gun parts. Due to the brazed joints in the gun region, it is not possible to subject the gun to the conventional radio-frequency heating during the activation process. This may result in somewhat higher gas evolution from the gun parts during tube operation than that obtained from guns which could be degassed by r-f heating. After the thermionic cathode has been activated, the getter is flashed and the tube sealed off by the closing and cutting of the copper tubulation with a pinching tool.

Finally, the external copper leads are soldered onto the metalized connecting strips on the outside of the tube.

D. Potting

The deflection yoke is formed into the proper cylindrical shape on an aluminum mandrel. The three continuous layers of the material (the outer layer consists of bare fiber glass and serves to protect the copper pattern) are cemented together with a thin layer of epoxy.

The vidicon is slipped into the deflection yoke and, after the yoke has been positioned properly, the assembly is potted in the magnetic shield. It was found that the ordinarily quite viscous potting compound can be made more fluid by slightly heating it (to less than 100°C). It is then sucked, by means of a mechanical vacuum pump, into the spaces between the tube, yoke, and magnetic shield.

The potted tube is kept at 80°C for four hours in order to polymerize the potting compound.

III. TEST PROCEDURES AND FAILURE MODE ANALYSIS

The sterilization and environmental tests prescribed for this project were outlined in Table I.

Suitable tests were performed on all tube parts which were considered to be potentially prone to failure due to the required sterilization or environmental conditions. The test level at which failure occurred and the mode of failure were determined, when appropriate. For the static-acceleration test a Schaevitz Model No. B-10-D centrifuge was used (Fig. 28). With a 4-1/2 ft. radius arm, it has a maximum acceleration capability of 200 g's.

The Ling Electronics Model No. 300 vibration unit, shown in Fig. 29, used for all vibration testing, can provide sinusoidal vibration to 100 g's peak amplitude or random vibration to 50 g's r.m.s. in the frequency range of 5 to 3000 cps. It can exert forces of up to 7000 lb.

One of the high acceleration shock machines designed for testing the ceramic vidicon and its components, is shown in Fig. 30. An 8 lb. magnesium drop table, sliding on Teflon bearings, has provided impact shocks of up to 3700 g's amplitude, in a 0.45 ms half-sine pulse. At the drop height of 60 inches, a 60% rebound is obtained. The total available drop height is 76 inches. Figure 31 shows a CRO trace of a typical shock pulse. The detection circuit contains a wide-band filter passing frequencies from 200 cps to 7000 cps. The 0.45 mc-duration, high-g shock profile is obtained by using fiber glass material as the impact "spring."

A similar, smaller machine was built for providing the 0.10 ms rise time 3000 g pulse. It uses a steel block for the impact spring.

The tests made on various tube components and complete tubes are discussed below:

A. Faceplate and Indium Seal

The resonant frequency of the faceplate subassembly is much higher than that corresponding to the shock-pulse duration. Thus no amplification of the pulse is caused and the maximum stress experienced by

Fig. 28. Centrifuge for Constant Acceleration Test

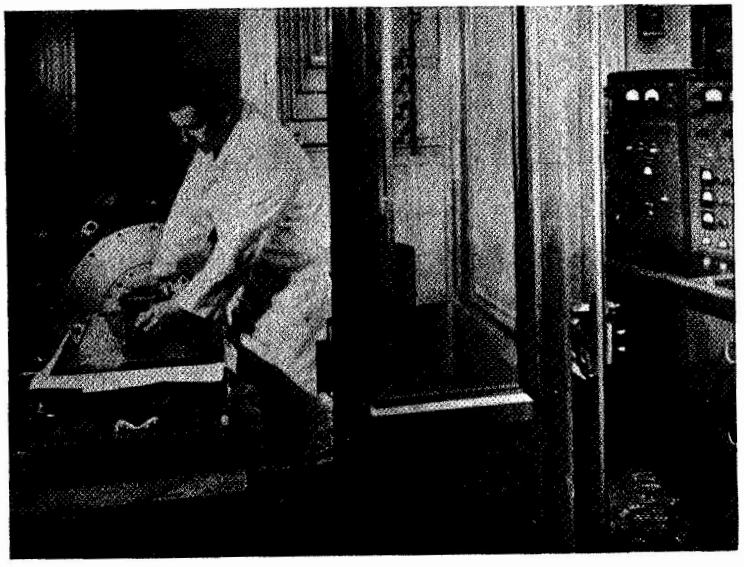

Fig. 29. Vibration Test Unit

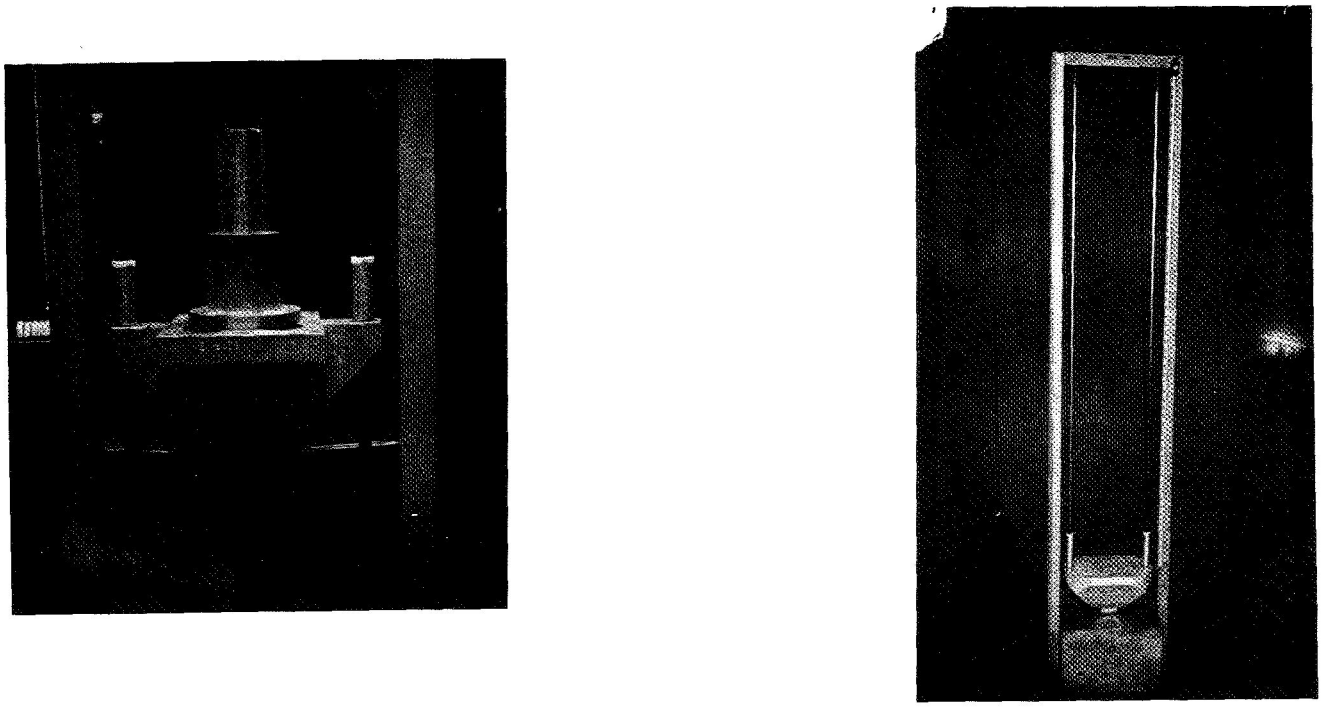

Fig. 30. High Acceleration Shock Machine and Detail of Drop Table (with holding fixture)

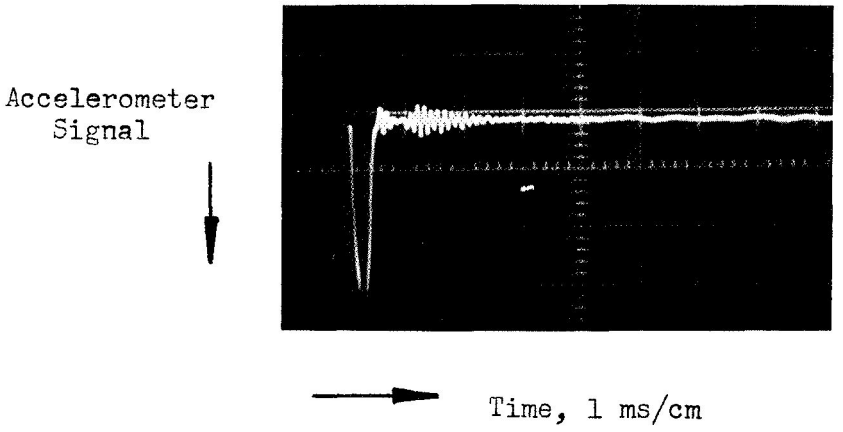

Fig. 31. Oscilloscope Trace of Typical Shock Pulse

the faceplate and indium seal can be deduced directly from the amplitude of the pulse. The weight of the quartz faceplate is about 0.0075 lb. If the pulse height is 3000 g, the maximum force on the indium seal is 3000 x 0.0075 or 22.5 lbs.

Static load tests were performed to establish the strength and failure mode of the indium seal on the vidicon. Two variations in sealing technique were investigated, differing in the method in which the ceramic seal surface is prepared. In the first kind of seal, the ceramic surface is ground and then metalized with molybdenum. Ten samples of indium seals formed on such a surface were tested under static loading, applied axially in the direction tending to push the faceplate away from the ceramic. The seals failed at forces varying from 75 lbs. to 270 lbs. In one case, the quartz faceplate cracked at 224 lbs. In all other samples, failure occurred due to separation of the indium seal. The average strength was 139 lbs.

The second kind of seal is formed on a bare ceramic surface which, after grinding, has been lapped smooth with a diamond compound. Six samples were tested. Three failed due to breakage of the quartz faceplate, at 161, 209 and 220 lbs., respectively. In the other three samples, the indium separated at forces of 114, 115 and 269 lbs., respectively. The average strength was 181 lbs. All seals had been found to be vacuum tight.

The second technique described above was chosen for the ceramic vidicon because tests showed it would yield seals which are at least four times as strong as required by the tube. Actually, since in the static tests the force was applied for many seconds before failure occurred, the seals can be expected to withstand a higher momentary force as in the case of the shock pulses.

Temperature tests on the indium seal indicated that no air leaks develop if the tube is exposed to a temperature of 152°C for 24 hours. Slight leakage occurs during a 24 hour exposure at 154 to 155°C and bad leakage during a 24 hour exposure at 155 to 156°C.

Tests were made on the feasibility of removing the stainless steel target ring after the indium ring had been formed. This would slightly reduce the maximum diameter of the tube and permit use of a magnetic shield of uniform diameter instead of requiring a step near the front end.

Target rings were removed from eight standard glass-envelope tubes. One of these developed an air leak, while the other seven remained

tight. Tests were then made on eleven specially mounted glass cylinders with indium seals. The faceplates of four samples, with target rings in place, were pushed off in the axial direction and were found to come off at an average force of 274 lbs. Three samples whose target rings had been removed, lost their faceplates at an average axial push of 185 lbs. Four further samples, without target rings, were tested with a lateral force applied to the faceplate. The faceplates started to slip at an average push of 60 lbs.

These tests indicated a small chance of a leak developing if the target ring is removed, and a pronounced reduction in mechanical strength of the indium seal. In view of these results it was decided to use the ceramic tube with the target ring in place.

B. Mesh

The nickel ring is attached to the 0.030" thick molybdenum support ring by means of four No. 0-80 stainless steel screws. Tension tests on these screws screwed into molybdenum sheet of 0.025" thickness, indicated that they failed at about 100 lbs. due to stripping of the threads and failure of the molybdenum sheet. As the weight of the mesh ring is about 3×10^{-3} lb, the total force experienced by the four screws at an axial acceleration of 3000 g's, is 9 lbs. The screws, therefore, have an adequate margin of safety.

Thirty-one mesh samples were tested with axial shock pulses of 3100 g's amplitude and 0.45 ms duration, five shocks being applied in each direction. Twenty-seven samples developed no wrinkles or other permanent damage. Their resonant frequency decreased by about 10% or less. The remaining four samples developed some wrinkles. However, it appears that these four samples were overstressed due to poor mounting in the testing fixture.

The resonant frequency of the mesh ranged from 2300 to 4000 cps with the average close to 3600 cps. The frequency of the mesh in one ceramic vidicon was found to be unchanged, at 3500 cps, after three heating cycles totaling 108 hours at 145°C.

Shock tests were made on two subassemblies consisting of mesh support rings brazed between ceramic cylinders. Mesh rings were attached to the support rings with four screws as used in the complete tube. Each sample was exposed to five 3000 g, 0.45 ms shock in five orthogonal directions. Due to mounting limitations, the pieces were not tested with shocks in the direction in which no force is exerted on the screws. One screw loosened in the first shock applied to it, presumably because it had not been properly tightened originally. After it was retightened, neither it nor the other seven screws showed any sign of loosening or other failure after the tests.

C. G_1-G_2 Subassembly

Early tests on the subassembly, consisting of the G_1 and G_2 cups brazed to a 14-mil thick ceramic spacer, showed that the ceramic tended to fail in shear perpendicular to the axis. The difficulty was clearly caused by the difference in thermal expansion of the metal and ceramic parts. Two remedial steps were taken. First, the spacer was made of a stronger ceramic. Second, slots were cut in the G_1 and G_2 cups making them more flexible.

Two subassemblies of this arrangement were exposed to five 3000 g, 0.45 ms shocks in each of the six directions, without showing any damage.

A static load test was made on two G_1-G_2 subassemblies with the force applied cantilever-fashion. Both samples failed at 125 lbs., one due to breakage of the ceramic spacer, the other due to separation of the epoxy in which the samples were mounted. The shear force transmitted by the spacer during a 3000 g transverse shock is less than ten pounds.

Three similar subassemblies were brazed in the ceramic G_1 support rings and cycled five times between 800°C and room temperature without showing any sign of damage. Cathode subassemblies and limiting apertures were then mounted in the G_1 and G_2 cups, respectively, and the test units were then exposed to 3000 g shock pulses. The brazed joint in one sample cracked during this test. This failure was found to have been caused by an unbalanced stress due to an incomplete braze, i.e. the joint was unsymmetrical and therefore produced localized stress concentrations. The other two test pieces passed satisfactorily through the complete set of sixty 3000 g shock pulses. Both units were then exposed to 5000 g shocks which caused fractures between the G_1 support ring and the G_1 cup.

It was well established that the G_1-G_2 ceramic spacer, if it is sound after being brazed, will be adequately strong to survive the environmental testing. However, the difference in expansion coefficients of the ceramic spacer and the stainless steel cups in some cases caused cracks in the spacer during cooling from the brazing temperature.

Two modifications were tried for reducing the remaining stress in the ceramic: (1) segmenting the ceramic spacer, and (2) using molybdenum instead of stainless steel for the metal parts.

G_1-G_2 subassemblies were made using ceramic spacers segmented into four and eight separate pieces. It was found that cracking still occurred, therefore this approach was abandoned.

7°

Since time did not permit the manufacture of molybdenum G_1 and G_2 cups, compound cups were made consisting of stainless steel sides with molybdenum bottoms. Although there is a tendency for the bottom section of these cups to be somewhat bowed, due to the difference in expansion coefficient of stainless steel and molybdenum, two subassemblies made with these cups had good brazed joints and withstood successfully the complete set of sixty 3000 g shock pulses. These tests, however, loosened the cathode subassembly within the G_2 cups indicating the need for more and heavier resistance welds. These two test pieces were also exposed successfully to 30 shocks of 0.12 ms duration and 4700 g amplitude.

D. Heater

The cathode heater consists of a double helix of rhenium-tungsten alloy wire just under 0.001" in diameter. Two straight sections of wire (the heater "legs") protrude from the cathode sleeve and are welded to two 30-mil kovar wires. The heater is coated with alumina.

In the first of several tests, eight heater-cathode subassemblies were mounted in ceramic test units (Fig. 32) in an arrangement similar to that used in the vidicon. Four of the heaters had short legs (.050" long) and four had longer legs (.140" long). The units were exposed to five 2500 g, 0.5 ms shock pulses in each of six orthogonal directions. The four long-legged samples failed: three due to the heater having left the cathode sleeve and one due to a welded contact opening up. The four short-legged units seemed to be intact although the heaters may have shifted inside the cathode sleeve.

A second set of test samples were made which were similar to the above except that they could be life tested with the cathode, hot. Since the first test had shown up the flexibility of the bare filament wire, care was taken to leave the insulation intact up to the weld point. The units were exposed to a complete set of shocks of 2500 g amplitude and 0.5 ms duration and then to another series of 3100 g amplitude and 0.42 ms duration. This test was followed by the complete series of vibration tests. Six of the eight samples survived all tests. The two failures (one during the first shock test, the other during vibration) occurred in units having the longer legs and consisted of loss of continuity. Four of the remaining samples (three with short legs, one with long legs) were then given a life test. Power was alternately on for 55 min. and off for 5 min. The filament voltage was 8V, instead of the design value of 6.3V. The heaters were still operable when the test was terminated at over 1200 hours.

X-ray pictures taken of these units at a later date showed that two of the heaters with short legs had shifted inside the cathode sleeve. One had moved away from the cathode by an appreciable amount and would probably have given unsatisfactory performance.

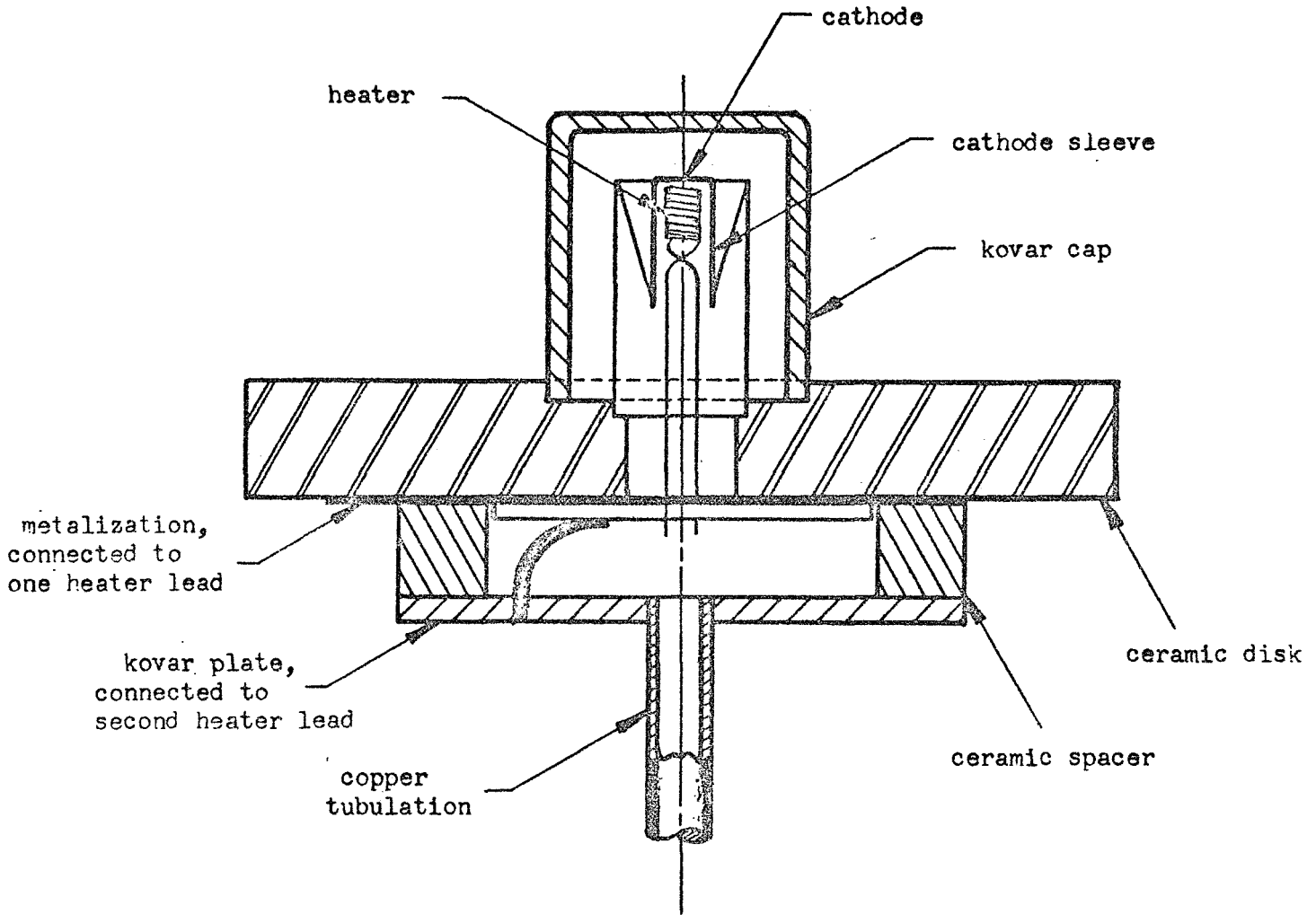

Fig. 32. Heater Test Assembly

The above environmental tests on heater samples had been made on heaters which had not yet undergone the cathode activation procedure. Since the recrystallization temperature of the filament wire is above the highest temperature reached during activation, it was felt that the properties of the heater would be similar before and after this process. In order to verify this assumption, eight more heater test units were made and, after cathode activation, were exposed to a complete set of 3000 g shocks. All eight heaters had short legs.

Three of the heaters failed by completely leaving the cathode sleeve and opening up. Four of the remaining filaments were found to have shifted somewhat within the cathode sleeve.

In order to strengthen the heater structure, tests were made on cementing the heater to the underside of the cathode. This prevents any appreciable shifting of the heater in the cathode sleeve. It also enhances thermal contact between heater and cathode and thus reduces the required filament power. Various materials were tried, including palladium, molybdenum, nickel and alumina, and some encouraging results were obtained. However, it was found that this technique was not satisfactory because it made the heater liable to failure under vibration. With the heater secured at both ends, the resonance of its unsupported section is within the frequency range of the vibration test which is likely to cause damage to the heater coating.

Various techniques were therefore investigated for completely embedding the heater in a suitable material in the cathode sleeve. After various attempts to surround the heater with a precast material which could be fitted into the cathode sleeve, the potting method described in section IIB was developed. The final set of test units, in this series of potting experiments, consisted of seven samples containing heaters potted in Linde A-1475 alumina with a Sauereisen-cement cap. They were exposed to the complete set of sixty 3000 g shocks and then were given a test during which they were operated, with 8V applied, for 55 minutes and turned off for 5 minutes during each hour. All seven units were still operable after 88 hours of this "accelerated life" test. This result implies a life expectancy of at least 2000 hours.

In addition, static tension tests were made on samples of straight filament wire welded to .030" kovar wire. The welding arrangement is similar to that used in the ceramic vidicon. Failure was found to occur at about 0.2 lbs. due in all cases to fracture of the wire. If one leg has to supply the total inertial force for accelerating the whole filament at 3000 g, the transmitted force is only 0.02 lbs.

E. Feedthrough

The molybdenum pins used for electrical contacts through the tube wall and to brazed joints, were found to form vacuum-tight and strong bonds to the ceramic. Static loading of the pins in the original design caused failures at about 200 lbs., due to cracking of the ceramic.

Strength measurements were also made on three test pieces incorporating the recessed pin arrangement used in the final design. The outside wall of the ceramic cylinder is ground flat under the pin head which, in the lower end section of the tube, reduces the wall thickness to about 0.038". The test sections were made similar to the lower end of the tube. The pins were found to be vacuum tight after being cycled five times between 800°C and room temperature. Forces were then applied radially outward. One sample failed at a force of 50 lbs., apparently due to being poorly supported during the test. The second sample was exposed to a push of 100 lbs., and the third to 120 lbs., without any evidence of failure. Forces were then applied to these two samples tending to bend the pins sideways, i.e. cantilever-fashion. One of the pins bent at 13 lbs. and the other pin broke at 30 lbs. Both brazed joints remained undamaged and vacuum tight. The maximum force exerted on any pin during a 3000 g shock is expected to be less than two pounds.

F. Ceramic-to-kovar Joint

Strength tests were made on three brazed test pieces consisting of ceramic cylinders with kovar cylinders attached at each end. Each unit contained two ceramic-to-kovar joints similar to those used in the actual tube. These pieces were tested under tension because the ceramic material is weakest in tensile strength. One of the test joints failed at a pull of 725 lbs., another at 1065 lbs., while the third did not fail at 1250 lbs.

The mass of the bottom section of the tube, supported by the brazed joint, is about six grams and exerts, at 3000 g acceleration, an inertial force of only about forty pounds.

G. Yoke

A sample deflection yoke was heated to 149°C and cooled rapidly to room temperature without damage. It was then exposed to the full dry-heat sterilization and ethylene-oxide decontamination procedure. Finally it was put onto a dummy tube, potted (with PR1538 polyurethane) inside a magnetic shield, and given all prescribed vibration and shock tests. It survived these tests successfully.

H. Magnetic Shield

Experiments were made on the magnetic shielding effect of Moly Permalloy shields before and after being exposed to shock. The four samples consisted of 0.020" material formed into cylinders of 6" length and 1-1/8" I.D. They were potted in C1100 epoxy and exposed to a complete set of 3000 g, 0.45 ms shock pulses.

Shielding efficiency was measured in an applied field of 90 gauss. The field observed inside the shield was found to be about 0.6 gauss initially and had a maximum value of 1.5 gauss after the shock test. Thus the shielding efficiency was still above 98%.

I. Potting Compound

Most of the potting compounds tested were found to have insufficient stiffness. The durometer reading of the compound should be at least 80 in order that the potted tube has a resonant frequency of 3000 cps or above as required. Epoxy which would satisfy this requirement, has an excessive thermal expansion coefficient which might cause damage to the tube at low temperatures.

A preliminary search indicated polyurethane to be the most promising material as far as stiffness and resistance to the sterilization procedures are concerned. Test samples were made of several formulations of this material with metal rods potted within metal tubes simulating the actual tube arrangement. PR1538 (Products Research Co.), cured at about 80°C for four hours, was found to have acceptable elastic characteristics and to be able to withstand the original dry-heat and ethylene-oxide sterilization procedures without appreciable change in physical properties. Samples of this material also were exposed to air at 160°F and relative humidity of 95% for 3 days without apparent changes.

The PR1538 polyurethane was not exposed to the final dry-heat sterilization and ethylene-oxide decontamination specifications because of lack of time and because of results obtained at JPL. As reported by S. H. Kalfayan and B. A. Campbell (as a result of work done for JPL Materials Section 351, D. P. Kohorst, cognizant engineer), PR1538 is compatible with the final specifications. They report that no change in hardness is experienced and it was assumed that the stiffness is similarly unaffected.

Unfortunately, when the final tubes made under this contract were tested according to the complete sterilization and test procedure required by the contract, it was discovered that the PR1538 potting compound did deteriorate during the dry-heat and ethylene-oxide exposures. The loss in tensile strength and stiffness was found to be so severe that the tubes could not safely be given the environmental tests while embedded in this material. This problem is discussed further in section J.

Since it is desirable to use a potting compound of considerably greater stiffness than the minumum durometer value of 80 mentioned above, tests were made on PR1538 to which various amounts of fine glass spheres (30 to 300 microns in diameter) and sand had been admixed.

Encouraging increases in stiffness have been obtained, but problems remain concerning proper mixing without inclusion of air bubbles and concerning the heat resistance of the resultant material.

Attempts were also made to pot tubes in epoxy. This material is very strong and stiff but suffers from a relatively high expansion coefficient. The latter tends to cause breaks in the tube envelope when the temperature of the assembly is varied. It was found however that epoxy could be used if it is in the form of separate longitudinal strips. In this case, differential expansion between the tube envelope and epoxy cannot cause any objectionable tangential stresses. Although the epoxy strips are continuous in the axial direction, no tube damage was caused. In this arrangement it is very important that the different epoxy strips are truly separated from each other. Even a very thin epoxy layer connecting the longitudinal strips was found to be sufficiently strong to crack the tube envelope when its temperature was raised to about 150°C. This approach to potting the ceramic vidicon was not pursued further because PR1538 polyurethane was believed to satisfy all requirements.

J. Complete Tube

A prototype ceramic bottle was made to indicate whether the various types of joints, used in the tube, are impervious to the ethylene-oxide decontamination gas. The ionization gage which had been incorporated in the unit, showed that no perceptible trace of the gas was allowed to penetrate the bottle.

In the first environmental test of a potted tube, a mechanical sample of the original design was used which did not contain a mesh or a heater. Thirty shocks (five along each of the six directions) of 3000 g amplitude and 0.45 millisecond duration were applied without causing apparent damage. The resonant frequency in the axial direction was found to be in excess of 3000 cps.

Three potted tubes (also of the original design) were exposed to nearly square shock pulses, of at least 3200 g amplitude and one-half millisecond duration in tests performed at the Jet Propulsion Laboratories. Two of the tubes were incomplete internally while the third was an operative vidicon. Altogether these tubes were exposed to thirteen transverse and six axial shocks.

No damage was found on the body of any of these tubes. The complete vidicon failed during the fifth transverse shock without having received any shock in the axial direction. The failure consisted of an open filament and a distortion of the G_2 cup structure. It is believed that the break in the heater, which occurred adjacent to the weld at the support wire, was caused by the motion resulting from the failure at the G_2 cup. The changes in the gun structure made in the final design are such that the joint which failed in this tube has been eliminated.

Experimental tests on the behavior of the ceramic vidicon under shock-pulse excitation indicated that the acceleration experienced by the tube components is greater than that applied to the fixture which holds the tube. The resonant frequency of the original design tube as mounted in the potting compound was about 3000 cps. The frequency corresponding to the 0.45 ms pulse duration is 2200 cps. These two frequencies are sufficiently close so that a shock pulse applied to the magnetic shield causes an acceleration of the tube which is greater than the applied acceleration by a factor of about 1.4.

Due to the flexibility inherent in the kovar joint at the gun of the original design tube (see Fig. 16), the amplification factor for the lower tube section is even larger. This is particularly true for transverse shocks in which the lower section is deflected in cantilever fashion. The amplification factor in this case is about 2.5.

At the end of Phase I of this contract a potted ceramic vidicon of the original design was exposed to a complete environmental test. The tube was first given an operational test which was repeated after the prescribed constant-acceleration and sinusoidal and random vibration tests. The tube was then exposed to five shock pulses in each of the six directions. These pulses were half-sinusoidal with 0.45 ms duration. The amplitude of the applied transverse shocks was 1200 g and of the axial shocks 2800 g. Presumably, therefore, all the accelerations experienced by the heater, as well as the axial accelerations of the mesh, were about 3000 g's. These, of course, are the critical aspects of the tube.

Since the tube was found to be in good condition, it was then exposed to the original sterilization conditions (two 24-hour cycles at 40°C in ethylene-oxide and three 36-hour cycles at 145°C in dry nitrogen). This treatment did not affect tube operation but resulted in some softening of the potting compound and a small amount of swelling at its exposed surfaces. However, the resonance frequency of the tube in the potting compound remained unchanged at 3600 cps.

The tube finally was given another set of axial shocks. The acceleration amplitude applied to the magnetic shield was over 3000 g and the lower end of the tube, containing the heater, received a maximum acceleration of about 5000 g. The filament was found to be still continuous after five shocks which were performed with the tube being dropped faceplate upward. However, the heater opened up during the fourth or fifth shock applied in the opposite direction. The resonance frequency of the mesh was about 2500 cps which was near its frequency measured before the shock test.

One tube of the final design was tested in accordance to the following plan:

(1) Ethylene-oxide decontamination.
(2) Heat sterilization.
(3) Static acceleration.
(4) Sinusoidal vibration.
(5) Wide-band noise vibration.
(6) Shock.

The tube was given a performance test at the beginning of this program and again at frequent intervals during the progress of the test procedure.

After the heat sterilization, it was found that the potting compound had become somewhat putty-like with reduced strength and stiffness. No deterioration in tube performance was evident at this stage or after the static-acceleration and the vibration tests. However, the filament was found to be open after the first shock test which consisted of a transverse pulse. After checking and recalibration of the test equipment, it was found that the input to the magnetic shield had been at least a 4800 g acceleration of 0.25 ms duration while the tube itself had been exposed to a shock of 7500 g amplitude and 0.30 ms duration. This unexpectedly high shock level was caused by the softening of the potting compound and the resultant lowering of the resonant frequency (of the tube in the potting compound) to 2000 Hz. The period of the resonance vibration therefore was close to the duration of the shock pulse, resulting in a large amplification factor. (The resonant frequency should be in excess of 5000 Hz.)

Two additional tubes were made successfully and potted in magnetic shields. The resonant frequency at this stage was about 7000 Hz. One of these was exposed to the complete dry-heat sterilization procedure and since the potting compound had become softened, it was repotted in fresh compound. It was then given the environmental test. The tube was in good condition after having undergone the constant-acceleration and the vibration tests, and after the first five (transverse) shocks, consisting of 3200 g amplitude pulses of 0.30 ms duration. However, one heater connection opened during the second set of transverse shocks.

The other tube also passed successfully through the constant-acceleration test. It was to be given the vibration test after the shock tests. The tube went through twenty-five shocks of 0.45 ms duration in good condition, but one heater connection opened during the final five shocks of this series. These five pulses were applied in the axial direction toward the base of the tube. The amplitude of the shocks was found to have been about 3700 g and the duration 0.35 ms.

A careful study of the results of these tests indicated that the failures were caused by breaks of the filament wires at, or very close to, the spot-welded joints by which they are connected to the 0.050 inch diameter kovar heater support rods. It appears that the deflection of the heater wires and the kovar rods under shock, though small, caused sufficient tension and flexing in the heater wires to break the wire.

It was decided that in any future tubes the aforementioned failures could be avoided by removing the alumina coating from the straight section of the heater wire, between the cathode sleeve and the support wire, and by loosely winding the heater wire around the support rod before spot welding the end of the heater wire to the kovar rod. These changes would (1) reduce the mass of the heater wire and thereby decrease the tension in the wire due to inertia forces produced during shock pulses, (2) reduce the flexing of the heater wire in the vicinity of the spot-weld where the wire tends to be relatively brittle, and (3) permit considerable deflection of the kovar support rod without causing appreciable tension in the heater wire.

IV. PERFORMANCE

A. Operating Conditions

The tubes were operated at a readout frame time of 1.0 sec. and horizontal line time of 1.6 millisec., so that the raster consisted of about 600 lines. Each readout frame was followed by an erase scan of equal duration and line number. The test pattern was projected onto the faceplate for a fraction of a second just prior to the readout scan.

Typical electrode voltages were as follows:

Target	20V	G_4	82V
G1	-11V	G_5	500V
G2	300V	Mesh	700V

B. Horizontal Response

Horizontal response was measured by means of a RETMA resolution pattern which contains square-wave resolution wedges. The results are shown on Fig. 33. The response at low line numbers was determined by means of a step between a white and a black stripe of relatively great width. Since the coarsest section of the test pattern corresponded to 200 TV lines, the response to lower line numbers was approximated by interpolation. The faceplate illumination was about 0.35 footcandle and the shutter speed 0.1 second, so that the total exposure was 0.035 fcs.

The relative response at 450 TV lines was about 0.15.

A value for the equivalent line number (N_e) was found from the area of a plot of the relative response squared versus line number. The resultant value of N_e is 158.

C. Vertical Response

The vertical response was measured by visual inspection on the monitor. A limiting response of 500 TV lines was observed.

D. Light Transfer Characteristic

The signal due to a black-to-white step was measured at various values of brightness, shutter speed and lens apertures. The face plate illum ination was computed for each exposure, assuming a lens

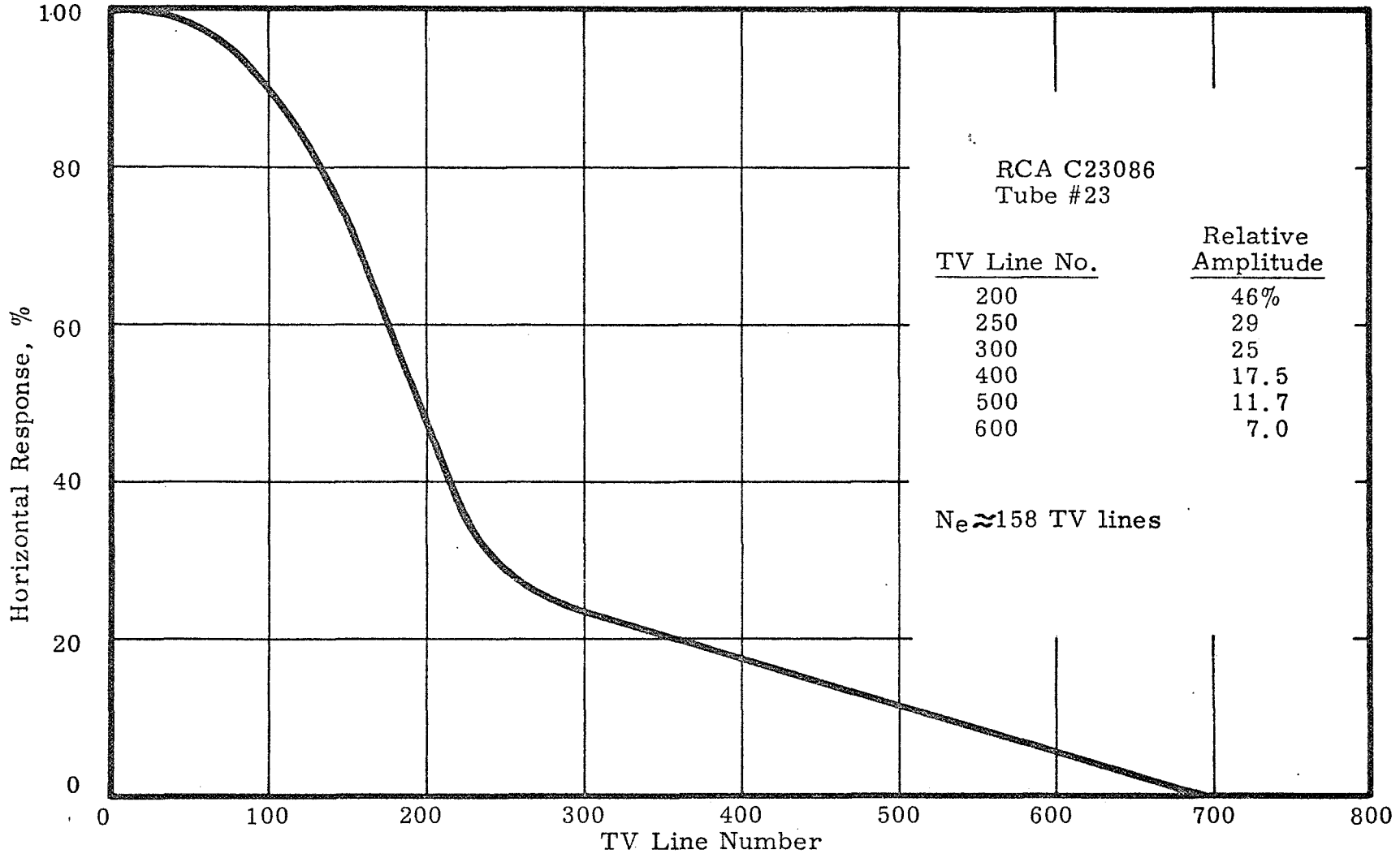

Fig. 33. Uncompensated Horizontal Peak-to-peak Response to Square-wave Test Pattern

transmission of 0.9. The results are shown on Fig. 34. Because of relatively low cathode emission in the tube used, the signal current saturates at a faceplate illumination of about 0.06 fcs. However, the tube is very sensitive and yielded a measurable signal less than 0.0003 fcs.

The slope of the linear portion of the transfer characteristic is 0.8. The ratio of the exposure corresponding to the maximum unsaturated signal to that causing the smallest measurable signal is about 200:1. The units used for plotting signal current in Fig. 34 are approximately equal to nanoamperes.

E. Signal-to-noise Ratio

The signal produced by a uniformly illuminated area was measured in terms of the corresponding vertical deflection on an oscilloscope, which was calibrated against a reference pulse. At a faceplate illumination of 0.14 fcs., a signal of 52 nA was observed.

An upper limit of the rms noise was determined, from the width of the oscilloscope trace, to be 0.75 nA.

The signal-to-noise ratio therefore was 69:1, or 37 db.

F. Spectral Characteristic

Spectral response was measured with the tube operated at standard television rate. With the target potential at 20 V., the light level was adjusted so that the signal current, for a 1/2" x 3/16" raster was 200 nA. Interference filters were then interposed and the signal current measured at several wavelengths. The measured values were corrected for the gamma of the tube and for the energy transmitted by each filter so as to yield the tube response as normalized for equal incident radiant power at all wavelengths. The results are shown in Fig. 35. Maximum response is seen to occur at about 575 mu.

G. Erase Characteristic

The signal corresponding to a white area was measured as well as the signal remaining at the next readout scan, without any light exposure having been made in the meantime. The erase scan, between the two readouts, consisted of a single scan similar to a

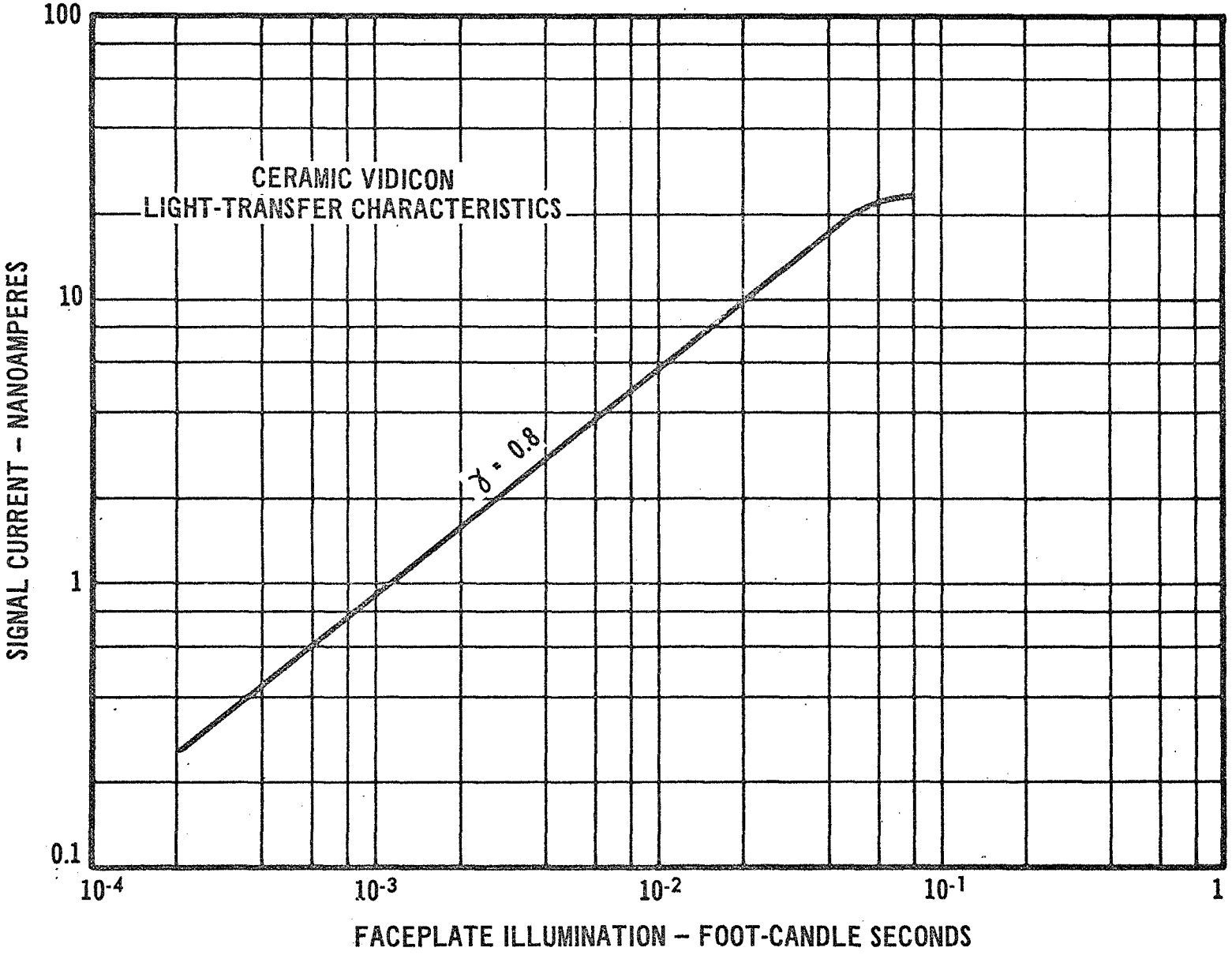

Fig. 34. Light-transfer Characteristics

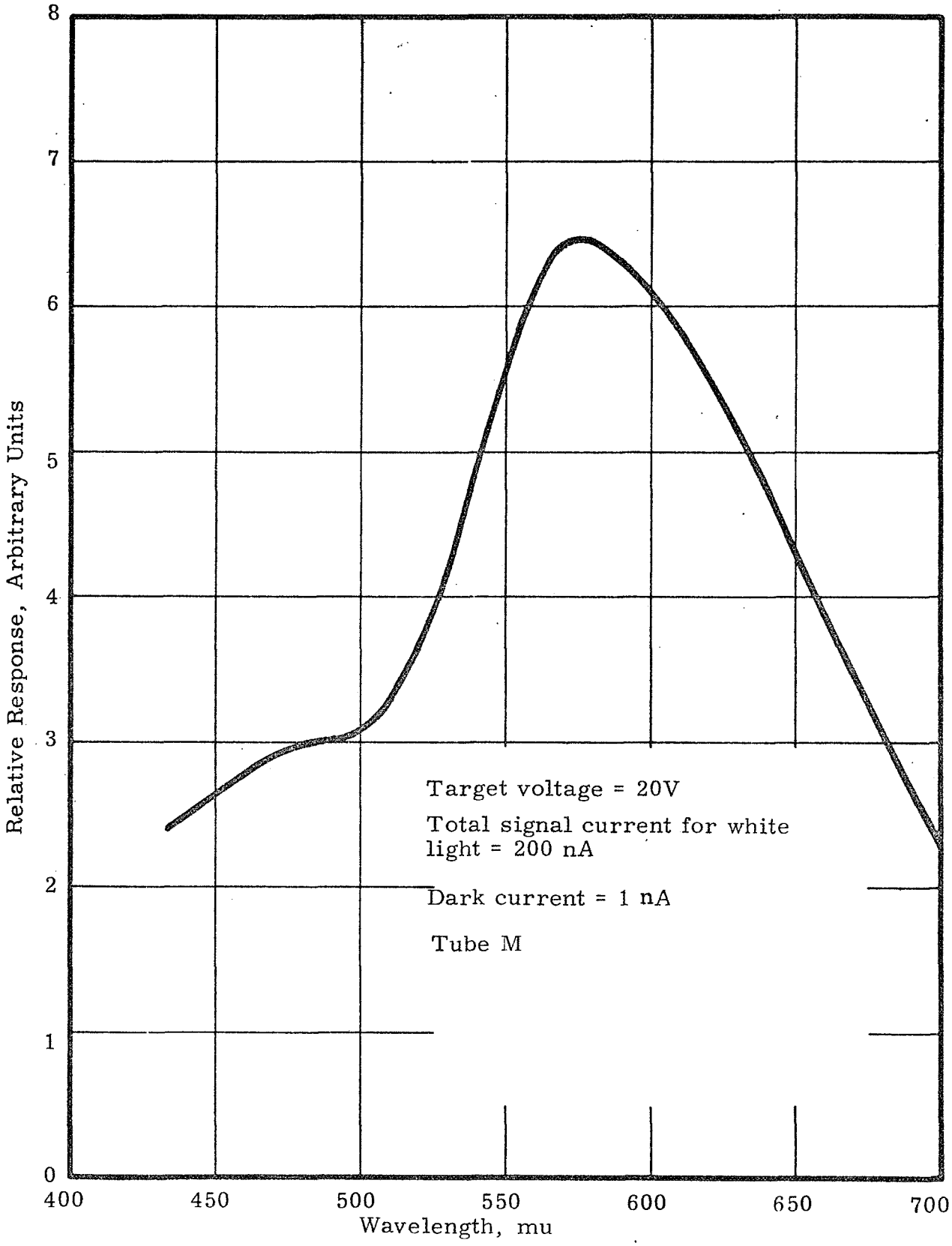

Fig. 35. Spectral Response, Corrected for Equal Power Incident at all Wavelengths

readout scan in frame time, line number and beam current.

At a faceplate exposure of 0.07 fcs., the remaining signal was 0.33 of the original, so that the reduction in signal was 10 db.

H. Shading

The test pattern used for this measurement consisted of eleven black vertical stripes in a white field. The signals corresponding to black-to-white transitions were recorded for four horizontal lines, located near the top, about 1/3 down, about 2/3 down and near the bottom of the raster, respectively. These measurements were then corrected for the nonuniformity of brightness of the test pattern, by multiplying each reading by the 0.8 power of the brightness for the corresponding region. The results are shown in Fig.36 in terms of response values given in arbitrary units. Approximate contours corresponding to equal response values also are indicated. The total variation of signal, from center-to-edge of the raster, is 60% of the maximum signal. The signal remains within 13% of the maximum value in one-third of the raster, and within 33% over two-thirds of the area.

V. TECHNICAL PROBLEMS AND SOLUTIONS

This contract encompassed the development of an electron tube of unconventional design utilizing materials and construction techniques not previously applied to similar devices. It therefore is not surprising that, in addition to the difficulties to be expected with any new tube design, many unusual problems arose in connection with the ruggedization requirements and the use of ceramic-and-metal construction. Two major problems (i.e. heater ruggedization and G_1-G_2 structure) and their solutions were discussed in part III. Several other problems that were encountered are discussed below:

A. Alignment of Tube Components

The various parts of the electron gun and the electrostatic lens system must be aligned, i.e. mounted on the same axis and with parallel transverse surfaces, to a high degree of accuracy. In particular, the limiting aperture in the accelerating electrode (G_2) should be located within 0.0005" of the tube axis.

Exact alignment of the brazed components was accomplished with precision brazing jigs. The design of these jigs was made difficult by the fact that the thermal expansion coefficient of the stainless steel

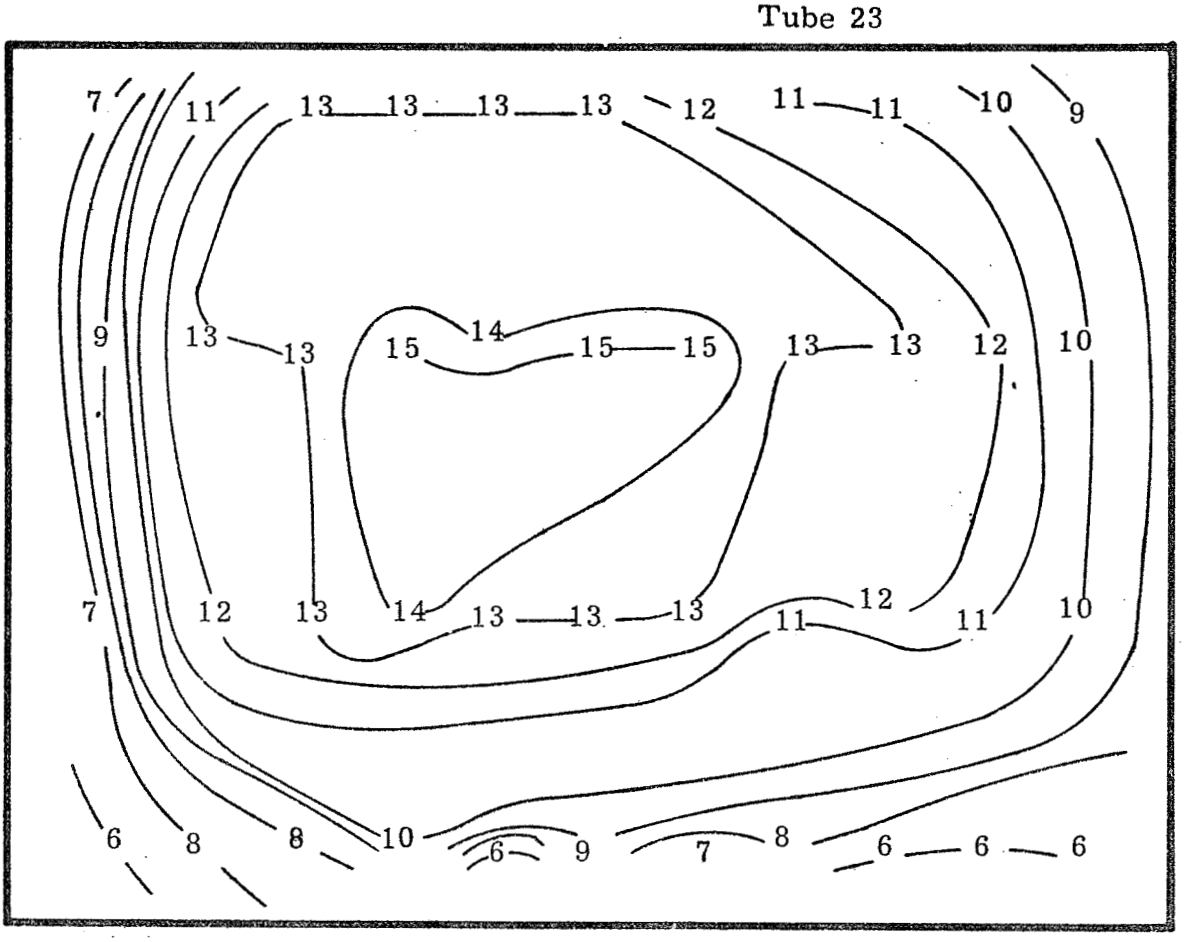

Fig. 36 Signal Distribution for Uniform Illumination

used in their construction is considerably greater than that of the alumina ceramic. The jig therefore cannot assure good alignm ent at both room and brazing temperatures.

The most desirable jig design appeared to be one that aligns the gun components relative to each other as well as to the tube body, by means of metal surfaces within the tube. The jig then fits loosely at room temperature and expands against the inner tube surfaces as the brazing temperature is approached.

Such an arrangement could not be utilized in the original tube design because of the presence of the deflectron with its conical shape. The final tube configuration, however, has a cylindrical inside wall which permits the use of an internal brazing jig. The jig developed for this purpose (Fig. 25) aligns the control grid (G_1) and accelerating electrode (G_2) by means of a ceramic pin which fits snugly within the 0.030" apertures of the two metal cups. Due to the small dimension of these holes, the differential thermal expansion between their diameter and that of the ceramic pin is negligible. The alignment between the 0.0015" limiting aperture and the 0.030" bottom hole of the accelerating electrode is accomplished ahead of the brazing operation. The two parts of the electrode are resistance-welded together under a microscope with which the alignment can be checked to within 0.0005".

The ceramic center pin of the brazing jig is aligned relative to the tube body by means of four metal rods which bear against the inside wall of the tube. The ceramic G_1 support ring has four holes which permit these rods to extend into the central portion of the tube. The exact radial spacing of the rods is assured by a hollow metal tube, which is inserted from the front end of the tube and which pushes the line-up rods outwards. The downward pressure required on the gun electrodes during brazing, is supplied by a cylinder fitting loosely within the metal tube.

This arrangement was found to line up the tube components with sufficient accuracy such that the tubes could be operated without the usual alignment coils.

B. Brazing Materials

Due to the conditions which had to be satisfied in the precision brazing step described above, it was necessary to make some of the required brazed joints in a separate operation. For instance, the jig described in the previous section could not be designed to allow the kovar-to-ceramic joint, at the bottom of the tube, to be brazed at the same time as the gun components. Therefore, two separate

brazes had to be made. Originally two different solders were used. The two materials which are suitable for brazing metalized ceramic surfaces are (1) "BT" silver solder, which is the eutectic alloy of silver (72%) and copper (28%), and melts at 780°C; and (2) the Palcusil alloys, containing silver, copper and palladium in various ratios so that the soldering temperature falls between 807 and 900°C. The material chosen for the first braze was Palcusil 5, with a soldering temperature of 807°C. The second braze, made with BT was then controlled so that the temperature of the work remained below 800°C. In this way the first braze joints were not remelted. However, it became apparent that some of the Palcusil joints were not air tight, due to fine cracks in the brazing material caused by the second temperature cycle.

Since BT solder joints were found capable of withstanding several heating cycles, it was decided to try to make both sets of brazed joints using BT. This material, when molten, was found to dissolve a small amount of nickel from the plating on the molybdenum metalizing layer. Hence, the joint formed in the first braze consists of an alloy with a slightly higher melting point than that of pure BT. By careful temperature control during the second braze it was possible to melt the BT without softening the previously made joints.

C. Wall Electrodes

The unipotential lens consists of three cylindrical electrodes which were formed by means of metal layers deposited on the inside wall of the ceramic tube body.

Initially these deposits were made by copper evaporation. However, it was found difficult to define the edges of the electrodes with sufficient accuracy. The spacing between the lens electrodes, and between the third lens section and the mesh electrode, should be no more than 0.02", but the segments have to be well insulated from each other. Masking these narrow separations during the copper evaporation was found to be very difficult. As an alternative, attempts were made to form the desired electrode configuration by evaporating a continuous copper layer and then cutting the separations on a lathe or with a slim grinding wheel. This technique seemed to result in well defined copper regions; however, the cutting operation tended to leave a semiconducting deposit which presumably consisted of metal particles embedded in the pores of the ceramic surface.

The material used for these electrodes was therefore changed to the molybdenum metalizing coating used for the brazed joints. This

material is originally in a pastelike form which is painted onto the ceramic with a brush. The metal is bonded to the ceramic by oven firing and is finally nickel plated. It was found that before the firing operation the metalizing could be readily removed with a diamond wheel. Good separation between electrodes was thereby obtained. The final metal deposit was found to be smooth and well conducting.

D. Ceramic Body

The ceramic tube envelope used with the original design consisted of various cylindrical sections of different cross-sections which were brazed together. The ceramic parts generally were found to be of good quality. In the final design, however, a single ceramic piece was used for the envelope, with a cylindrical outside but with two shoulders cut on the inside surface such that the end portions had thinner walls than the central (lens) region.

Considerable trouble was experienced due to (1) chipping of the end surfaces, and (2) fine cracks in the thinner sections of the envelope. The chipping was particularly serious at the front end where the indium seal to the faceplate has to be made. No ceramics were used in which any chipped area extended more than halfway across the surface rim. It was found that a crack could be usually discovered by means of an indicating dye. Naturally, no piece was used if a crack was observed.

Of fifty pieces which had been purchased, eighteen were found to be unacceptable due to excessive chipping or because of cracks. These rejects were eventually replaced by eighteen substitute pieces, nine of which had to be replaced once more because of defects. At least two tubes had to be discontinued because of defective ceramic, one losing a large chip at the front surface, the other cracking at one of the feedthrough pins.

E. Heliarc Weld

In general, strong and reproducible heliarc welds were obtained (between the kovar bottom section and header) once the proper surface speed, gas flow, weld current and probe spacing had been ascertained. However, at first, considerable difficulties were encountered which were traced to the presence of silver (from the brazing joints) on the kovar surfaces. Even a very small amount of silver near the arc would cause bad sputtering and prevent the formation of a proper joint. Meticulous removal of all traces of silver was found to remove this problem.

F. Pinch-off

Three tubes were lost while being sealed off after exhaust and cathode activation. The copper tubulation is pinched off by means of a tool containing two hardened steel edges with which the tubing is flattened in a narrow region and squeezed until the copper separates. At the point of separation the copper is generally pinched together in an air-tight seal. In the case of the three failures, some air was able to leak in at the seal.

Careful analysis, including spectrographic and microscopic studies of the copper material, of the seal areas and the copper-to-kovar brazes, indicated that (1) some of the barium getter material was flashed onto the inside wall of the tubulation, and (2) in at least one case the brazed joint was weakened by the pinch-off operation.

In accordance with these findings, the direction in which the getter is flashed was shifted to avoid the possibility of depositing the material on the copper surface and all subsequent pinch-offs were made at a greater distance from the brazed joint than used before. No further tubes were lost at pinch-off after these measures were taken.

G. Mesh

Although the mechanically tensioned, 1000-line nickel mesh as mounted in the ceramic vidicon, was found to be capable of withstanding the required environmental tests, its factor of safety was smaller than that of most other tube components. In particular, it was felt that a significant increase in the resistance of the mesh to shock pulses could be achieved by raising the resonance frequency from the usually obtained value in the 3600 to 3800 hertz range to 5000 hertz or above. This would greatly reduce the axial motion of the central region of the mesh during and after the application of the shock pulses.

It appeared likely that local heating of the mesh was caused when it was resistance welded, under tension, to the mesh ring. Such heating would cause a decrease in mesh tension and result in a reduced resonance frequency. Therefore, other techniques were considered for attaching the mesh to its ring.

One sample was fastened by means of epoxy and was found to have a frequency of 4900 cps. Some effort was made to attach the mesh by gold plating all contact surfaces and welding by use of sufficient pressure at room temperature. However, reliable welds could not be obtained. These techniques were not perfected because of lack of time.

Work was also done on plating nickel and copper onto a copper mesh in order to increase its internal damping. This approach showed some promise but was not pursued because of the magnitude of the job involved.

Some work was done on chromium-plating the nickel mesh in order to strengthen it against shock pulses by increasing its internal damping. Preliminary tests showed that high damping values can thus be obtained. However, this technique could not be applied because of two difficulties, (1) the mesh did not have enough conductivity to carry the required plating current, so that the deposit could not be made sufficiently thick or uniform, and (2) bubbling of the bath was found to cause breaks and poor reproducibility in the coatings.

VI. CERAMIC CATHODE STRUCTURE

As a separate project, some work was performed on a ceramic cathode structure consisting of a directly heated cathode on a ceramic substrate, as indicated in Fig. 37. Such a cathode unit should provide greater strength, longer life, simpler construction and, possibly, lower power consumption than the present design. Improved thermal coupling can be obtained by putting the heater pattern on the same side of the ceramic support as the cathode coating. The two can be separated by a thin insulating layer such as alumina or quartz (see Fig. 38).

It was found that the geometry of the heater configuration is quite critical. Initial tests of metalized heater patterns had shown them to crack at the temperatures needed for thermionic emission, either immediately or after several cycles of heating and cooling. The principal cause for these failures was the internal stress set up in the ceramic support by the temperature differences between various areas within and surrounding the heater pattern. The geometry shown in Fig. 37 was therefore developed so as to result in a uniform temperature along lines parallel to the shorter sides of the rectangular shape of the device. All temperature gradients, and the resultant differential expansions, then occur only in a single dimension (i.e. along the longer side of the rectangle). If the unit is mounted so as to permit some dimensional fluctuation in this direction, the major source of internal stress is eliminated. Since the heat loss from the edges of the slab is somewhat greater than from its center, the outside strips of the heater pattern are made slightly narrower than the inner strips. Therefore, more heat is generated near the edge than in the center and a uniform transverse temperature is generated. The ceramic support plate is made as thin as practical, particularly under the heater area, in order to minimize the temperature gradient across the thickness of the ceramic.

It would be desirable to cover the underside of the support plate with a reflecting coating in order to minimize heat loss by radiation to other portions of the tube.

In a more advanced form, which has not been attempted, this structure might incorporate the control grid as suggested in Fig. 39. Here another

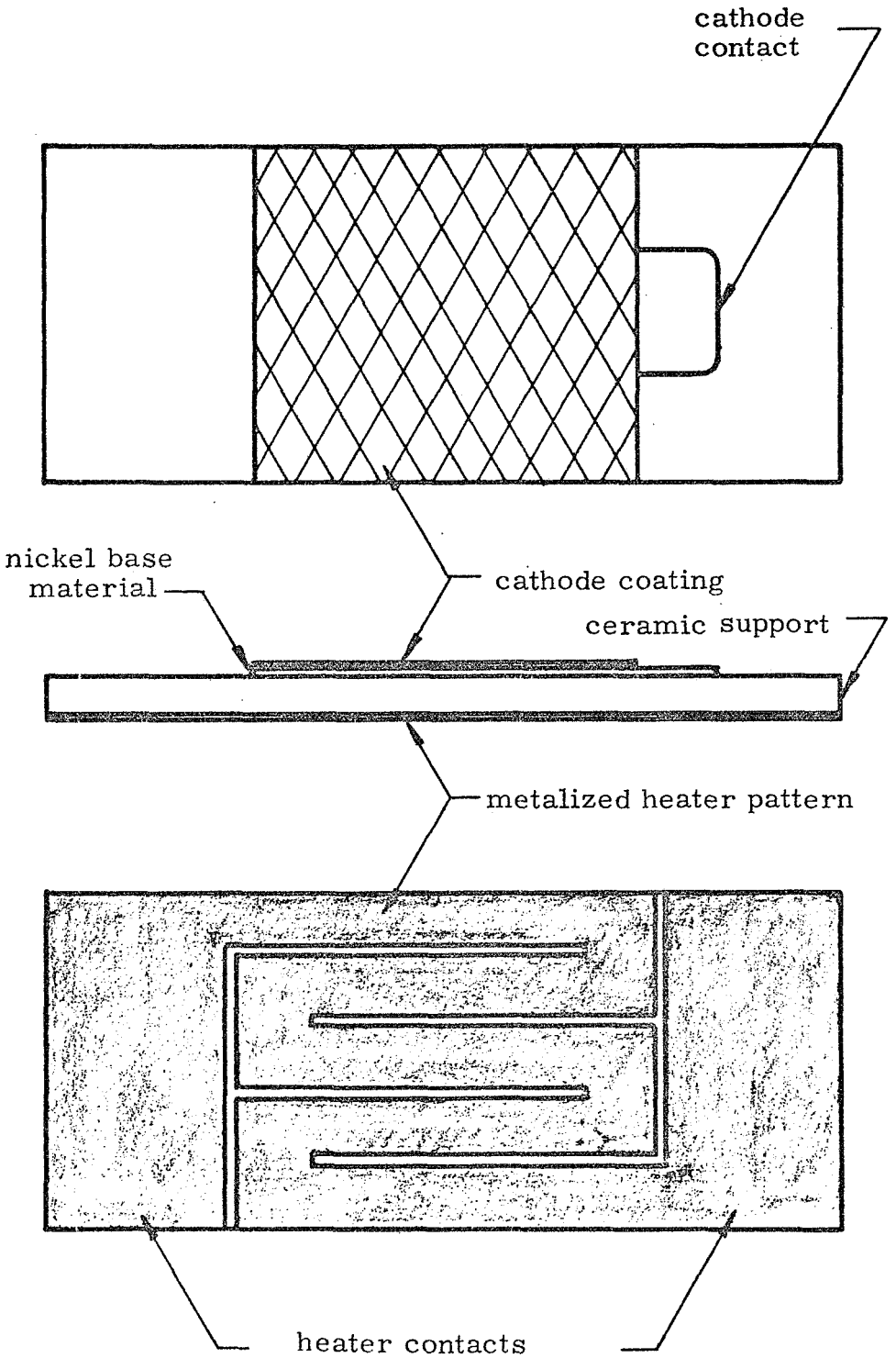

Fig. 37. Simple Ceramic Cathode

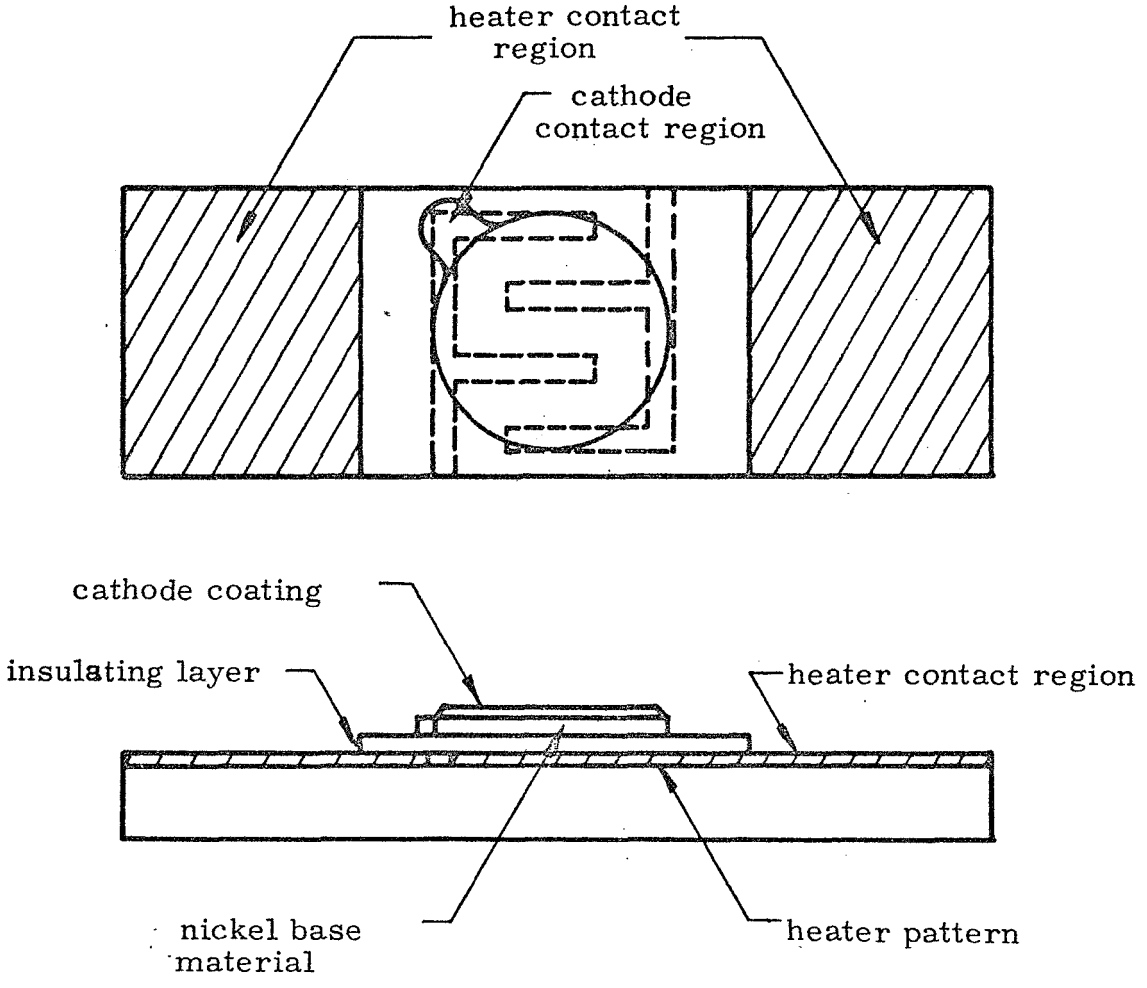

Fig. 38. Improved Ceramic Cathode Structure

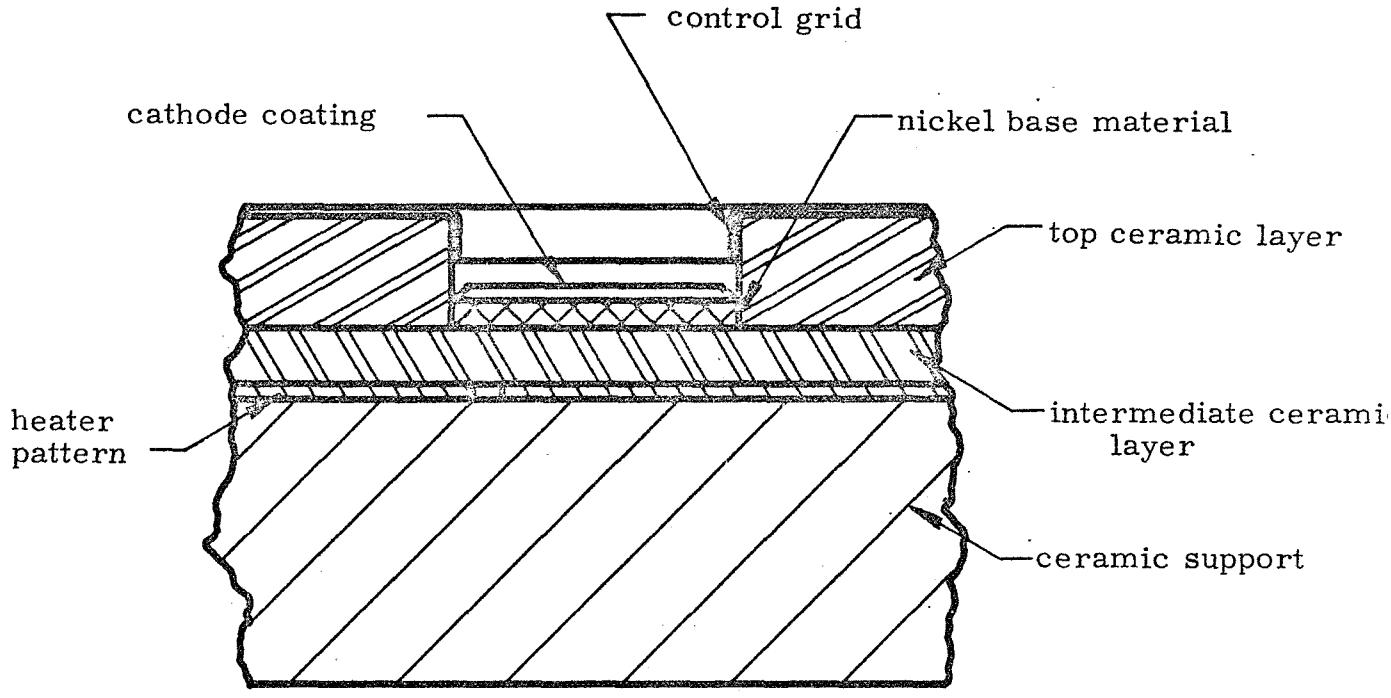

Fig. 39. Ceramic Cathode With Control Grid

ceramic layer, surrounding the cathode region, carries the control electrode. This arrangement provides an accurately controlled and rigidly maintained cathode-grid spacing, which would reduce the difficulty of tube assembly and strengthen the gun structure against shock pulses.

VII. POST-DESIGN CRITIQUE AND RECOMMENDATIONS

The ceramic vidicon which was developed during the course of this contract represents a major advance in ruggedization of camera tubes and its design incorporates many unconventional construction techniques. The tube was shown to be capable of surviving the compatibility tests for heat sterilization and ethylene oxide decontamination prescribed by JPL for piece parts to be used in Voyager flight equipment. It also passed successfully through almost all required environmental tests.

The present version of the tube has several areas in which improvement would be desirable, as can be expected in a device with many radically new construction features which had to be "frozen" into a final design within 1-1/2 years from the start of the developmental program. These areas include some of the structural features inside the tube, the potting compound and the electron optics. None of them present any basic difficulties. If further development were to be done on the ceramic vidicon, it is suggested that the following items be considered:

a. The gun structure (comprising the cathode subassembly and the control and accelerating grids) is difficult to assemble with the required spacings and alignment. Therefore it would be desirable to redesign this structure, preferably as a pre-assembled package which is mounted in the tube after the proper spacing and alignment of its elements has been accomplished. It is recommended that two possible arrangements be considered: (1) A pre-brazed structure similar in design to the present gun, but using a metal with an expansion coefficient close to that of the ceramic, and (2) a ceramic structure as described in Section VI, including the filament, cathode and control grid, and to which the accelerating electrode is attached previous to mounting in the tube.

b. The modification in the method for attaching the heater leads (stripping the alumina coating from the end portion of the wires and winding the wires around the support rods before making the welds) should be put into effect and environmental tests made on suitable subassemblies, and complete tubes, incorporating these changes.

   In addition, further work on potting the heater in the cathode sleeve is recommended as a means of extending the ruggedization of the tube to higher levels of vibration and shock exposure.

c. Similarly, it is suggested that further work be done on increasing the resistance of the mesh to shock and vibration by increasing its tensile strength, raising its resonance frequency (i.e. increasing the ratio of tension to mass) and by providing greater internal or external damping. It would also be desirable to change to a finer mesh, e. g. a 1500-line or 2000-line pattern, in order not to limit resolution when the tube is operated with small beam current.

d. A considerable reduction in power requirement of the deflection yoke could be achieved by redesigning its metal pattern and by increasing the number of flat coils used for each deflection direction.

e. It is clear that the PR 1538 potting compound, as used on this contract, is not satisfactory. Further work is therefore necessary to improve the resistance of this material to the sterilization treatments (possibly by changes in the mixing and curing procedures) or to replace it with a more suitable material. In particular, it is suggested that further consideration be given to the use of epoxy.

f. It would be worthwhile to study further the electron optics of the tube, including the precise dimensions of the unipotential lens and the geometry of the mesh-target region.

VIII. SUMMARY AND CONCLUSIONS

In Task I the slow scan photoconductor was evaluated in the commercial 7735A type vidicon. Performance characteristics studied consisted of:

(a) Dark current vs. target voltage,
(b) Signal current (at constant, uniform illumination) vs. target voltage,
(c) Signal current (at constant target voltage) vs. illumination,
(d) Spectral response,
(e) Ultimate resolution,
(f) Gray-scale rendition,
(g) Lag.

The tubes were tested for some or all of these characteristics before and after the dry-heat sterilization procedure which consisted of three 36-hour 145°C bakes in dry nitrogen. In addition, many tubes were tested following the first bake, and some also after the second.

In testing, primary consideration was given to the dark current and signal current characteristics and, to some degree, resolution. No significant changes, from tube to tube or from before to after sterilization, were observed in either gray-scale rendition or lag characteristics. In some tubes, sterilization caused a perceptible change in the shape of the spectral response curve but not of sufficient degree to be of significance in this program.

The major effect of the sterilization procedure on tube characteristics consisted of an increase in dark current and a smaller increase in signal current. These changes varied considerably from tube to tube. On the average, the dark current at 20V target voltage approximately doubled and the signal current increased by about 25%.

While the resolution in most tubes did not change much during sterilization, several tubes did show an appreciable loss while a few exhibited an increase.

Most of the tubes showed some spurious signal (spots). It was found that this problem can be greatly reduced by proper cleaning of the faceplates prior to the photoconductor evaporation. In no instance did sterilization cause an increase in spottiness.

At the beginning of this project the slow scan photoconductor used was found to be suitable for sterilization. Only a minor adjustment in its chemical composition was made, in order to cause a small decrease in dark current. The major portion of the work in Task I consisted of improvements in freedom from spurious signals and of obtaining experimental data for establishing the characteristics of the photoconductor.

In Task II it was demonstrated that an operable vidicon can be built which is capable of good performance as well as being able to withstand sterilization procedures and severe environmental testing.

In the original design, the tube design was based on a ceramic-metal modular construction. Electrostatic focusing and deflection were employed with the deflectron, an integral portion of the ceramic envelope. The final design consists of a hybrid vidicon having a unipotential electrostatic lens and a magnetic deflection yoke consisting of a thin copper pattern on an insulating support sheet.

The quartz faceplate is attached with an indium seal. Mechanically tensioned, unfired, nickel mesh was found to be the most rugged electroformed mesh material as far as resistance to vibration and shock are concerned. The low-power gun is made in a brazed construction and a technique was developed for cementing the heater inside the cathode sleeve.

Continual emphasis was put on ensuring the reliability of the tube under environmental testing. Critical components and subassemblies were tested and an effort was made to anticipate all possibilities of eventual failure.

It was shown that the ceramic vidicon developed under this contract can give good performance and can withstand the prescribed dry-heat and

gas sterilization treatments, and constant-acceleration and vibration tests. Although no tube finished the complete series of sixty 3000 g shocks, the tubes were found to be capable of surviving several such shocks, with the final tube tested lasting through at least 25 shock pulses. A simple change suggested for the heater connection should allow any future tubes to withstand a considerably larger number of 3000 g shocks.

Two tubes of the final design were delivered to JPL.

APPENDIX

Bill of Materials

Part No.	Part Name	Description	No. Needed Per Tube
1	Ceramic tube envelope	Fig. 40	1
2	Bottom ring	Fig. 41	1
3	Header	Fig. 42	1
4	Exhaust tubulation	Copper tube, 1/4" O.D., OFHC, 2-1/2" long	1
5	Faceplate	RCA part No. FP8-1/4B1 (quartz)	1
6	Target ring	RCA part No. 60341C	1
7	Electroplated mesh	RCA part No. L605V (nickel)	1
8	Mesh welding ring	Fig. 43	1
9	Mesh ring	Fig. 44	1
10	Mesh support ring	Fig. 45	1
11	Mesh-mounting screw	0-80 screw, r.h., stainless steel, 0.050" long (excluding head)	4
12	G_1 support	Fig. 46	1
13	Beam disk support assembly	RCA part No. FM60766	1
14	G_2 cup	RCA part No. RA681 (molybdenum)	1
15	G_1-G_2 spacer disk	Fig. 47	1
16	G_1 cup	RCA part No. RA684 (molybdenum)	1
17	Brazed ceramic-cathode assembly	RCA part No. FM60765	1
18	Coated double helical heater	RCA part No. MCH6100-1	1
19	Heater support	Kovar rod, .050" D, .556" long	2
20	Pin connector	Fig. 48	4
21	Getter	RCA part No. FZ6241	1
22	Feedthrough pin A	Fig. 49	3
23	Feedthrough pin B	Fig. 49	4
24	Feedthrough pin C	Fig. 49	4
25	Target ring contact ribbon	Nichrome ribbon, .004" x 1/16" x 1-1/2"	1
26	Deflection yoke	Figs. 50-51	1
27	Potting compound	Polyurethane type PR 1538 (Products Research Co.)	
28	Magnetic shield	Fig. 52	
29	Insulated copper leads		13

Scale - 1:1
Dimensions in inches

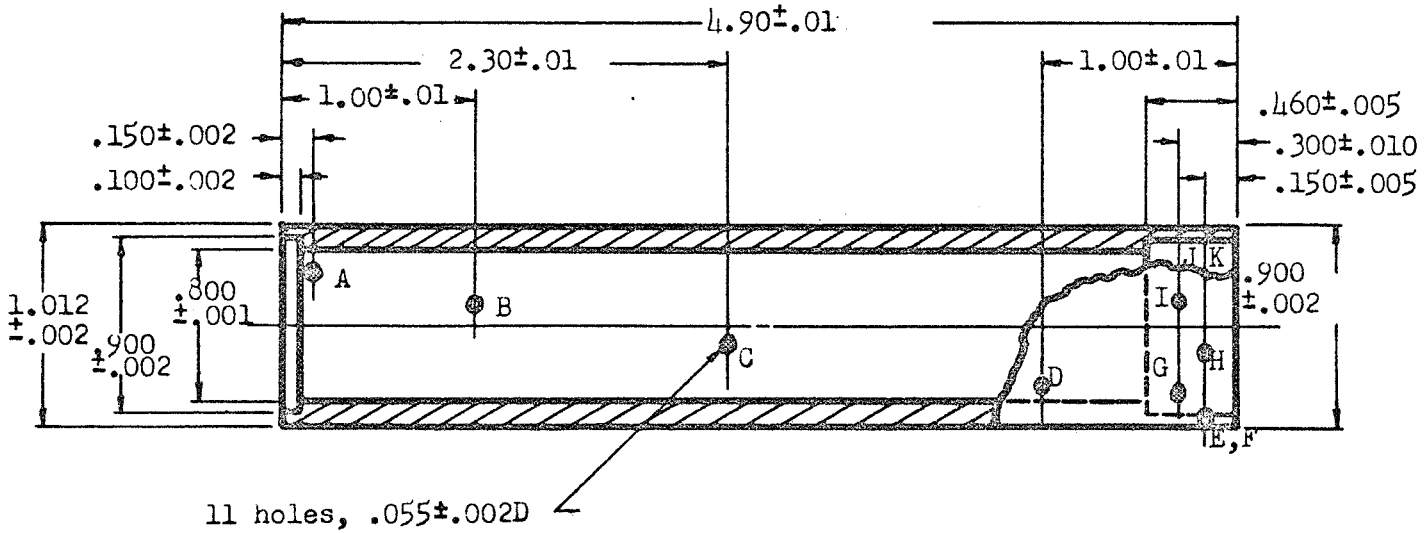

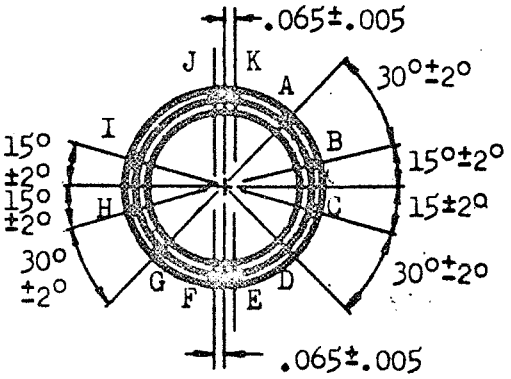

Note 1 - End surfaces (including internal shoulders) to be flat within 0.001" and perpendicular to ℄ within 0.001".
Note 2 - Finish on 0.800" I.D. surface to be 30 or better.
Note 3 - Internal radii to be concentric within 0.002".
Note 4 - Holes E,F,J and K are parallel to each other, all other holes are radial.

Fig. 40. Ceramic Tube Envelope

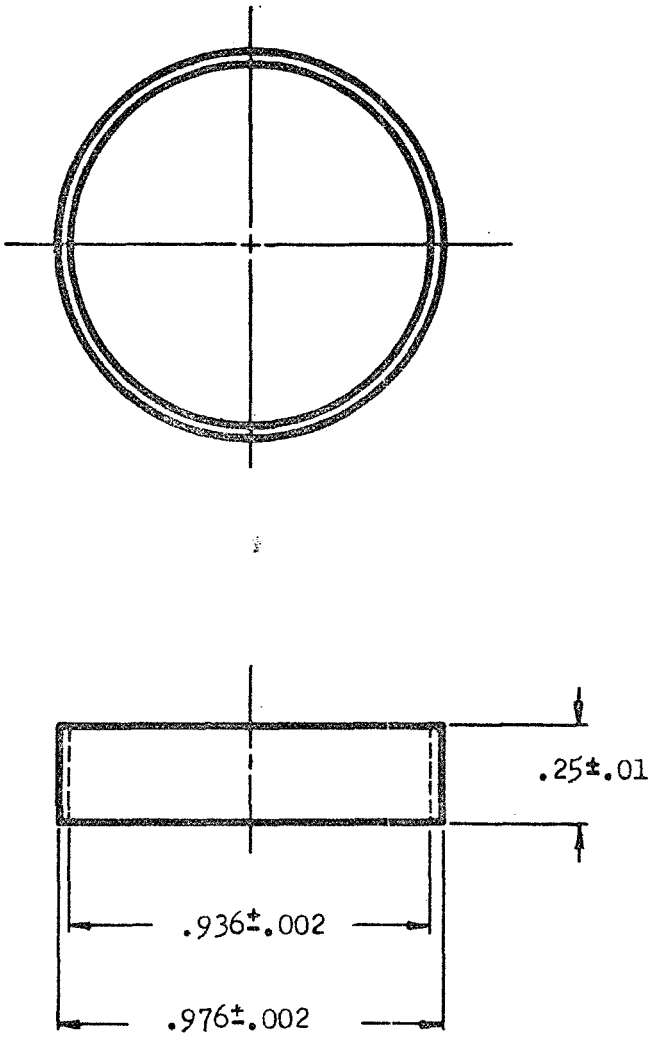

Scale - 2:1
Dimensions in inches

Material - Kovar

Fig. 41. Bottom Ring

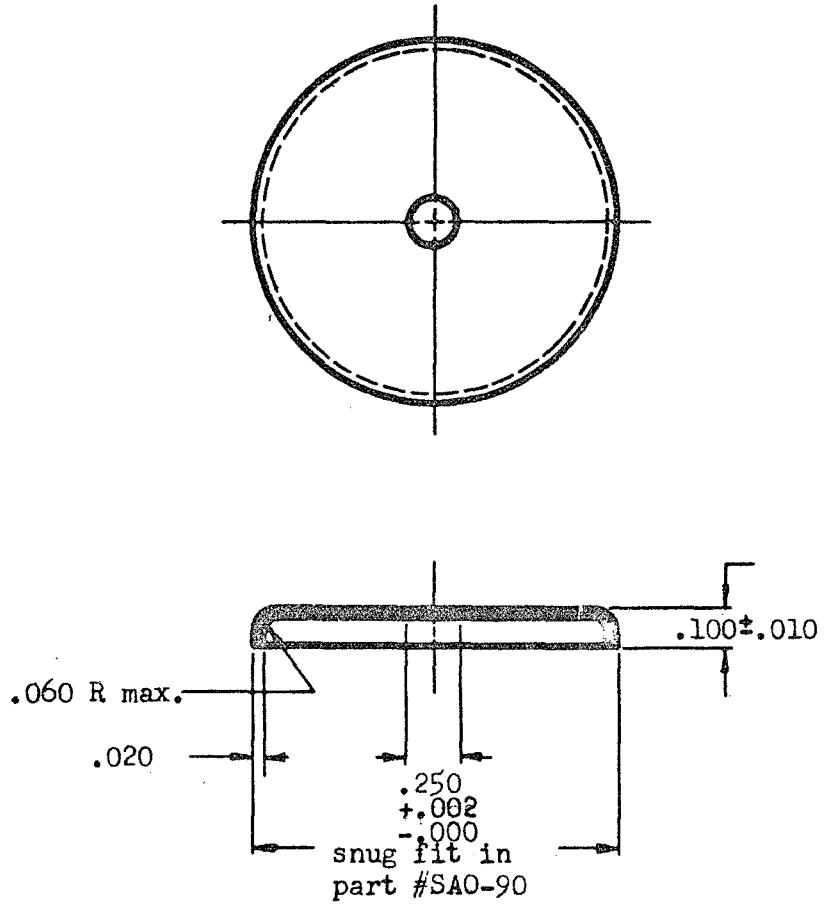

Scale - 2:1
Dimensions in inches
Material - Kovar

Note - center hole to be snug fit for 1/4" copper tubing

Fig. 42. Header

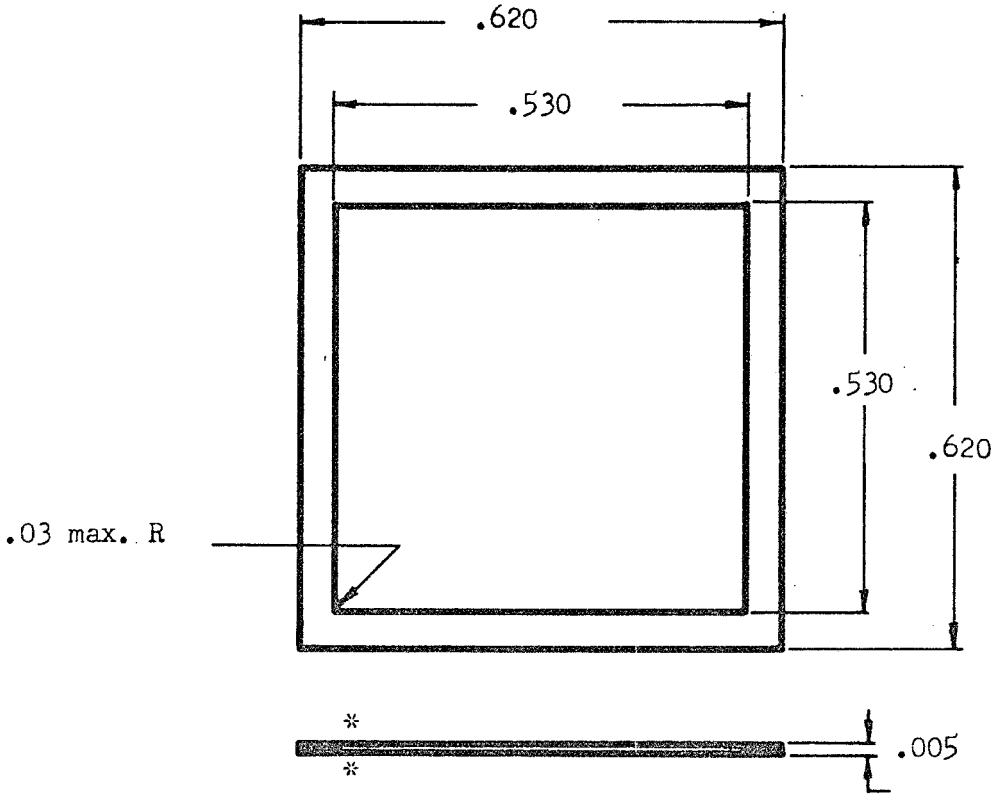

*Surfaces to have no spots over .001" high.

Scale - 4:1

Material - nichrome

Fig. 43. Mesh Welding Ring

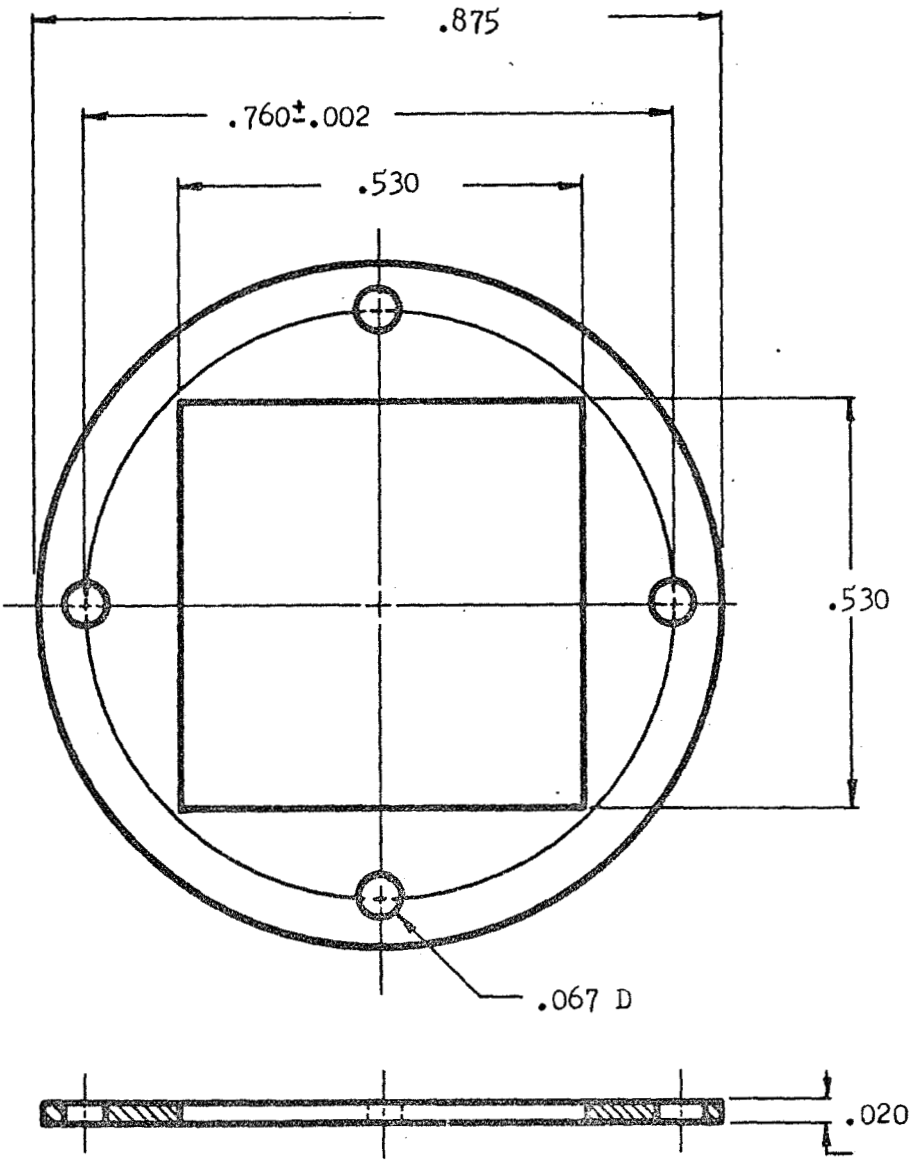

Note 1 - Punch square hole and O.D. in same direction.
Note 2 - Flat surfaces are not to have any spots over .001" high.

Scale - 4:1
Dimensions in inches

Material - nichrome

Fig. 44. Mesh Ring

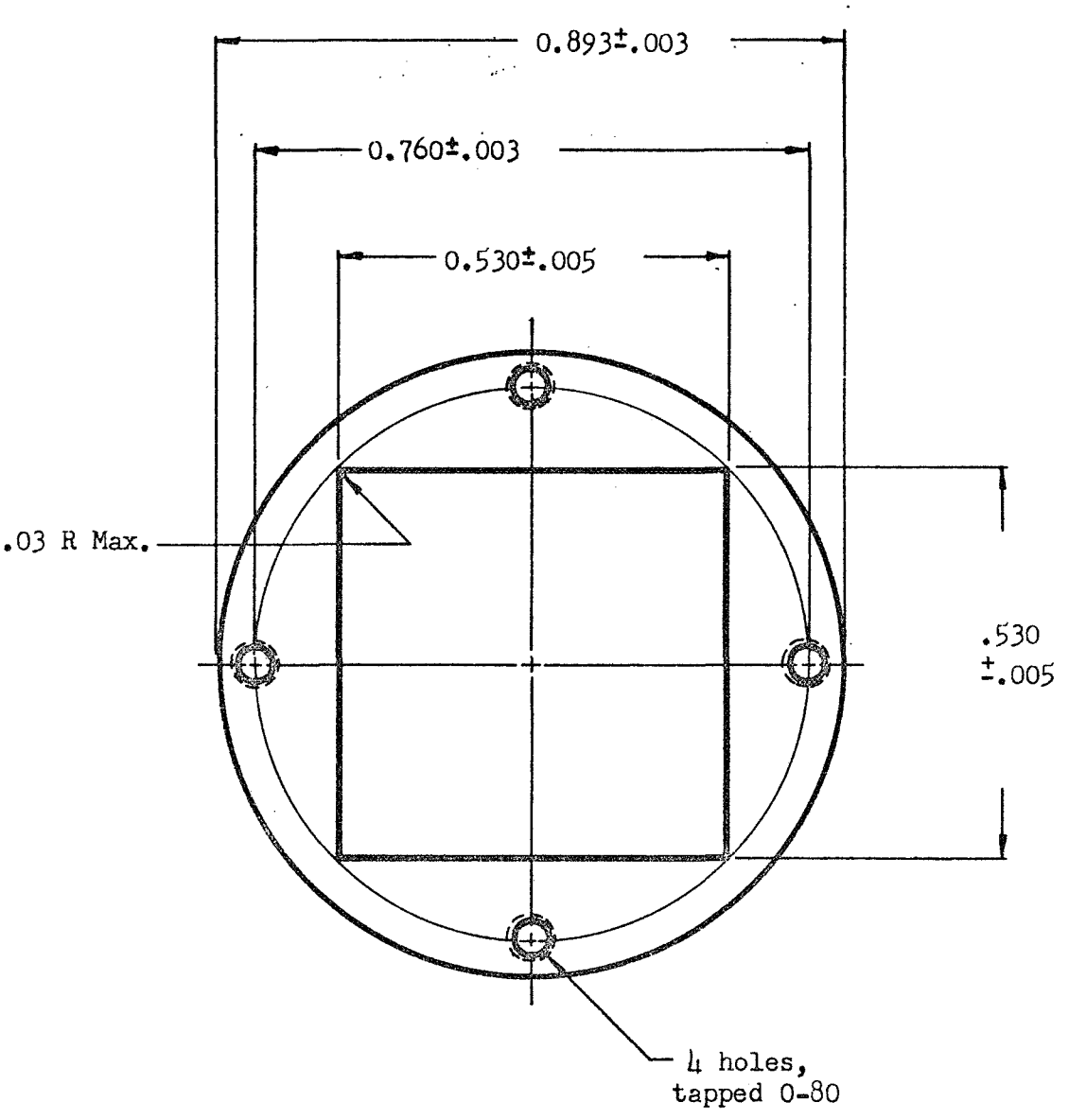

Note - Flat surfaces are not to have any spots over .001" high.

Scale - 4:1 Material - molybdenum

Fig. 45. Mesh Support Ring

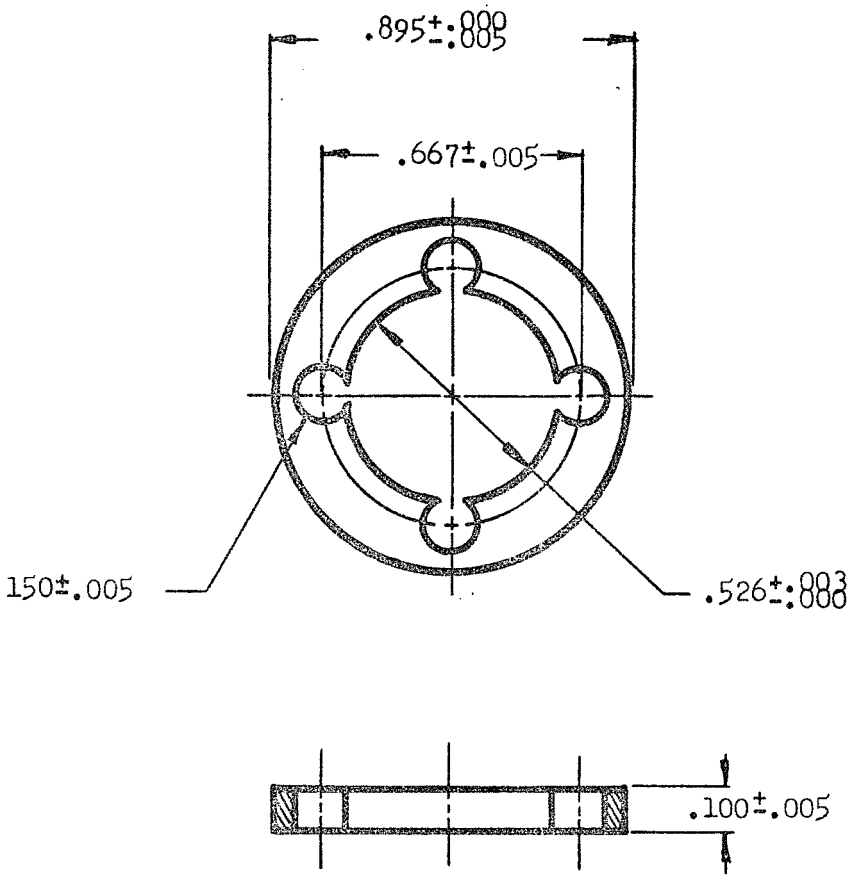

Scale - 2:1
Dimensions in inches

Material - alumina ceramic

Fig. 46. G_1 Support

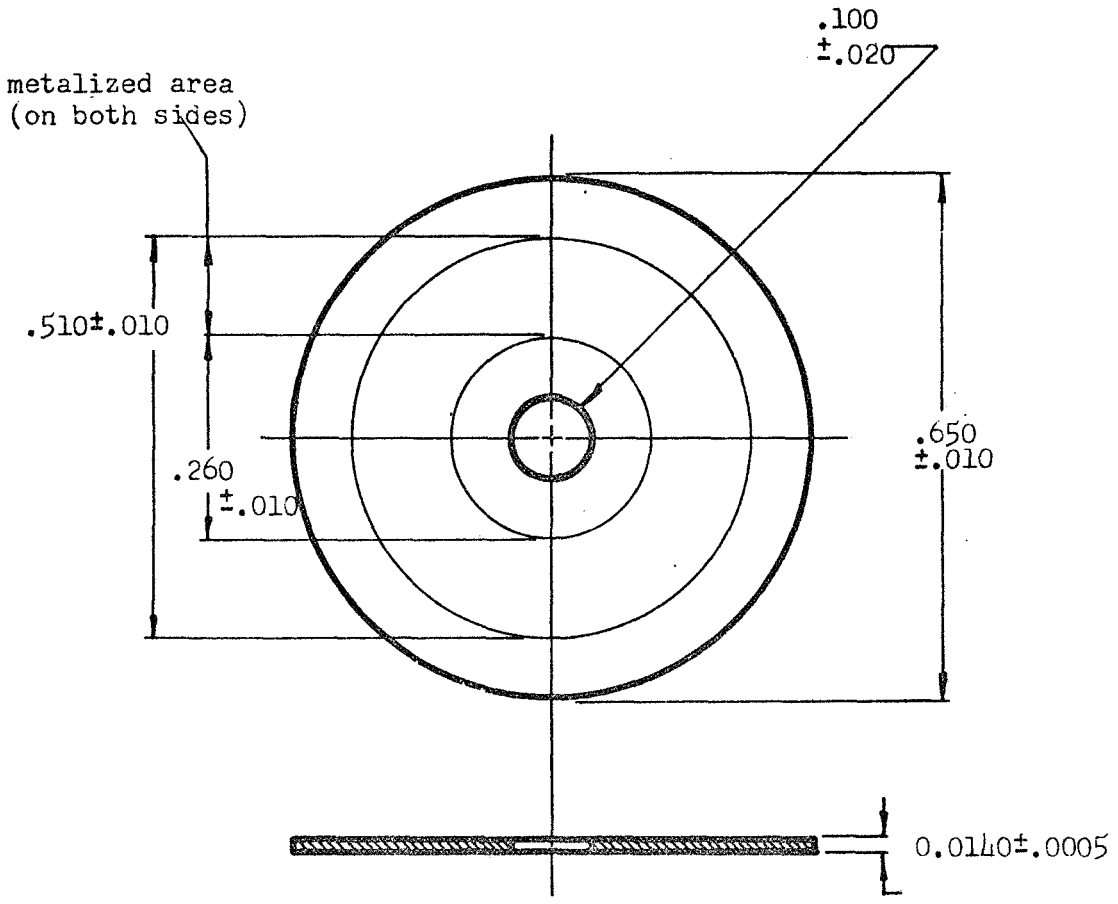

Note - End surfaces to be flat within 0.001"

Material - ceramic

Fig. 47. G_1-G_2 Spacer Disk

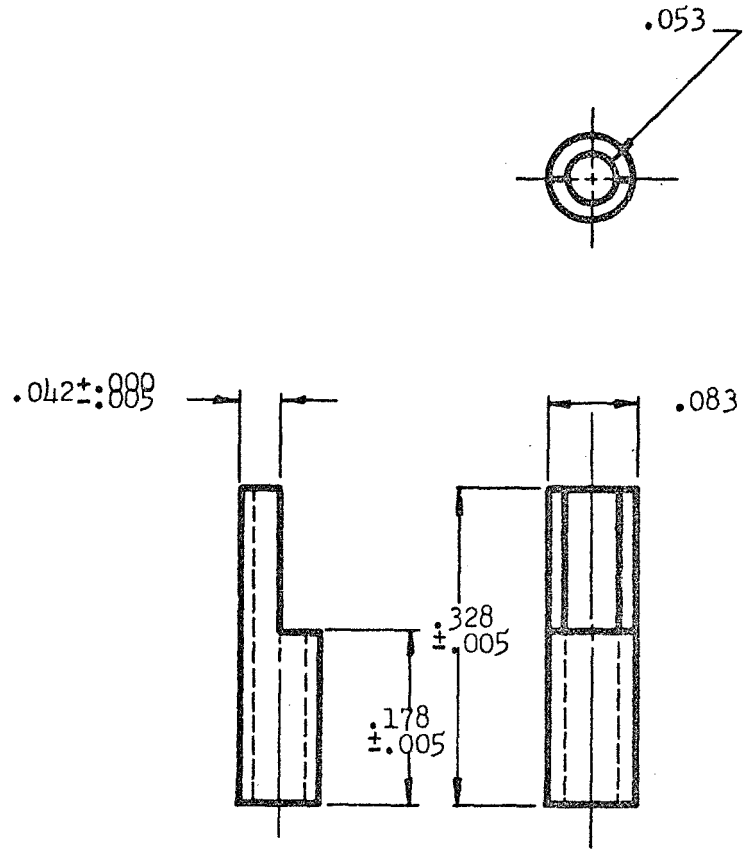

Scale - 5:1
Dimensions in inches

Material - stainless steel, type 321

Fig. 48. Pin Connector

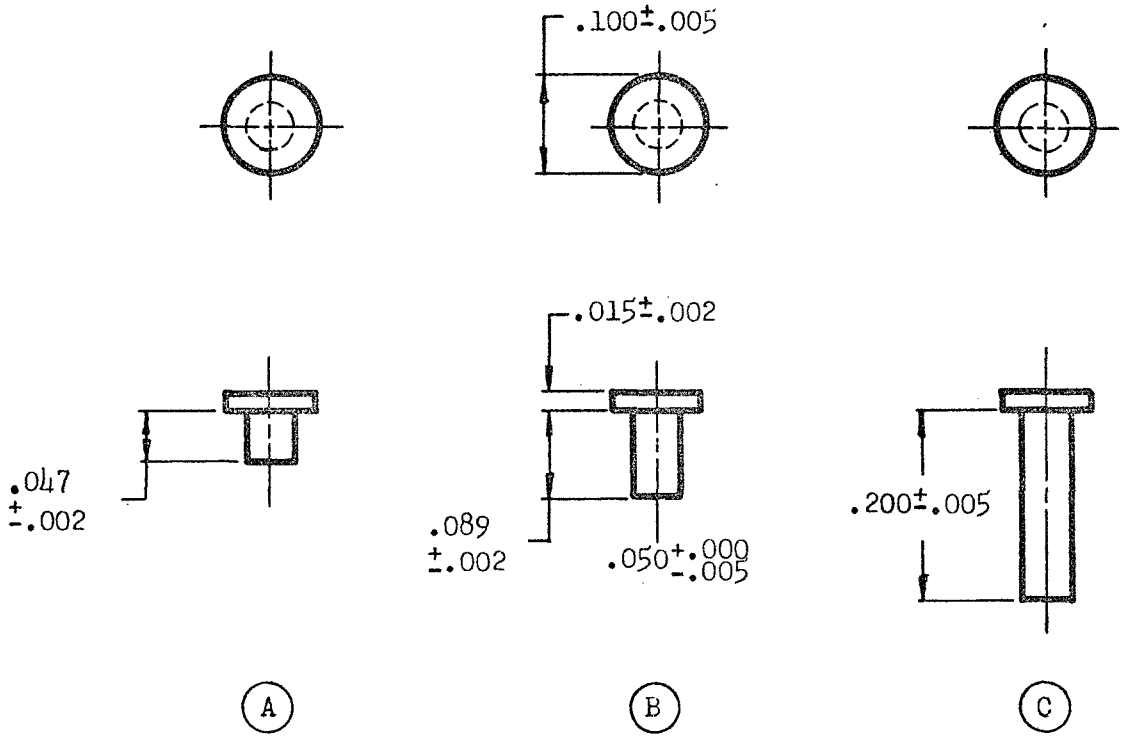

Scale - 5:1
Dimensions in inches

Material - (A), (C): Kovar
(b): molybdenum

Fig. 49. Feedthrough Pin

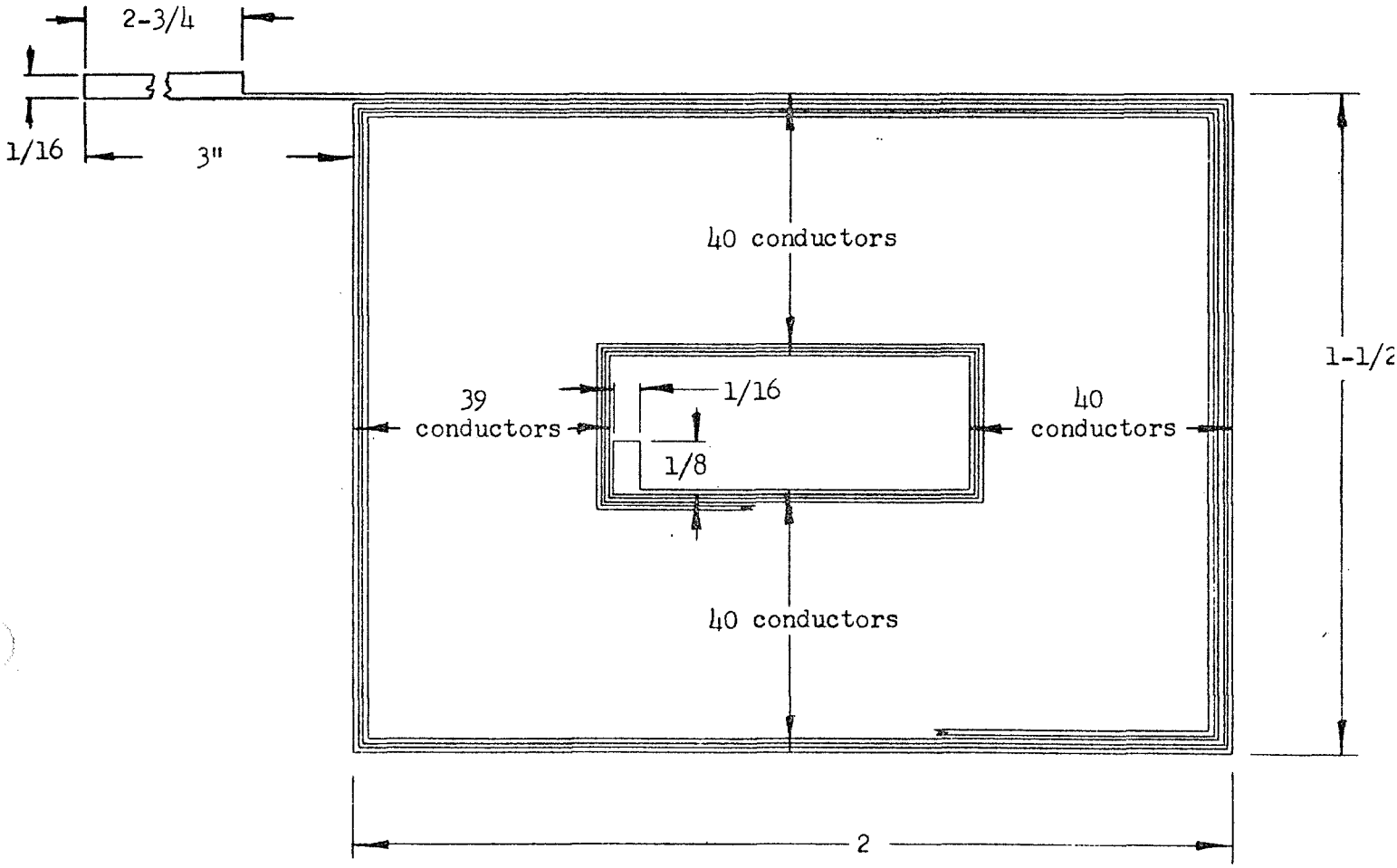

Conductor: thickness - 2 oz. copper per 4 etched coils
width - .010"
spacing - .005

Fig. 50. Deflection Coil (detail)

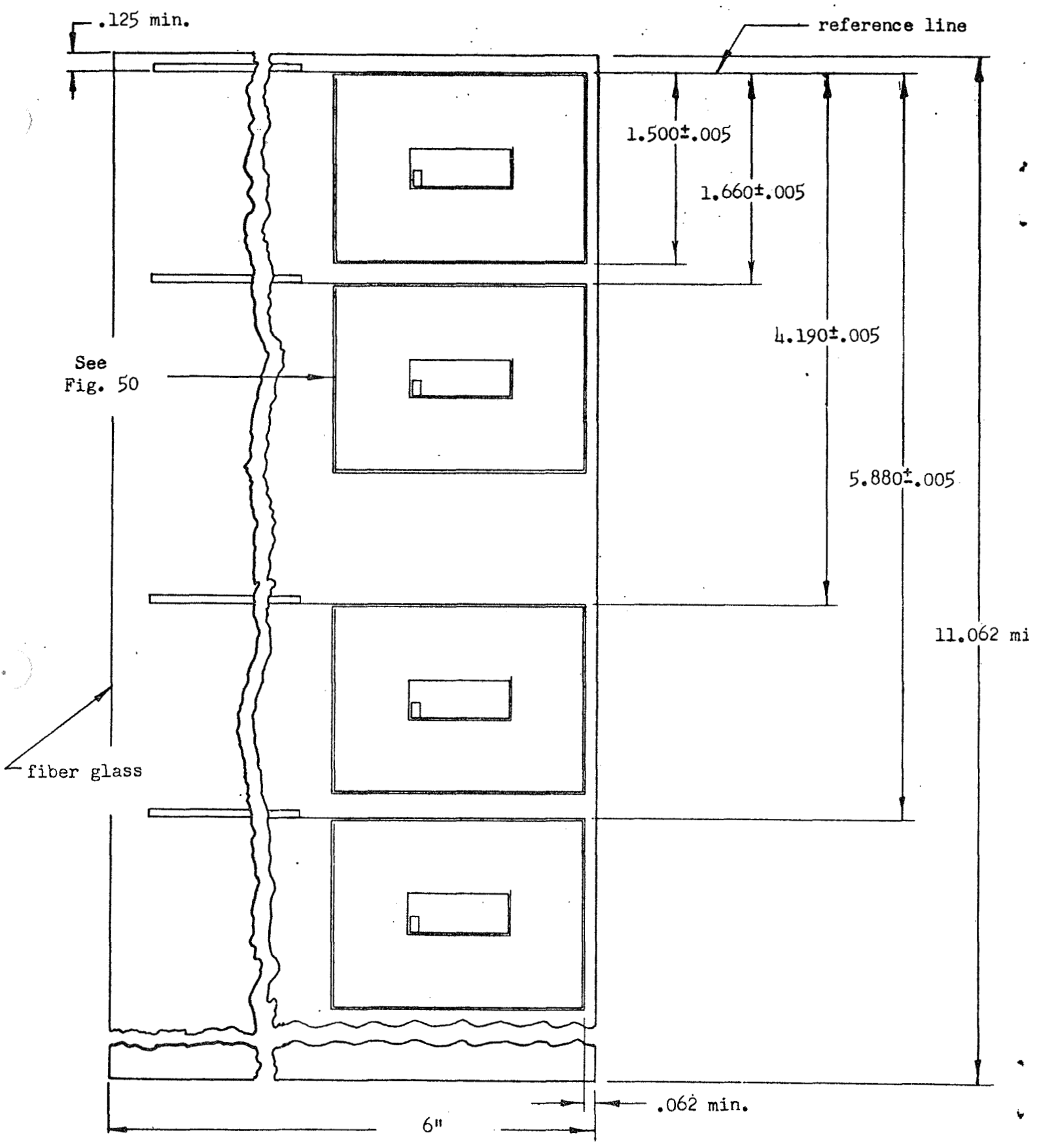

Fig. 51. Deflection Coil Pattern

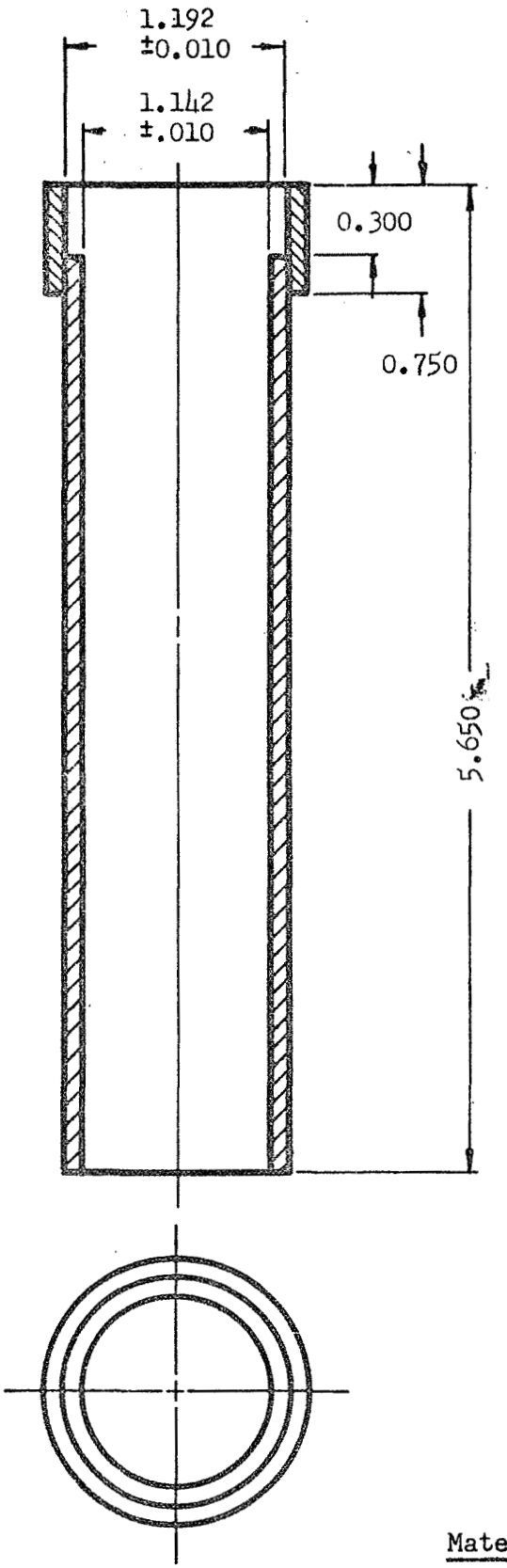

Material - Moly-permalloy

Fig. 52. Magnetic Shield